

REPORT DOCUMENTATION PAGE			Form Approved OMB NO. 0704-0188		
<p>The public reporting burden for this collection of information is estimated to average 1 hour per response, including the time for reviewing instructions, searching existing data sources, gathering and maintaining the data needed, and completing and reviewing the collection of information. Send comments regarding this burden estimate or any other aspect of this collection of information, including suggestions for reducing this burden, to Washington Headquarters Services, Directorate for Information Operations and Reports, 1215 Jefferson Davis Highway, Suite 1204, Arlington VA, 22202-4302. Respondents should be aware that notwithstanding any other provision of law, no person shall be subject to any penalty for failing to comply with a collection of information if it does not display a currently valid OMB control number. PLEASE DO NOT RETURN YOUR FORM TO THE ABOVE ADDRESS.</p>					
1. REPORT DATE (DD-MM-YYYY)		2. REPORT TYPE		3. DATES COVERED (From - To)	
		New Reprint		-	
4. TITLE AND SUBTITLE			5a. CONTRACT NUMBER		
Four Decades of the Chemistry of Planar Hypercoordinate Compounds			W911NF-12-1-0083		
			5b. GRANT NUMBER		
			5c. PROGRAM ELEMENT NUMBER		
			206022		
6. AUTHORS			5d. PROJECT NUMBER		
Li-Ming Yang, Eric Ganz, Zhongfang Chen, Zhi-Xiang Wang, Paul von Ragué Schleyer					
			5e. TASK NUMBER		
			5f. WORK UNIT NUMBER		
7. PERFORMING ORGANIZATION NAMES AND ADDRESSES			8. PERFORMING ORGANIZATION REPORT NUMBER		
University of Puerto Rico at Rio Piedras P. O. Box 21790  San Juan, PR 00931 -1790					
9. SPONSORING/MONITORING AGENCY NAME(S) AND ADDRESS (ES)			10. SPONSOR/MONITOR'S ACRONYM(S)		
U.S. Army Research Office P.O. Box 12211 Research Triangle Park, NC 27709-2211			ARO		
			11. SPONSOR/MONITOR'S REPORT NUMBER(S)		
			60435-MS-REP.53		
12. DISTRIBUTION AVAILABILITY STATEMENT					
Approved for public release; distribution is unlimited.					
13. SUPPLEMENTARY NOTES					
The views, opinions and/or findings contained in this report are those of the author(s) and should not be construed as an official Department of the Army position, policy or decision, unless so designated by other documentation.					
14. ABSTRACT					
<p>The idea of planar tetracoordinate carbon (ptC) was considered implausible for a hundred years after 1874. Examples of ptC were then predicted computationally and realized experimentally. Both electronic and mechanical (e.g., small rings and cages) effects stabilize these unusual bonding arrangements. Concepts based on the bonding motifs of planar methane and the planar methane dication can be extended to give planar hypercoordinate structures of other chemical elements. Numerous planar configurations of various central atoms (main-group and transition-metal elements) with coordination numbers up to ten are discussed herein. The evolution of such planar</p>					
15. SUBJECT TERMS					
Hypercoordination;coordination numbers;nonclassical molecules;planar coordination;theoretical chemistry					
16. SECURITY CLASSIFICATION OF:			17. LIMITATION OF ABSTRACT	15. NUMBER OF PAGES	19a. NAME OF RESPONSIBLE PERSON
a. REPORT	b. ABSTRACT	c. THIS PAGE	UU		Zhongfang Chen
UU	UU	UU			19b. TELEPHONE NUMBER
					787-764-0000

## Report Title

Four Decades of the Chemistry of Planar Hypercoordinate Compounds

### ABSTRACT

The idea of planar tetracoordinate carbon (ptC) was considered implausible for a hundred years after 1874. Examples of ptC were then predicted computationally and realized experimentally. Both electronic and mechanical (e.g., small rings and cages) effects stabilize these unusual bonding arrangements. Concepts based on the bonding motifs of planar methane and the planar methane dication can be extended to give planar hypercoordinate structures of other chemical elements. Numerous planar configurations of various central atoms (main-group and transition-metal elements) with coordination numbers up to ten are discussed herein. The evolution of such planar configurations from small molecules to clusters, to nanospecies and to bulk solids is delineated. Some experimentally fabricated planar materials have been shown to possess unusual electrical and magnetic properties. A fundamental understanding of planar hypercoordinate chemistry and its potential will help guide its future development.

---

**REPORT DOCUMENTATION PAGE (SF298)**  
**(Continuation Sheet)**

---

Continuation for Block 13

ARO Report Number 60435.53-MS-REP  
Four Decades of the Chemistry of Planar Hyper...

Block 13: Supplementary Note

© 2015 . Published in Angewandte Chemie International Edition, Vol. 54 (33) (2015), ( 33). DoD Components reserve a royalty-free, nonexclusive and irrevocable right to reproduce, publish, or otherwise use the work for Federal purposes, and to authorize others to do so (DODGARS §32.36). The views, opinions and/or findings contained in this report are those of the author(s) and should not be construed as an official Department of the Army position, policy or decision, unless so designated by other documentation.

Approved for public release; distribution is unlimited.

# Four Decades of the Chemistry of Planar Hypercoordinate Compounds

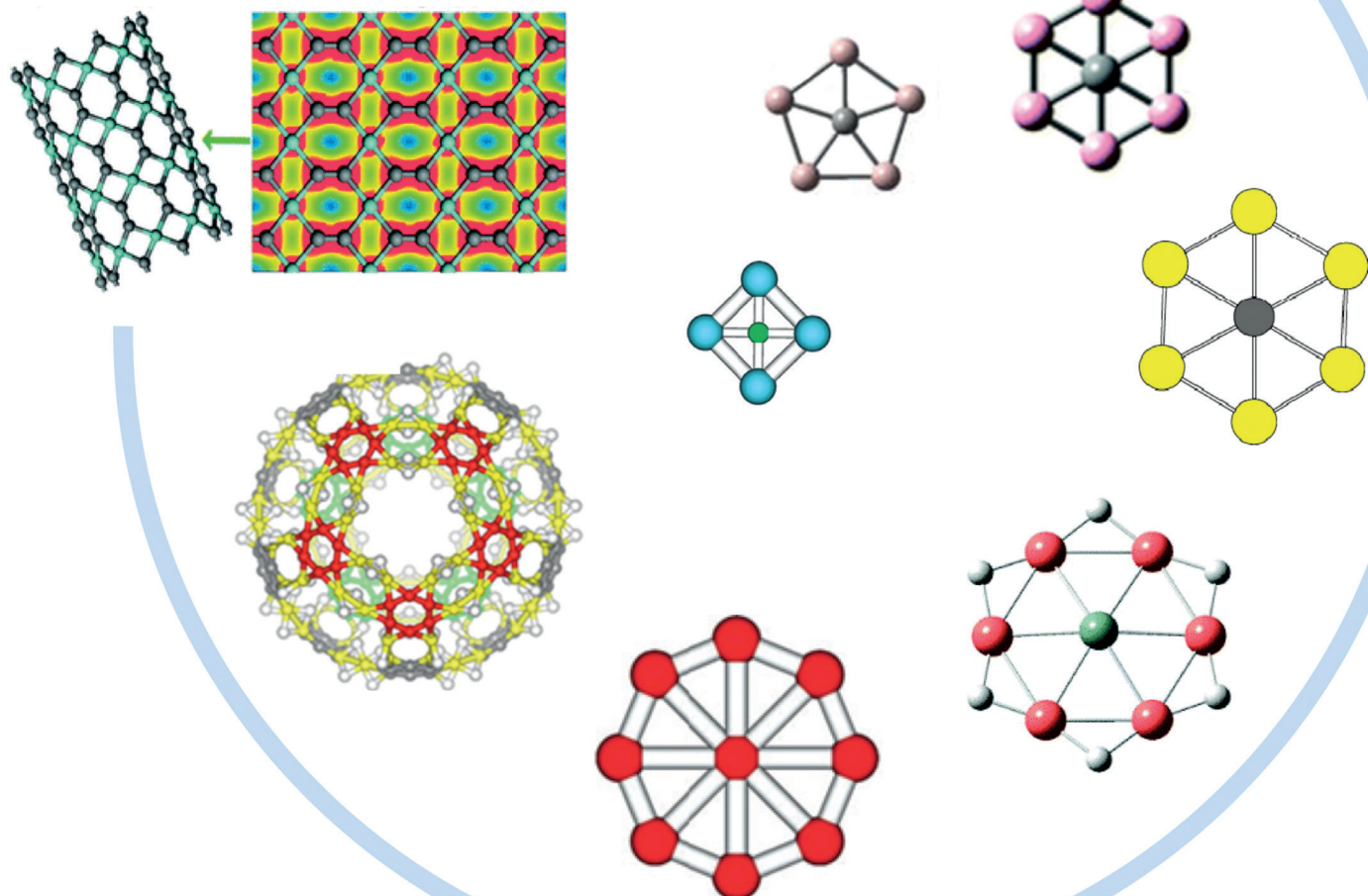
Li-Ming Yang,\* Eric Ganz, Zhongfang Chen,\* Zhi-Xiang Wang, and Paul von Ragué Schleyer†

**Keywords:**

Hypercoordination ·  
coordination numbers ·  
nonclassical molecules ·  
planar coordination ·  
theoretical chemistry

*In memory of Hans Wynberg*

## Planar Hypercoordinate Chemistry



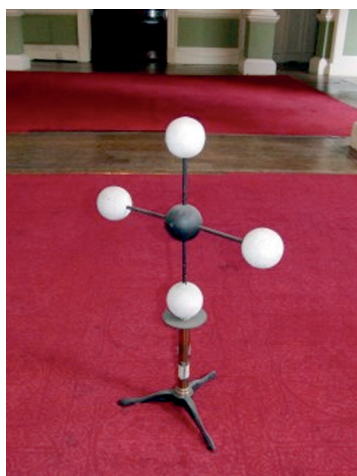


**T**he idea of planar tetracoordinate carbon (ptC) was considered implausible for a hundred years after 1874. Examples of ptC were then predicted computationally and realized experimentally. Both electronic and mechanical (e.g., small rings and cages) effects stabilize these unusual bonding arrangements. Concepts based on the bonding motifs of planar methane and the planar methane dication can be extended to give planar hypercoordinate structures of other chemical elements. Numerous planar configurations of various central atoms (main-group and transition-metal elements) with coordination numbers up to ten are discussed herein. The evolution of such planar configurations from small molecules to clusters, to nanospecies and to bulk solids is delineated. Some experimentally fabricated planar materials have been shown to possess unusual electrical and magnetic properties. A fundamental understanding of planar hypercoordinate chemistry and its potential will help guide its future development.

## 1. Introduction

Non-classical molecules<sup>[1]</sup> with atypical geometries and exotic electronic structures enrich chemical bonding theory and offer the potential for novel applications owing to their exceptional electronic, magnetic, and optical properties. Molecules with planar tetracoordinate carbon are seminal examples.

Although A. W. von Hofmann's beautiful mechanical model of planar methane from 1860 is still applicable, the



Source: Ref. [2]

tetrahedral preference of tetracoordinate carbon, deduced by van't Hoff<sup>[3]</sup> and Le Bel<sup>[4]</sup> independently, has been a basic structural principle of organic and biological chemistry since 1874. But what was not fully appreciated at that time is the remarkably large extent to which the tetrahedral model is true quantitatively. The energy associated with planar tetracoordinate deformation is enormous! A century passed and over a million molecules had been characterized before such planar configurations were discovered.

## From the Contents

<b>1. Introduction</b>	9469
<b>2. How to Achieve Planar Tetracoordinate (Hypercoordinate) Carbon</b>	9472
<b>3. Designing ptC Compounds using New Principles</b>	9474
<b>4. Planar Pentacoordinate Carbon</b>	9480
<b>5. Planar Hexa- and Higher Coordinate Carbon</b>	9482
<b>6. Other Planar Tetracoordinate (or Hypercoordinate) Elements</b>	9487
<b>7. Sandwich-Type Complexes and Extended Systems</b>	9492
<b>8. Experimental Realization of Planar Motifs</b>	9495
<b>9. Conclusion</b>	9497

Hans Wynberg, the first modern chemist who kindled interest in planar tetracoordinate carbon, is the unsung hero of this development. Wynberg was concerned by the fact that the  $CR^1R^2R^3R^4$  hydrocarbons (with four different alkyl groups) that his Groningen group had synthesized by chiral

[\*] Dr. L.-M. Yang, Prof. P. v. R. Schleyer  
Center for Computational Quantum Chemistry  
Department of Chemistry, University of Georgia  
Athens, GA 30602-2525 (USA)  
E-mail: lmyang.uio@gmail.com

Prof. E. Ganz  
Department of Physics, University of Minnesota  
116 Church St. SE, Minneapolis, MN 55416 (USA)

Prof. Z. Chen  
Department of Chemistry, Institute for Functional Nanomaterials  
University of Puerto Rico  
Rio Piedras Campus, San Juan, PR 00931 (USA)  
E-mail: zhongfangchen@gmail.com

Prof. Z.-X. Wang  
School of Chemistry and Chemical Engineering, University of the Chinese Academy of Sciences  
Beijing, 100049 (China)

Dr. L.-M. Yang  
Present address: Hanse-Wissenschafts-Kolleg (Institute for Advanced Study)  
Lehmkuhlenbusch 4, 27753 Delmenhorst (Germany)  
and  
Bremen Center for Computational Materials Science, University of Bremen  
Am Falturm 1, 28359, Bremen (Germany)

[†] Deceased, November 21, 2014.

routes did not have measurable optical activity.<sup>[5]</sup> While this probably was due to the similarity of the alkyl ligands, Wynberg wanted to rule out the seemingly unlikely possibility of thermal racemization. As the barrier heights for such stereomutation were unknown, Wynberg employed his powerful personality to persuade theoreticians to compute examples. The resulting papers he inspired, including those by his Dutch colleague, Hendrik Monkhorst, who led the way in 1968,<sup>[6]</sup> as well as by the Roald Hoffmann<sup>[7]</sup> and the Pople–Schleyer<sup>[8]</sup> groups, acknowledge Wynberg's influence. Although the theoretical levels available to them were crude by today's standards, Monkhorst's very large computed relative energy of planar methane ruled it out as a possibility.<sup>[6]</sup> High *ab initio* levels verified this conclusion later (see Scheme 4 in Section 2).<sup>[8,9]</sup>

Monkhorst's<sup>[6]</sup> interconversion pathways of methane enantiomers with hypothetical asymmetric carbon atoms

(without breaking bonds) are reproduced in Scheme 1. His goal was not to find a planar tetracoordinate carbon (ptC) minimum; instead, he pointed out that the stereomutation of methane via a ptC seems quite impossible. The tetrahedral tetracoordinate carbon (ttC) configuration is very rigid and the energy difference (ca. 130 kcal mol<sup>-1</sup>) between ttC (*T<sub>d</sub>*) and ptC (*D<sub>4h</sub>*) is extremely high, even higher than the dissociation energy (ca. 103 kcal mol<sup>-1</sup>) of a methane C–H bond.<sup>[10]</sup> The challenge of ptC chemistry is to find ways to overcome such huge interconversion barriers and to stabilize planar configurations.

Roald Hoffmann, along with colleagues Roger Alder and Charles Wilcox (together abbreviated to HAW), were the next to address Wynberg's problem. However, their stated goal was not (as is often misreported) to find a ptC, but rather to consider “how to stabilize a planar geometry so that it could serve as a thermally accessible transition state for



Li-Ming Yang received his Ph.D. in physical chemistry at Jilin University (China) in 2008. He joined Prof. Schleyer's group at University of Georgia (USA) as a postdoc in 2011. In 2014, he joined Prof. Frauenheim's group at University of Bremen (Germany) as a fellow of the Hanse-Wissenschafts-Kolleg. He is also a visiting scientist at Prof. Heine's group at Jacobs University Bremen. His research interests include planar hyper-coordinate chemistry, aromaticity, catalysis, reaction mechanism, and the computational exploration of various materials.



Zhi-Xiang Wang obtained his Ph.D. from the Beijing Normal University (China) in 1996, under the supervision of Prof. Ruozhuang Liu. He joined Prof. Schleyer's group in 1998 at the University of Georgia. In 2003, he became a member of Prof. Duan's group at the University of California, Davis. He has been a Professor since he joined the University of Chinese Academy of Sciences in 2007, as a scholar of “one hundred person project” of the Chinese Academy of Sciences. His research is focused on applying computational chemistry to understand catalytic mechanisms and design catalysts in the context of sustainable chemistry.



Eric Ganz received his PhD in physics from the University of California at Berkeley in 1988. He did a post-doc at Harvard University, and then joined the faculty of the physics department at the University of Minnesota in 1991. He worked on the construction of scanning tunneling microscopes and studied atomic diffusion and growth on Si surfaces in vacuum. Recently, he has been studying hydrogen storage by spillover on metal–organic and covalent–organic frameworks using density functional theory calculations.

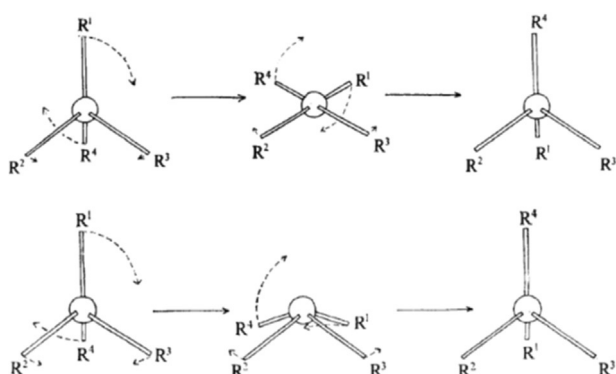


Paul von Ragué Schleyer studied chemistry in Princeton and Harvard (Ph.D. with P. D. Bartlett). He was named Eugene Higgins Professor of Chemistry in 1969. In 1976 he became Co-Director of the Organic Chemistry Institute of the University of Erlangen-Nuremberg (Germany) where he founded the Computer Chemistry Center in 1993. He was Professor Emeritus at Erlangen since 1998, and continued as Graham Perdue Professor of Chemistry at the University of Georgia, Athens. He was President of the World Association of Theoretically Oriented Chemists (WATOC) and Editor-in-Chief of the *Encyclopedia of Computational Chemistry*.



Zhongfang Chen earned his degrees at Nankai University (China; Ph.D. 2000) and stayed for four years as a postdoc in Germany with Prof. Andreas Hirsch and Prof. Walter Thiel under the support of Alexander von Humboldt foundation and Max Planck society. In 2003, he joined Prof. Schleyer's group at the University of Georgia. After a short stay at Rensselaer Polytechnic Institute (2008) he moved to the University of Puerto Rico, Rio Piedras campus, where he is a Professor in the Department of Chemistry. He applies modern computational tools

to investigate rules and trends in chemistry and to design new materials for energy, environment and human health applications.



**Scheme 1.** Monkhorst's possible exchange pathways of tetrahedral carbon enantiomers illustrated by showing the relationship among hypothetical ligands around the chiral central carbon atom. (Reprinted with permission from Ref. [6], Copyright 1968 The Royal Society of Chemistry). Scheme 2 lists the high-level theoretical data for comparison.

a classical racemization experiment" to ascertain ways to reduce the ptC stereomutation barriers. None of their extended Hückel theory (EHT) computations on prospective model compounds (e.g., those employing ring strain) came anywhere close to having a ptC minimum,<sup>[7]</sup> HAW concluded, "it would seem too much to hope for a simple carbon compound to prefer a planar to a tetrahedral structure." Nevertheless, this paper (and Hoffmann's subsequent account of the work in *Pure and Applied Chemistry*)<sup>[7]</sup> had enormous influence. HAW's<sup>[7a]</sup> 1970 breakthrough was the insightful analysis of ptC bonding in hypothetical planar methane. They suggested strategies to stabilize ptCs electronically, for example, stabilizing its lone pair by  $\pi$ -acceptor substituents, and its electron-deficient bonding by  $\sigma$ -donors.

Hans Wynberg next convinced Paul Schleyer, during his many visits to Groningen, to undertake the ptC search. Schleyer's initiation to ab initio computations under John Pople's tutelage already had begun in the late 1960s. The challenge of finding ptCs by systematic investigations in collaboration with Pople using his Gaussian 70 program was irresistible. But computer time was severely limited in those days.

The opportunity came during Schleyer's 1974–1975 sabbatical year in Munich which he spent there with many members of his research group, including Eluvathingal Jemmis and Yitzhak Apeloig (both later become Presidents of Universities). Rolf Huisgen kindly arranged access to Bavarian computational facilities, which afforded the use of the ab initio Gaussian 70 program to explore ptC candidates by employing Pople–Schleyer<sup>[8]</sup> systematic surveys of comprehensive sets of molecules.

At George Olah's suggestion, small rings were added to HAW's ptC-promoting  $\sigma$ -donor/ $\pi$ -acceptor substituents strategies; this led to the discovery of the first molecule computed to have a ptC minimum, 1,1-dilithiocyclopropane (Figure 1a). As a consequence of this landmark achievement, Schleyer's and other research groups have been pursuing planar hypercoordinate chemistry ever since.

A comprehensive high-level theoretical investigation of  $\text{CH}_4$  in 1995<sup>[9]</sup> characterized its potential-energy surface

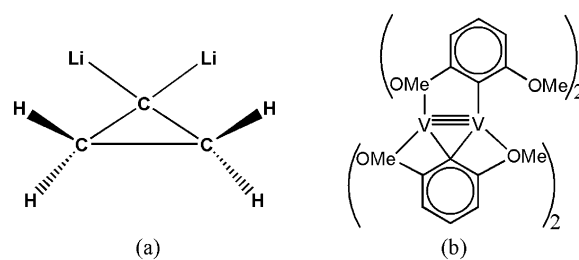
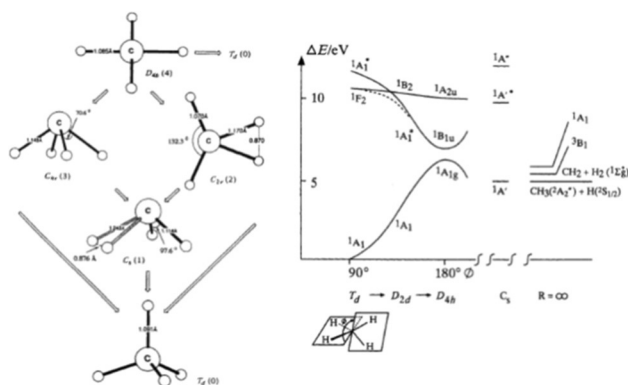


**Figure 1.** a) 1,1-dilithiocyclopropane, the first ptC molecule predicted by calculation in 1976; b) the vanadium 2,6-dimethoxyphenyl complex, the first ptC compound, synthesized in 1977.



**Scheme 2.** Correlation diagrams with  $T_d$   $\text{CH}_4$  and  $C_{4v}$   $\text{CH}_4$ . (Reprinted with permission from ref. [9], Copyright 1995 Wiley-VCH.)

definitively (Scheme 2; see also Scheme 1), and provided valuable information for the understanding of planar tetra-coordinate carbon energetics. Neither the unstable  $D_{4h}$  nor the  $C_{2v}$  planar  $\text{CH}_4$  geometries are minima or even transition states, but rather are higher order saddle points (see Scheme 4 in Section 2).

Although not recognized by the original authors, the first experimental example of a carbon with planar tetracoordination was reported in the X-ray structure of a vanadium 2,6-dimethoxyphenyl complex (Figure 1b) in 1977.<sup>[11]</sup> Numerous compounds with ptCs have been characterized experimentally as well as theoretically ever since. Significant progress in this "flatland" has been made in the last four decades; many interesting planar motifs with exotic geometries and unusual chemical bonding have been predicted theoretically and/or observed experimentally. This Review extends earlier Reviews of this research area<sup>[12]</sup> substantially.

This Review covers the past 44 years of progress in planar hypercoordinate chemistry of carbon and other main-group elements and transition metals. Since the highest planar coordination of carbon is usually three (e.g., in alkenes, arenes, etc.), planar carbon attachment to four (or more) atoms in the same plane is considered to be "planar hypercoordination." Similar definitions are applied to other elements. All types of planar hypercoordinated species including molecules, ions, clusters, nanotubes, nanosheets, nanoribbons, and bulk assemblages are included. The experimental realizations of planar motifs and potential applications of planar



species are emphasized. The mechanical and electronic strategies as well as the electron-counting rules used to design and help achieve planar configurations are explained, and the relationships of aromaticity and antiaromaticity to planar motifs are clarified. We hope to achieve a fundamental understanding of planar hypercoordination that, along with the numerous known and possible examples, will help dispel its seemingly exotic character. For simplicity, compounds are identified by their Figure number; for example, **1a** denotes the structure presented as (a) in Figure 1.

## 2. How to Achieve Planar Tetracoordinate (Hypercoordinate) Carbon

Strategies favoring ptC arrangements were suggested by HAW based on an analysis of the electronic structure of simple  $D_{4h}$  planar methane. This analysis revealed its two unfavorable features: 1) the non-bonding p- $\pi$  lone pair on the central carbon is “wasted” akin to that in the methyl carbanion,<sup>[13]</sup> which also prefers pyramidal distortion, and 2) the  $\sigma$  electron deficiency for the four in-plane CH bonds of  $D_{4h}$  methane. Consequently, the energy of an imposed square-planar methane structure is very high, approximately 130 kcal mol<sup>-1</sup> relative to that of the tetrahedral global minimum.<sup>[9]</sup> Since the C–H bond dissociation energy of methane is only 103.2 kcal mol<sup>-1</sup>,<sup>[14]</sup> tetrahedral methane prefers to undergo cleavage of a C–H bond to deformation into its planar,  $D_{4h}$ -symmetric form. Nevertheless, planar tetracoordinate carbon arrangements in other molecules can be stabilized mechanically (by strain effects), electronically (by appropriate substituents), or by using both strategies simultaneously.

The mechanical approach employs small-ring strain and/or an annulene perimeter or cylindrical cage or tube, to force the central carbon atom to be planar.<sup>[7b,12]</sup> Initially, the fenestranes (e.g. **2a**, Figure 2) and the aromatic unsaturated

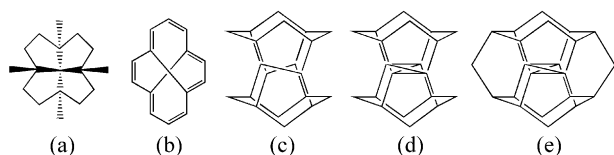


**Figure 2.** Schematic presentations of various mechanically stabilized ptC molecules.

fenestrenes (e.g. **2b**) were proposed as promising organic ptC candidates. Although no ptC compound was found later in line with this thinking, their study led to “fenestrane chemistry”.<sup>[15]</sup> Another approach (only explored computationally) positions a carbon atom at the center of a rigid three-dimensional cage, such as octaplane (**2c**).<sup>[12c,16]</sup> Many attempts failed to achieve ptC in alkaplans (including octaplane (**2d**),<sup>[12c,16]</sup> which closely approaches having a ptC minimum), until Rasmussen and Radom finally computed the first successful example, dimethanospiro[2,2]octaplane, (**2e**), by further modifying the “alkaplane” cage (**2d**) by adding “buttresses”.<sup>[12c,17]</sup>

HAW’s electronic approach involves substituents functioning as strong in-plane  $\sigma$  donors and out-of-plane  $\pi$  acceptors, which compensate the deficiency of  $\sigma$  bonding electrons and stabilize the energetically unfavorable  $\pi$  lone pair.<sup>[7a]</sup> In the extreme case, the lone pair can be entirely removed (as in the planar methane dication).<sup>[18]</sup> Alternatively,  $\pi$  acceptors can be used to delocalize the single  $\pi$  electron remaining in the corresponding radical cation (after removing only one electron.)

Using HAW’s “electronic” strategy, many ptC compounds have been characterized both theoretically and experimentally.<sup>[7a,12]</sup> In accord with HAW’s extended Hückel molecular orbital (EHMO) computations showing the planar methane HOMO to be a nonbonding lone pair in a perpendicular carbon  $\pi$ -orbital, analogous electronic structures also were found in many ptC compounds, such as **1a** and Radom and coworkers’ alkaplans **2e** (Figure 3).<sup>[12c,16,17]</sup>

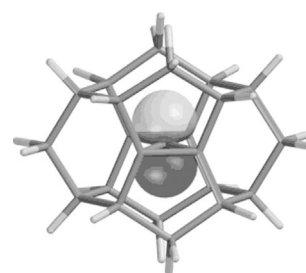


**Figure 3.** An isosurface showing the  $\pi$  HOMO of **2e**.<sup>[17]</sup> (Reprinted with permission from Ref. [17], Copyright 1999 WILEY-VCH.)

However, Siebert and Gunale have noted that genuine planar methane derivatives whose central carbon atom is indeed stabilized by  $\sigma$  donors and  $\pi$  acceptors are rare in the largest class of ptC molecules found experimentally—organometallic compounds. “In most cases investigated, the mode of stabilization is different from that predicted for planar  $CH_4$ . Very often the delocalization of  $\pi$  electron density does not play a role in stabilization of the geometry, as sufficient density is already distributed into the  $\pi$  system of the arene or olefin.”<sup>[12e]</sup>

Moreover, HAW’s planar methane model does not succeed with its isoelectronic analogues. Although planar  $CH_4$ , and  $NH_4^+$  have  $\pi$ -type HOMOs, the other  $ZH_4$  ( $BH_4^-$ ,  $AlH_4^-$ ,  $SiH_4$ ,  $PH_4^+$ ) molecules prefer  $\sigma$ -type HOMOs. The electronic configuration is determined by the central atom’s electronegativity. Species with  $\pi$  HOMOs are stabilized by  $\pi$ -acceptor and/or  $\sigma$ -donor groups, for example, electropositive substituents.<sup>[19]</sup> In contrast, species with  $\sigma$  HOMOs require  $\pi$ -donor and/or  $\sigma$ -acceptor groups such as OR,  $NR_2$ , and F for stabilization.<sup>[19]</sup> In addition, strong ligand–ligand bonding was first employed by Schleyer and Boldyrev to achieve the planar tetracoordinate geometries of **4a–f** (with five atoms being the smallest possible number; Figure 4).<sup>[20]</sup> When the O atom is embedded in the ring ( $Al_4O$ , **4a**), the main contributor to the HOMO is the oxygen lone-pair electrons (conforming with the HAW planar methane concept, Scheme 3), which are delocalized to the perimeter (Figure 5, left). In contrast, when

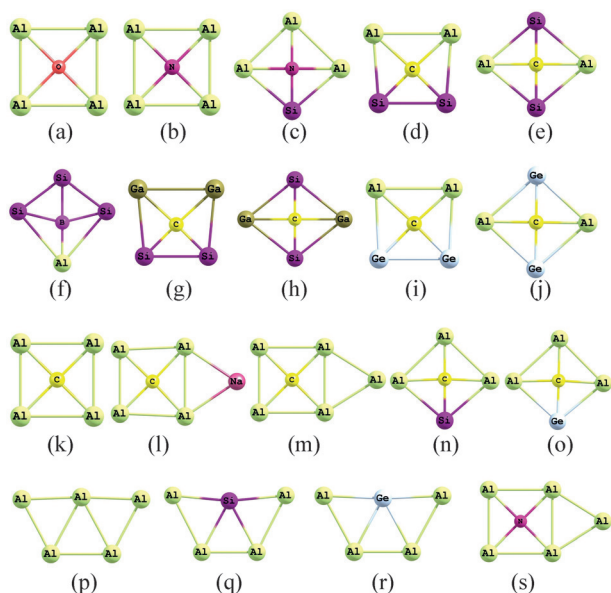
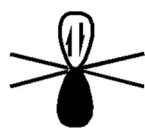


**Figure 4.** Five-atom planar tetracoordinate structures. a)  $\text{Al}_4\text{O}$ , b)  $\text{Al}_4\text{N}^-$ , c)  $\text{NAl}_3\text{Si}$ , d) *cis*- $\text{CSi}_2\text{Si}_2$ , e) *trans*- $\text{CAL}_2\text{Si}_2$ , f)  $\text{BAlSi}_3$  computationally predicted by the Schleyer–Boldyrev design principle;<sup>[20]</sup> later extended to g) *cis*- $\text{CSi}_2\text{Ga}_2$ , h) *trans*- $\text{CSi}_2\text{Ga}_2$ , i) *cis*- $\text{CGe}_2\text{Al}_2$ , j) *trans*- $\text{CGe}_2\text{Al}_2$ ,<sup>[24a]</sup> k)  $\text{CAL}_4^-$ ,<sup>[21]</sup> l) salt  $\text{Na}^+(\text{CAL}_4)^{2-}$ ,<sup>[22]</sup> m)  $\text{CAL}_5^-$  (i.e.,  $\text{Al}^+(\text{CAL}_4)^{2-}$ ),<sup>[27]</sup> n)  $\text{CAL}_3\text{Si}^-$ ,<sup>[23]</sup> o)  $\text{CAL}_3\text{Ge}^-$ ,<sup>[23]</sup> p)  $\text{Al}_5^-$ ,<sup>[24b]</sup> q)  $\text{SiAl}_4^-$ ,<sup>[24c]</sup> r)  $\text{GeAl}_4^-$ ,<sup>[24c]</sup> s)  $\text{Al}_5\text{N}^-$  (together with  $\text{Al}_4\text{N}^-$ ).<sup>[28]</sup> Among these structures, **4b** and **4k–s** were detected experimentally using photoelectron spectroscopy by the Wang and Boldyrev groups.

1970 Hoffmann, Alder, Wilcox  
(Based on planar  $\text{CH}_4$ )



Use  $\pi$ -acceptor substituents  
Use  $\sigma$ -donor substituents,  
eg.  $\text{BH}_2$ ,  $\text{SiH}_3$ , Li

2000 Exner, Wang, Schleyer  
(Based on planar  $\text{CH}_4^{2+}$ )



Use  $\pi$ -donor substituents  
Provide a good alternative MO  
for the extra electrons  
Apply to higher planar hypercoordination  
(penta, hexa, hepta)

**Scheme 3.** Two different models to achieve ptC

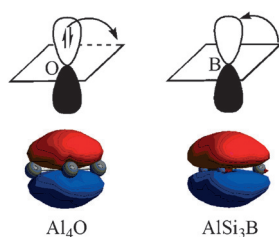
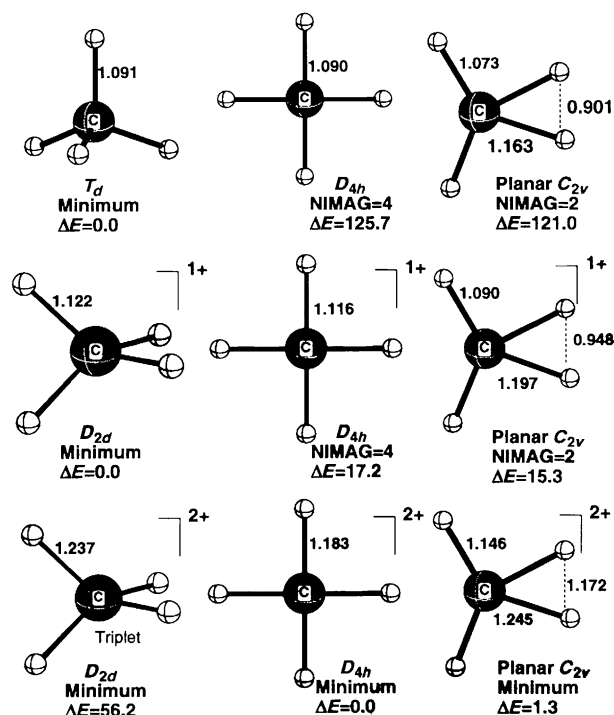


**Figure 5.** Diagram of the  $\pi$ -MO of  $\text{Al}_4\text{O}$  and  $\text{AlSi}_3\text{B}$ .

the central atom is B ( $\text{BAlSi}_3$ , **4f**), since the central boron has only a vacant p orbital initially, p electrons from the perimeter atoms flow in to form the  $\pi$  orbital (Figure 5, right), and the resulting HOMO is dominated by the perimeter atoms (this

follows the planar methane dication model of Scheme 3). Eighteen valence electrons are necessary to fill the bonding orbitals completely. The general Schleyer–Boldyrev strategy of strong perimeter bonding has been extensively developed further by Boldyrev and Wang. They have computed various planar molecules (including  $\text{CAL}_4^-$ ,<sup>[21]</sup>  $(\text{Na}^+)(\text{CAL}_4)^{2-}$ ,<sup>[22]</sup> and  $\text{CAL}_3\text{X}^q$  ( $\text{X} = \text{Si}, \text{Ge}$ ;  $q = -1, 0$ )<sup>[23]</sup> and have verified some experimentally (**4b**, **4k–s**).<sup>[21–24]</sup> They have predicted a series of isoelectronic substituted planar species (with general formula  $\text{XY}_4$ , X is Group IVa; Y is Group IIIa).<sup>[25]</sup> The pentatomic planar tetracoordinate carbon shown in Figure 4 is an important prototype of planar motifs which are stabilized solely by electronic factors. Many subsequent studies on pentaatomic planar molecules with different central elements and peripheral ligands involve same-group element substitution and isoelectronic systems.<sup>[25a,26]</sup>

Removal of the ptC lone-pair electrons helps planarize the central carbon arrangement. As shown in Scheme 3,  $\text{CH}_4^{2+}$ , the simplest ptC species, prefers to be planar because the perpendicular carbon  $\pi$  orbital is vacant. The six valence electrons in  $\text{CH}_4^{2+}$  bind best in planar  $\text{sp}^2$  hybridization (as in  $\text{CH}_3^+$ ).<sup>[18]</sup> Moreover, the planar methane radical cation is only modestly less stable than its tetrahedral alternatives (see Scheme 4).<sup>[29]</sup> Thus, planar  $\text{CH}_4^{2+}$  provides a new design principle for ptC molecules, and may be a better model than planar methane for this purpose.<sup>[30]</sup> As this Review shows, successful examples of ptC and planar hexacoordinate carbon (phC) compounds generally lack  $\pi$  electrons at the planar carbon sites.



**Scheme 4.** Planar versus  $T_d$  configurations of  $\text{CH}_4$ ,  $\text{CH}_4^+$ , and  $\text{CH}_4^{2+}$  (B3LYP/6-311 + G\*\* + ZPE, energy values in  $\text{kcal mol}^{-1}$ ).<sup>[30]</sup> (Reprinted with permission from Ref. [30], Copyright 2002 American Chemical Society.)

### 3. Designing ptC Compounds using New Principles

#### 3.1. PtCs Based on the Planar Methane Dication Model

Owing to the ionic character of its bonding, lithium prefers bridging positions and the structures of lithium compounds often do not follow classical considerations.<sup>[31]</sup> In addition to the first computed ptC compound (**1a**), several ptC species were predicted, such as  $C_6Li_6$  ( $D_{6h}$ ) **6a**<sup>[32]</sup> and **6b** (Figure 6). The ptC predicted in 1981 for the isolated dimer in

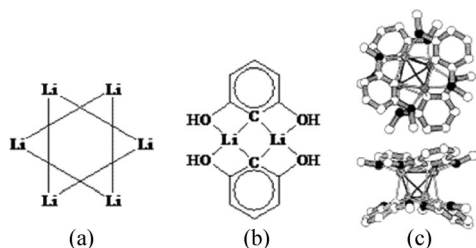


**Figure 6.** Theoretically predicted (a and b) and experimentally verified (c) lithium-based ptC compounds. Note that later work has revealed that the lowest energy configuration of  $C_6Li_6$  is not flat.<sup>[34]</sup> ((b) and (c) reprinted with permission from Ref. [33], Copyright 1988 American Chemical Society.)

**6b** was verified experimentally in 1988<sup>[33]</sup> with the crystal structure of (2,6-dimethoxyphenyl) lithium tetramer, **6c**, which comprises two interacting dimer units. Later work<sup>[34]</sup> has revealed that the lowest energy configuration of  $C_6Li_6$  is not flat, and is different than the predicted flat structure **6a**.

By utilizing the strong bridging proclivity of lithium to heteroatoms, as well as its strong electron-donating ability, a series of ptC compounds can be prepared.<sup>[35]</sup> The ptC arrangement in 1,1-dilithiocyclopropane (**1a**) is due to the combination of electronic and strain (bond angle) effects. The  $CH_2$  groups in 1,1-dilithiocyclopropane can be replaced by the more electronegative but isoelectronic groups NH (**7a**) and O (**7b**; Figure 7). Embedding **7a** into a heterocyclic system (**7c**), or further fusion of a benzene ring (**7d**) leads to more feasible

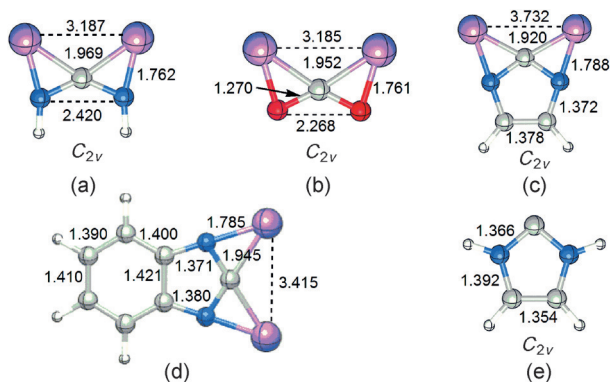


**Figure 7.** Computationally predicted dilithium ptC compounds.<sup>[35]</sup> The bond lengths are given in Å. C gray, H white, N blue, O red, Li lilac.

synthesis targets, because both **7c** and **7d** can take advantage of the aromaticity of imidazole.

To some extent, the electronic structures of **7a–d** are similar to those of the related carbenes, for example, **7e**, rather than the usual ptC compounds, such as **1a**. They have no p lone pair located on the ptC carbon with p- $\pi$  occupancy less than 1.0 e, in comparison with that (1.72 e) in **1a**. The strong ionic interactions between lithium atoms and the central carbon atoms in **1a** decrease significantly in **7a–d** owing to the smaller charge on the quaternary carbon atoms, but are compensated by the ionic interactions between the lithium atoms and the adjacent nitrogen (in **7a**, **7c** and **7d**) or oxygen (in **7b**) atom.

Recently, beryllium substituents have been successfully used to stabilize the ptC molecules, although they are not good  $\pi$  acceptors. This stabilization has been demonstrated by a class of ptC species (**8a–k**; Figure 8) based on  $C(BeH)_4$  computationally predicted by Wang and co-workers.<sup>[36]</sup>

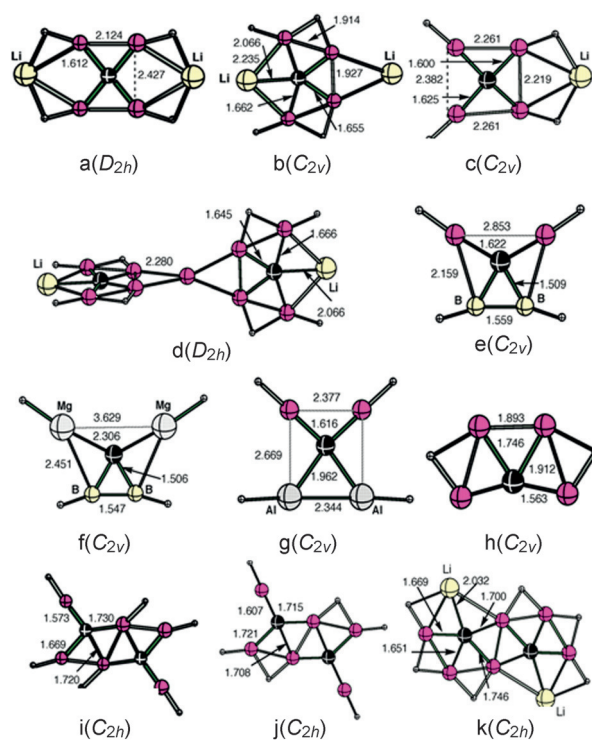


**Figure 8.** Lowest energy configurations of ptC species obtained by beryllium-based substituents. The unlabeled red, black, and white balls represent beryllium, carbon, and hydrogen atoms, respectively. (Reprinted with permission from Ref. [36], Copyright 2009 American Chemical Society.)

Radom's group<sup>[16]</sup> designed a family of alkaplane molecules (for example, spirooctaplane, **2c**) which constrain the ptC candidate in hydrocarbon cages. Although approaching a planar  $C(C)_4$ -type ptC more closely than ever before, such “mechanical” designs without “electronic” assistance must struggle to overcome the enormous strain of a ptC with a  $\pi$  lone-pair HOMO. More buttresses are needed to achieve planarity (for example, in dimethanospiro[2,2]octaplane **2e**).



As noted by Radom and co-workers,<sup>[17]</sup> **2c** is a minimum at the potential energy curve calculated at MP2/6-311 + G(2d,p) level but not quite so at B3LYP/6-311 + G(3df, 2p) level. It was later found that **2c** has a 279i cm<sup>-1</sup> imaginary frequency at B3LYP/6-31G\*.<sup>[30]</sup> Note that both **2c** and **2e** have lone-pair HOMOs (Figure 3), which conforms to the HAW planar methane model, but is not favorable for the ptC arrangement.

One way to achieve a ptC based on these compounds is to remove the lone-pair electrons completely from the HOMO, which follows our planar CH<sub>4</sub><sup>2+</sup> example. For example, the spirooctaplane dication, **2c**<sup>2+</sup> is a minimum in *D*<sub>2h</sub> symmetry,

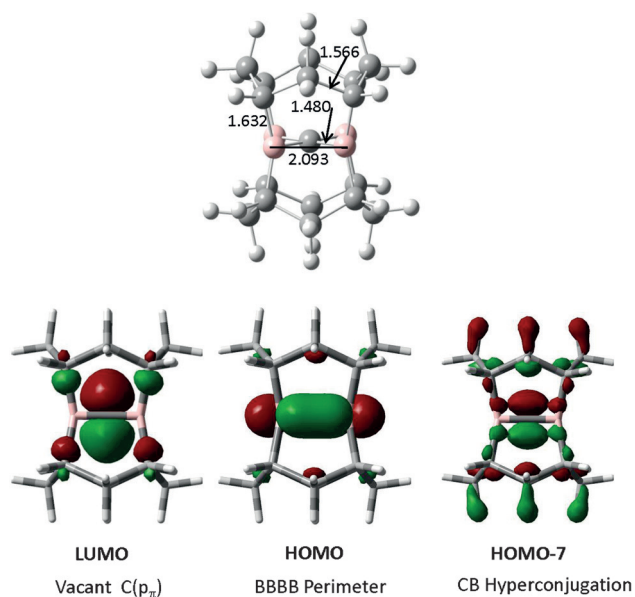


**Figure 9.** Octaboraplane and its key molecular orbitals.<sup>[10]</sup> The bond lengths are given in Å.

and the  $\pi$  orbital on the central carbon is the LUMO rather than the HOMO. Following the CH<sub>4</sub><sup>2+</sup> model, a family of neutral compounds called boraplanes (e.g. **9** Figure 9) was prepared.<sup>[10]</sup> The central carbon p orbital in **9** is formally vacant and is the LUMO, rather than the HOMO. The two “missing” electrons are accommodated in an energetically more favorable orbital, the 4c-2e BBBB perimeter HOMO.

To achieve more challenging C(C)<sub>4</sub>-type ptC arrangement, Wang and Schleyer developed “charge-compensation principle”.<sup>[30]</sup> Exemplified by **10a–j** (Figure 10), this principle uses two formal anionic -BH<sub>2</sub><sup>-</sup> groups to compensate the formal double positive charges on the ptC. In these compounds, the ptC  $\pi$  orbitals are the LUMOs. The “missing” electrons are utilized effectively for bonding. The HOMO of **10b** (shown in Figure 11) is an example. As a simple extension of Wang and Schleyer’s principle, in 2009, Wang<sup>[37]</sup> predicted several unsaturated pure and boron-substituted hydrocarbons containing a perfectly planar tetracoordinate carbon by means of a combined scheme: stabilized mechanically through the strain of a rigid cage framework, and electronically through the electron delocalization in a three-dimensional  $\pi$ -conjugated system.

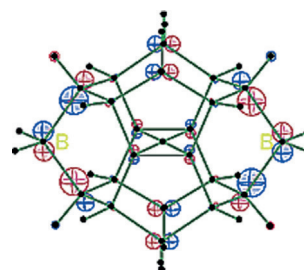


**Figure 11.** The HOMO<sup>[30]</sup> of **10b**. (Reprinted with permission from Ref. [30], Copyright 2002 American Chemical Society.)

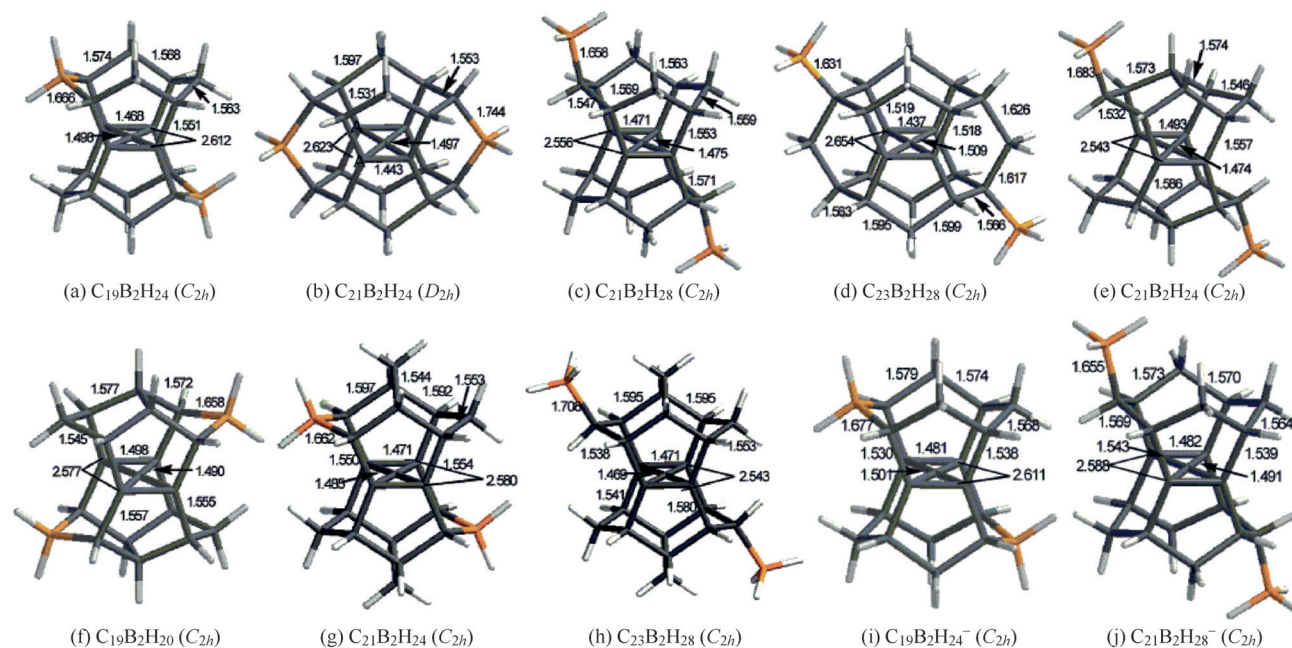


**Figure 10.** The calculated ptC motifs (a)–(j) using Wang–Schleyer’s charge-compensation principle.<sup>[30]</sup> The bond lengths are given in Å. (Reprinted with permission from Ref. [30], Copyright 2002 American Chemical Society.)

In contrast to the alkylanes, these new species have unambiguous, perfectly planar tetracoordinate C(C)<sub>4</sub> minima, and positively charged ptCs with much lower p-π occupancies. Although **10a-h** can be considered to be zwitterions, none of the atoms has a large positive or negative charge. The charges are spread out over the whole molecule. Consequently, in conceiving ptC candidates, it is more fruitful to base designs on the inherently planar methane dication as the parent, rather than on methane itself. However, note that these ptCs come from the synergy of the mechanical and electronic strategies. For example, C(BH<sub>2</sub>)<sub>4</sub> prefers C<sub>2v</sub> (**12a**) over D<sub>4h</sub> symmetry (**12b**). Using the same strategy to transform hemispiroalkylanes, such as **12c** failed.<sup>[16b,38]</sup> The HOMO of **12c** displays the spread out charge (Figure 12d).

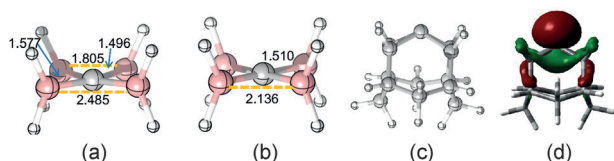
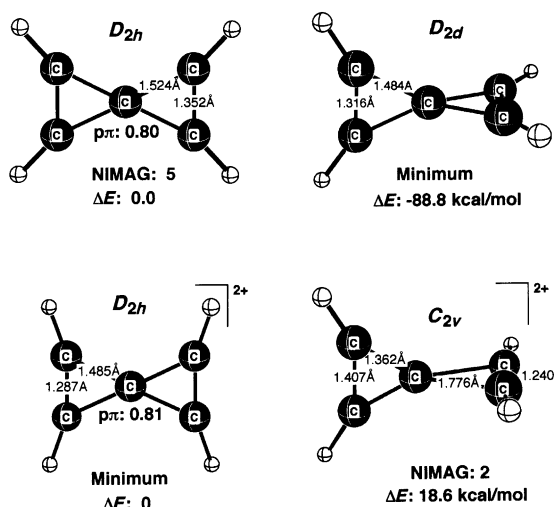
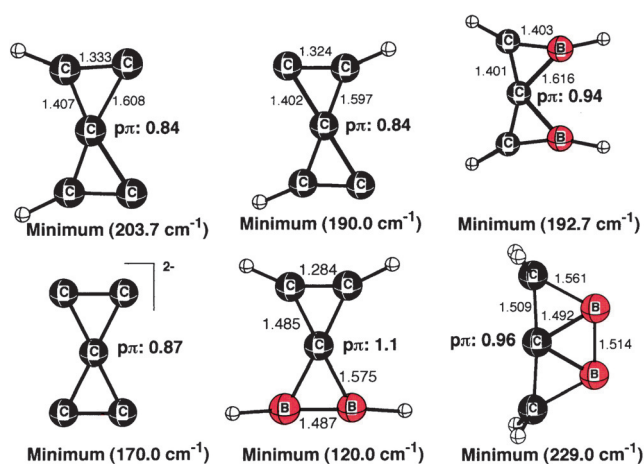


**Figure 12.** Calculated unsaturated pure and boron-substituted hydrocarbons featuring ptC and pyramidal configurations. (a) and (b) are from Ref. [10], (c, d) are from Ref. [12c]. The bond lengths are in Å.

Can we achieve ptC in hydrocarbons only using the electronic effect? The answer is definitely yes.<sup>[39]</sup> The removal of two electrons from spiropentadiene does lead to a perfect ptC arrangement (Scheme 5). The electron pair of the ptC atom is involved in two aromatic subsystems which stabilize the planar structure over its tetrahedral isomer. The same stabilization principle holds true for the isoelectronic analogues of C<sub>5</sub><sup>2+</sup> (Scheme 6). Fusing these basic ptC units with various mono- and bicyclic ring systems leads to many novel ptC compounds, such as **13a-n** (Figure 13). These species are characterized by central carbons with p-π occupancies around 1.0 e, close to the value in arenes.



**Scheme 5.** ptC stabilization principle of C<sub>5</sub>H<sub>4</sub> and related species.



**Scheme 6.** Isoelectronic analogues of C<sub>5</sub><sup>2+</sup>. The bond lengths are given in Å.

Using the stable spiropentadiene dication building block (D<sub>2h</sub> symmetry, C<sub>5</sub>H<sub>4</sub><sup>2+</sup>, Scheme 4)<sup>[39a]</sup> and the charge-compensation methodology,<sup>[40]</sup> neutral structures with a ptC (**14c-e**; Figure 14) were designed by Esteves and co-workers.<sup>[41]</sup> The planarity at the central carbon atom is achieved by using aromaticity to stabilize a positively charged core moiety. The neutrality is obtained by compensating the positively charged ptC core by negatively charged functional groups (such as HPO<sub>3</sub><sup>-</sup> in **14e**) or cyclopentadienyl rings (**14c** and **14d**). The same procedure can be applied to isoelectronic analogues, such as (**14g**). However, ring opening is an easy process with a small barrier. Therefore, the stability of the spiropentadiene dication and its derivatives needs further to be confirmed.

Some building blocks in Scheme 5 have also been employed to build ptC compounds. For example, using C<sub>5</sub><sup>2-</sup>, the smallest carbon cluster containing a ptC as the starting point, Vela and co-workers<sup>[42]</sup> designed a series of ptC compounds **15a-c** (Figure 15). Minkin and co-workers<sup>[43]</sup> found new building blocks similar to those in Scheme 5 and constructed **15d** and **15e**. Four cyclic hydrocarbons containing a ptC, including **13i-l**, were proposed by Merino and co-workers.<sup>[44]</sup> More isoelectronic analogues of the structures in Schemes 4 and 5 were designed by Sastry and co-workers.<sup>[45]</sup>

Subsequently, Merino and co-workers<sup>[44,46]</sup> reported a series of ptC-containing cyclic hydrocarbons (**16a-h**; Figure 16). These molecules were created by combining the C<sub>5</sub><sup>2-</sup> skeleton with cyclic hydrocarbon fragments. Almost at the same time, Esteves and co-workers<sup>[47]</sup> analyzed the spiropentadiene dication and concluded that the ptC is mainly stabilized by σ electrons and that the ptC has a negative charge. The total positive charge is spread along the skeleton structure. Moreover, the spiropentadiene dication has a 2.3 kcal mol<sup>-1</sup> activation barrier for ring opening. Following this work, the same group predicted and analyzed a class of tetrasubstituted derivatives of the spiropentadiene dication with ptC. However, owing to thermodynamic instability these ptC species will all be difficult to synthesize as they are all highly energetic local minima on the potential energy surface. Furthermore, these materials suffer from



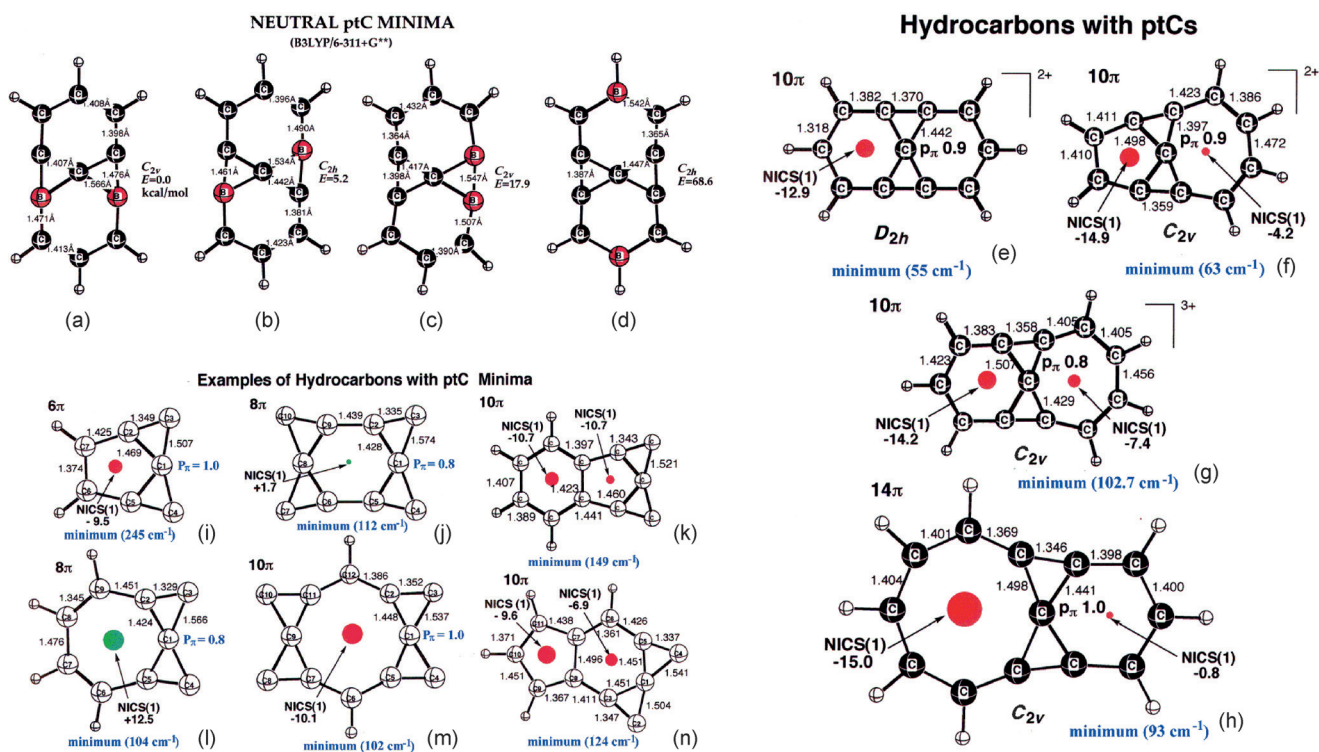


**Figure 13.** Calculated ptC motifs obtained by fusing basic ptC units with various mono- and bicyclic systems. The bond lengths are given in Å. The values of nucleus-independent chemical shifts (NICS) are given in ppm.

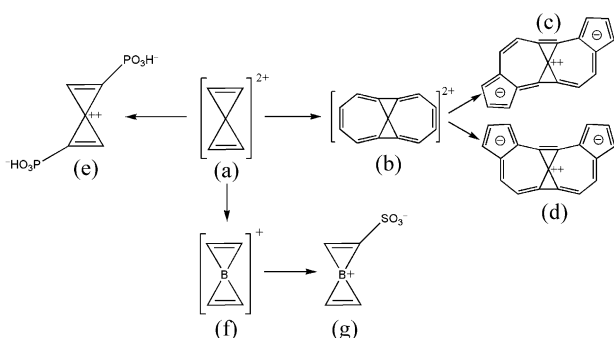


**Figure 14.** Calculated neutral ptC motifs based on  $C_5H_4^{2+}$  and isoelectronic  $BC_4H_4^+$  obtained as a result of aromaticity and compensation of the positively charged ptC core by negatively charged functional groups.

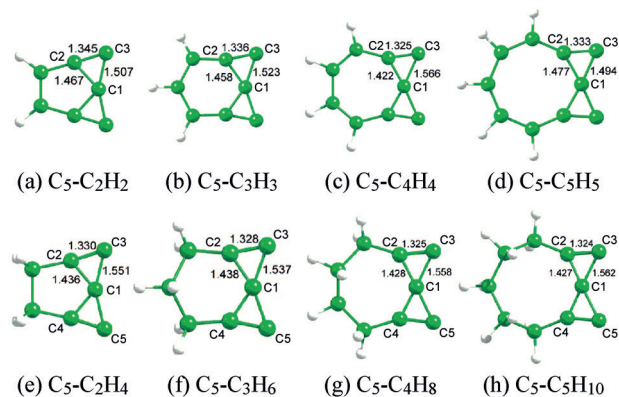


**Figure 16.** Calculated  $C_5^{2-}$  based hydrocarbons featuring ptC motifs.<sup>[46]</sup> The bond lengths are given in Å. (Reprinted with permission from Ref. [46], Copyright 2008 American Chemical Society.)

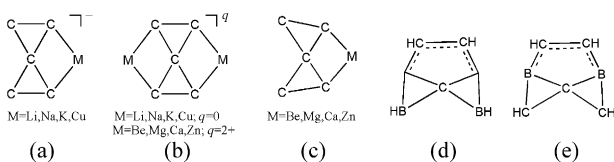


**Figure 15.**  $C_5^{2-}$  based ptC compounds (a–c) and  $C_3B_2$ -based ptC species (d,e).

instability caused by ring opening and structure rearrangement.

In 2008, Minyaev and Minkin<sup>[48]</sup> predicted a series of extended belt-like organoboron structures containing several

ptCs, such as **B1–B4** in Figure 17. Almost at the same time, on the basis of the building block  $C_3B_2H_4$  (neutral analogue of spiropentadiene dication), Zhang and Cao<sup>[49]</sup> predicted a series of ptC-containing tubular structures (**T1–T5** in Figure 17) and star-shaped species (see Figure 18). Some of the belt-shape ptC species are similar to the extended organoboron species investigated by Minyaev and co-workers.<sup>[48]</sup> The oligomers of diboraspriopentadiene featuring ptC motifs have been studied by Minkin and co-workers.<sup>[50]</sup> Moreover, several research groups have tested variants of boron-substituted spiropentadiene ( $C_5$ ) to probe the planar motifs (multi-ptC/B).<sup>[48–50]</sup> However, these “beautiful” planar

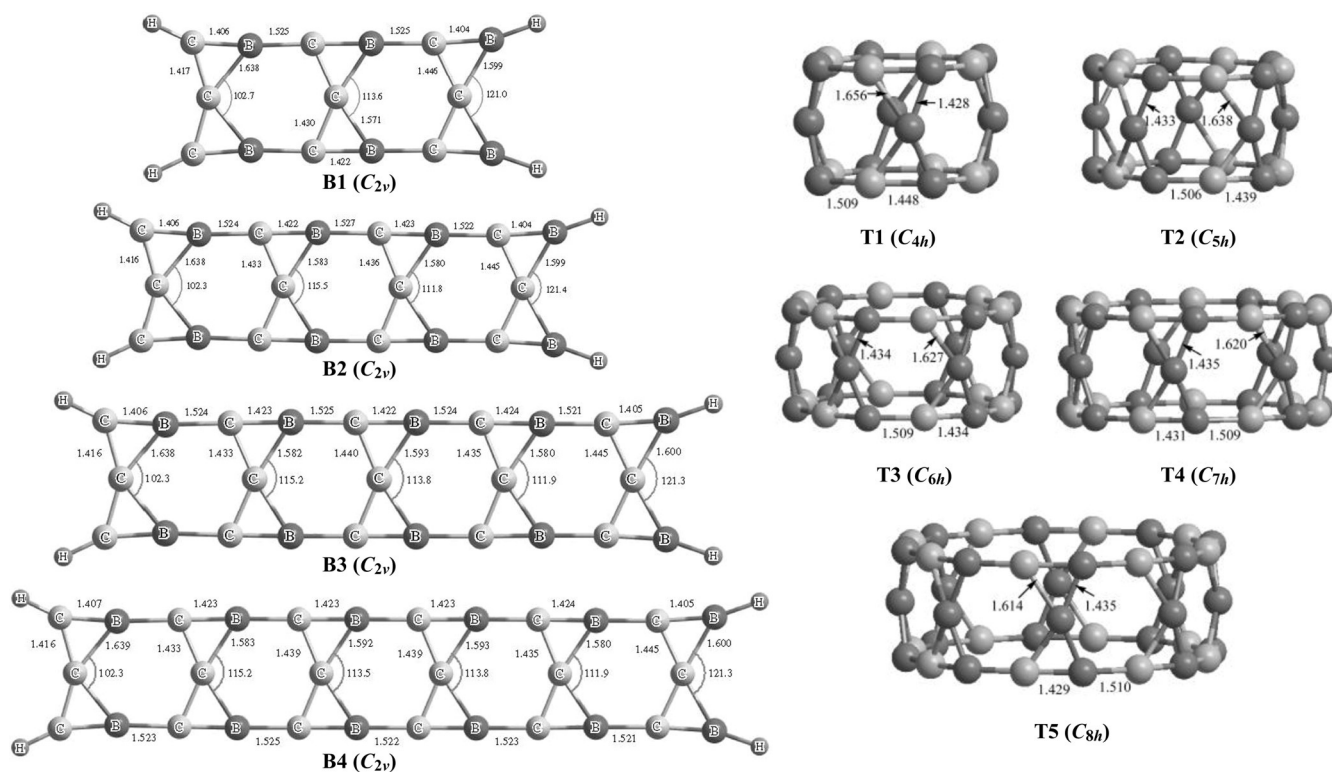


**Figure 17.** Calculated extended species featuring multiple ptC motifs in the belt forms (B1–B4)<sup>[48]</sup> and tubular forms (T1–T5)<sup>[49a]</sup> based on ptC unit  $C_3B_2$ . The bond lengths are given in Å. (Reprinted with permission from Ref. [48], Copyright 2008 Pleiades Publishing, Ltd. and from Ref. [49a], Copyright 2008 American Chemical Society.)

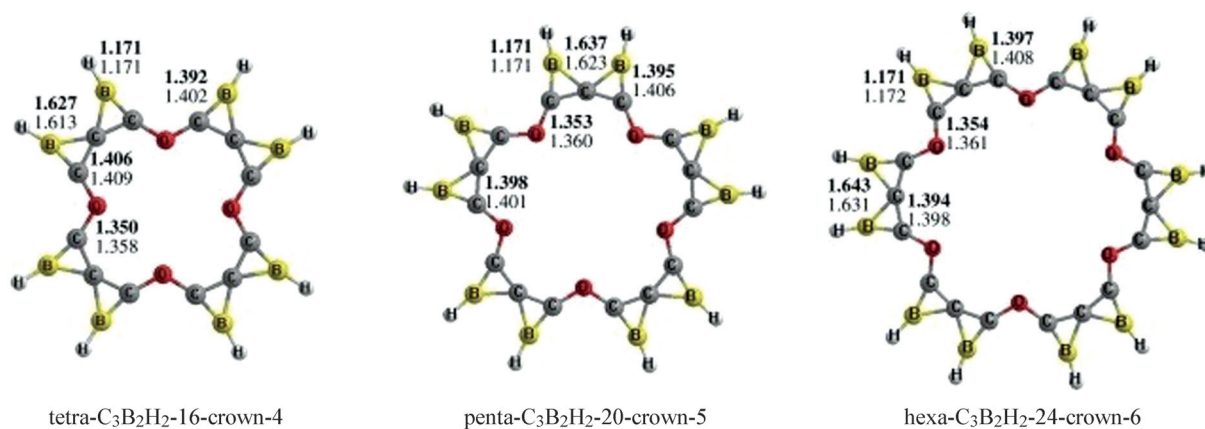


**Figure 18.** Calculated star-shaped multiple ptC species based on  $C_3B_2$ .<sup>[49b]</sup> The bond lengths are given in Å. (Reprinted with permission from Ref. [49b], Copyright 2009 Elsevier B.V.)

motifs are highly unstable, just high-energy local minima. This may make these materials difficult to synthesize.

Note that the carbon–boron mixed clusters ( $C_xB_y$ )<sup>[51]</sup> have been extensively studied during the search for planar carbon motifs during the past decade. The higher electronegativity of carbon compared to boron disfavors the hypercoordinate carbon forms.<sup>[51e–g]</sup>

In 2010, Wang, and co-workers computationally designed families of flat, tubular, and cage molecules containing ptC, which are assembled with “starbenzene” building blocks (i.e. **19a**) through hydrogen bridging bonds, as represented by

**19c–19e** (Figure 19). These structures are geometrically akin to graphenes, carbon nanotubes, and fullerenes, but have fundamentally different chemical bonds. The “starbenzene” monomer is a local minimum, and the fused polymers (e.g. **19c**) exhibit high thermodynamic stability because of the bridging bondings, implying the possibility for experimental realization. Extending the “starbenzene”, Wu and co-workers<sup>[52]</sup> further predicted the star-like aromatic  $C_5Al_5^-$  species (**19b**) which could be a global minimum for experimental synthesis.

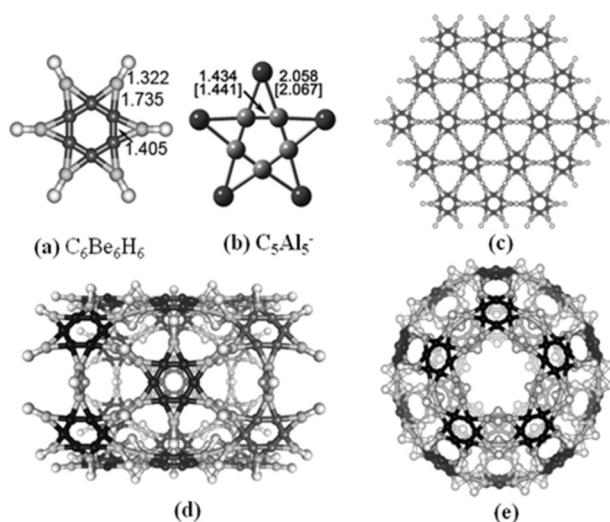


**Figure 19.** Calculated multiple ptC motifs based on starbenzene building blocks with hydrogen bonds.<sup>[53]</sup> The bond lengths are given in Å. (Reprinted with permission from Ref. [53], Copyright 2010 Wiley-VCH.)

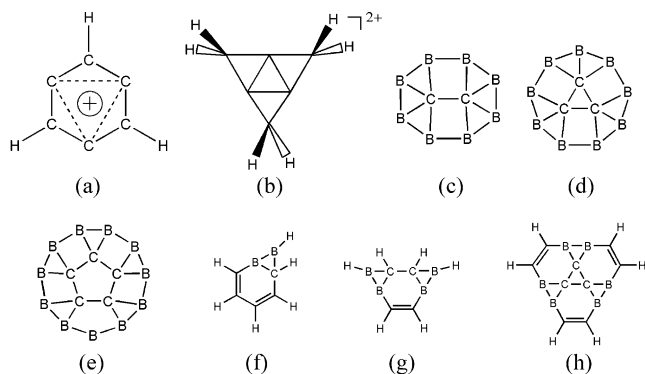


**Figure 20.** Calculated multiple ptC motifs inside boron and carborane rings.

More than one ptC can reside in a single molecule. The simplest is  $C_6H_3^+$  (**20a**,  $D_{3h}$  symmetry), whose ptCs participate in both the  $\pi$ -electron delocalization and the in-plane  $\sigma$ -delocalization.<sup>[54]</sup> This is a good example of “double aromaticity”.<sup>[54]</sup> Another simple example is the benzene dication isomer **20b** (Figure 20),<sup>[55]</sup> which contains three contiguous ptCs and is a local minimum on the potential-energy surface. More examples, such as **20c–e**, were designed by Frenking, Schleyer and co-workers.<sup>[51c]</sup> Using  $C_5^{2-}$  and its isoelectronic analogues (Scheme 5) as building blocks, Minyaev and co-workers<sup>[56]</sup> designed a series of stable structures with one, two, and three ptC centers (e.g., **20f–h**). They attributed the stability of these structures to a combination of electronic and steric effects, including 1) surrounding the C atom with  $\pi$ -accepting and  $\sigma$ -donating boron centers, 2) inclusion of carbon into strained three-membered aromatic rings, and 3) strong interligand attractive interactions between the peripheral ligating centers.

### 3.2. ptCs Based on the Planar Methane Model

Stimulated by the proposal of aromatic hydrocopper  $Cu_4H_4$  ( $D_{4h}$  symmetry),<sup>[57]</sup> Li and co-workers investigated the possibility of using d-block transition metals Cu and Ni to stabilize the ptC and other planar tetracoordinate elements including B, N, and O (Figure 21).<sup>[58]</sup> Although  $D_{4h}$ - $[BCu_4H_4]^-$

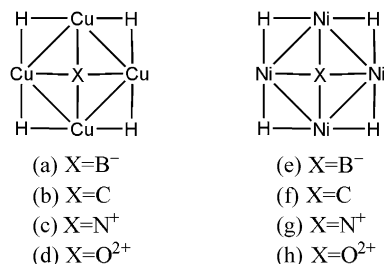


**Figure 21.** Calculated single ptC motifs enclosed by transition-metal hydride rings.

(**21a**) and  $D_{4h}$ - $CCu_4H_4$  (**21b**) are not local minima but transition states, other  $D_{4h}$  structures, such as  $XM_4H_4$  (**21c–h**), are true minima on the potential-energy surface. However, it is not clear whether these structures are the global minima or not. More planar molecules can be expected for the larger analogues (see Sections 4 and 5). Bridging of the above hydrometal complexes can lead to compounds containing double ptCs (see Figure 22).<sup>[59]</sup> However, all of the double ptC species predicted by Li and co-workers are only highly energetic local minima in a shallow well on the potential-

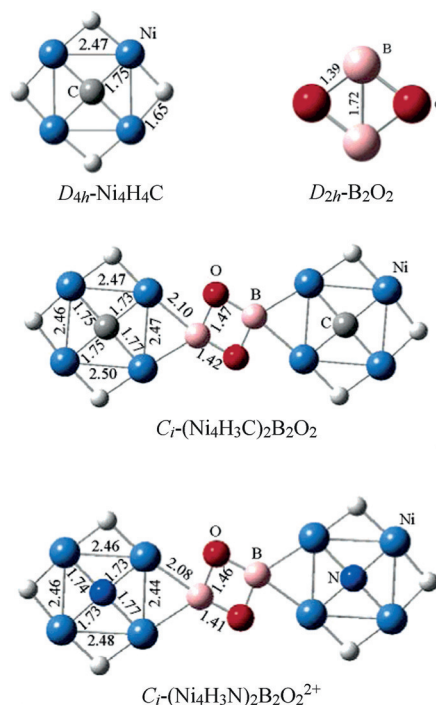


**Figure 22.** Calculated double ptC motifs based on the single ptC building blocks.<sup>[59]</sup> The bond lengths are given in Å. (Reprinted with permission from Ref. [59], Copyright 2005 American Chemical Society.)



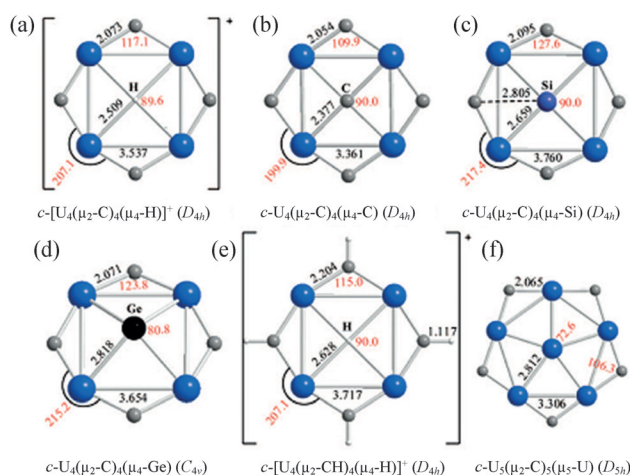
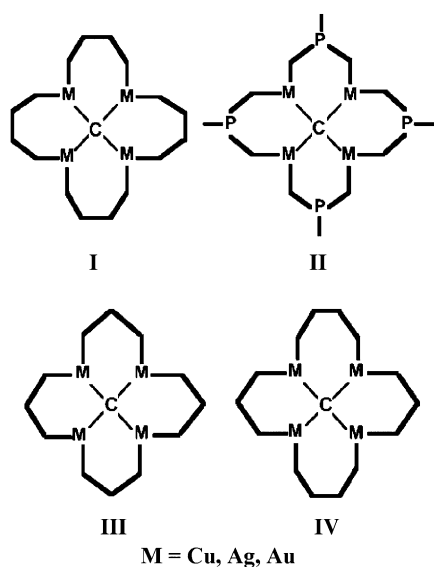


**Figure 23.** Computationally predicted planar motifs in  $E@[c-U_4(\mu_2-C)_4]$ , ( $E = H^+$ , C, Si, Ge) and  $U@[c-U_5(\mu_2-C)_5]$  molecules.<sup>[60]</sup> The bond lengths are given in Å. (Reprinted with permission from Ref. [60], Copyright 2008 American Chemical Society.)

energy surface, and are therefore very challenging to be synthesized experimentally because of their high instability.

Another type of cyclic ring cluster featuring planar motif centers was reported by Tsipis and co-workers<sup>[60]</sup> in 2008 (Figure 23). They predicted the planar isocyclic and heterocyclic uranium clusters (**23 a–f**), among which  $E@[c-U_4(\mu_2-C)_4]$  ( $E = H^+$ , C, Si, Ge; **23 a–e**) feature planar tetracoordinate motifs with central elements (H, C, Si) and distorted Ge. The planar pentacoordinate uranium motif in **23 f** will be discussed in the following Section on planar hypercoordinate transition-metal atoms and actinides. However, it is not clear whether these planar motifs are global minima or not.

Su<sup>[61]</sup> computationally studied twelve organometallic molecules containing Cu, Ag, and Au (Scheme 7) to determine if a central ptC atom is present. Model molecules **I** and

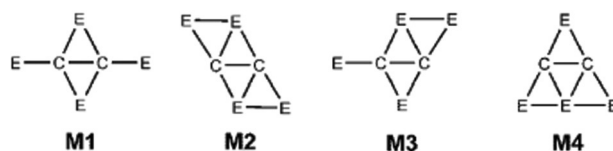


**Scheme 7.** Computationally designed ptC motifs enclosed by organometallic molecular rings.<sup>[61]</sup> (Reprinted with permission from Ref. [61], Copyright 2005 American Chemical Society.)

**II** have large cavities that can accommodate ptC atoms, and the exact planarity of the central carbon has been predicted by theoretical calculations. However, owing to the small size of the central cavity in **III** and **IV**, planar **M-III** and **M-IV** (except **Cu-III**) are not local minima, the central carbon atom is about 0.1–0.5 Å above the  $M_4$  plane.

The strong metal–ptC interactions (arising from the considerable electron transfer from the metal ligands to the more electronegative central ptC) together with the intermolecular metallophilic attractions are the main driving forces in maintaining the planarity of the above organometallic ptC species. In all these compounds, the central ptC atom has three  $sp^2$  hybridized chemical bonds and a nearly pure lone pair of  $2p_z$  electrons perpendicular to the  $M_4$  plane. This is in line with the HAW planar  $CH_4$  model which has a pure lone pair of  $2p_z$  electrons. There is also considerable electron transfer from the H ligands to the central C atom. The aromaticity in Li's series (Figure 21) also contributes to the stability of these unusual structures. In 2012, several (nearly) ptC configurations in small molecules have also been predicted by Crigger and co-workers.<sup>[62]</sup>

Carbon–aluminum binary clusters have attracted attention because of their non-classical structures and exotic chemical bonds. In 2008, Naumkin<sup>[63]</sup> explored the flat structural motifs in small aluminocarbon clusters  $C_nAl_m$  ( $n = 2–3$ ,  $m = 2–8$ ) using ab initio MP2 calculations. They identified some clusters featuring planar tetra- and hypercoordinate carbon motifs. On the basis of simple models potentially containing double ptC motifs, Wu and co-workers<sup>[64]</sup> predicted that the simplest neutral singlet  $C_2E_4$  ( $E = Al, Ga, In, \text{ and } Tl$ ; Scheme 8) is a global minimum with two ptCs.



**Scheme 8.** Simple models potentially containing double ptCs motifs, with  $E = Al, Ga, In, \text{ and } Tl$ .<sup>[64]</sup> (Reprinted with permission from Ref. [64], Copyright 2009 American Chemical Society.)

As a continuation of this work, Wang and co-workers<sup>[65]</sup> used a bifunctional scheme to extend  $C_2Al_4$  with two planar tetracoordinate carbons to a new class of ptC molecules (**24 a–h**; Figure 24).

#### 4. Planar Pentacoordinate Carbon

In 2001, Wang and Schleyer proposed the construction principles of “hyparenes” and designed families of molecules with planar pentacoordinate carbon (ppC).<sup>[51b]</sup>  $-CH-CH-CH-$  is a common fragment in arenes and allyls. Replacing some of the atoms in the traditional trigonal  $sp^2$  arrangement results in ppC building blocks, such as  $-C_3B_3-$  (type A),  $-C_2B_4-$  (type B), and  $-CB_5-$  (type C; Figure 25). With such building blocks, simple molecules (**25 a–c**) as well as elaborate aromatic and

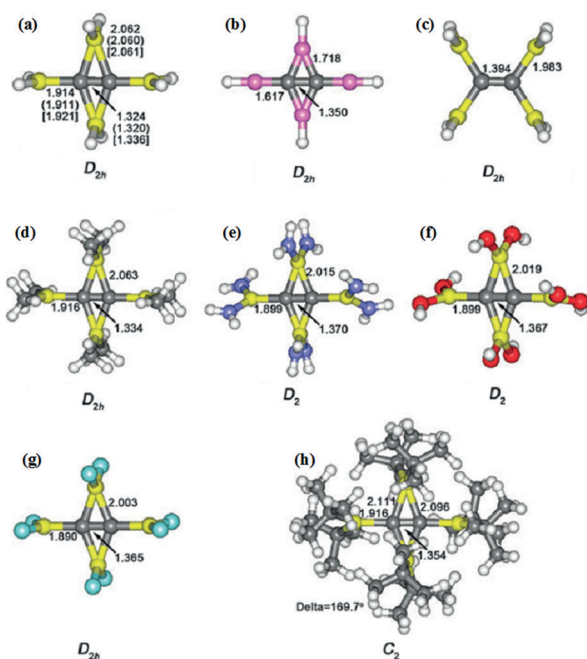


**Figure 24.** Computationally predicted double ptC species based on the skeleton of M1 in Scheme 8.<sup>[65]</sup> The point groups are listed underneath each structure. Atom colors, yellow Al, cyan F, red O, blue N, gray C, pink Be, and white H. (Reprinted with permission from Ref. [65], Copyright 2010 The Royal Society of Chemistry.)

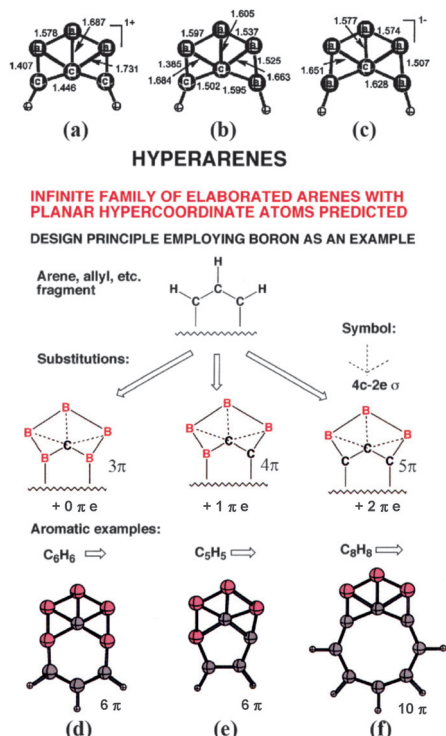


**Figure 25.** Design principles for ppC compounds.<sup>[51b]</sup> The bond lengths are given in Å. (Reprinted with permission from Ref. [51b], Copyright 2001 AAAS.)

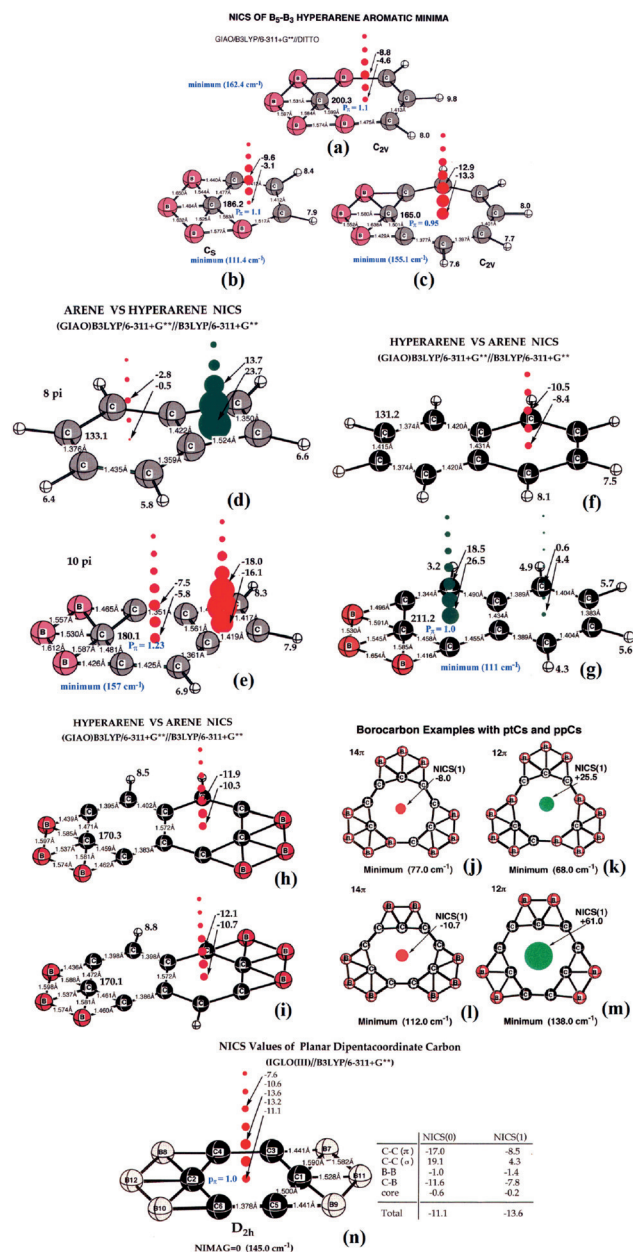


**Figure 26.** NICS (in ppm) grid plots of ppC compounds.<sup>[51b]</sup> (Reprinted with permission from Ref. [51b], Copyright 2001 AAAS.) The red and green colors denote negative (diatropic) and positive (paratropic) NICS values, respectively.

antiaromatic hydrocarbons can be created. We call these molecules “hyparenes” (hypercoordinated arenes). These hyperarenes include **25 a–f**, **26 a–c**, and **26 e–n** (Figure 26). All of these species have computed structures with normal bond lengths, vibrational spectra with no imaginary frequencies, and magnetic properties [nucleus-independent chemical shifts (NICS)] as well as proton chemical shifts<sup>[66]</sup> that reveal the aromatic or antiaromatic character of the individual rings. The planar pentacoordination results from multicenter bonding. The total Wiberg bond indices (WBI) for the central carbons are close to 4 demonstrating that the octet rule is not violated.

Most mono- and polycyclic aromatic (and even antiaromatic) species (which we generically call “arenes”) can be extended geometrically and electronically by the borocarbon groups of Type A, B, or C. Appropriately chosen, these extensions can maintain existing aromaticity (for example **25b**). Alternatively, they can convert antiaromatic into aromatic systems (for example Type C in **26e**) or vice versa (**26g**). Some ppC compounds, such as **26n**, can be more aromatic than benzene owing to the significant diatropic contribution from the multicenter C–B bonds.

Other rings involving atoms other than boron and carbon in the perimeters are also possible (Figure 27). For example,

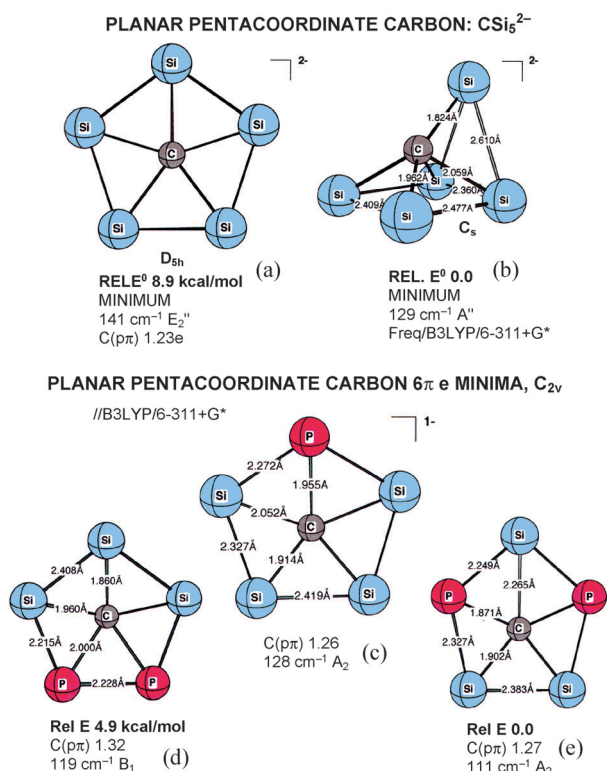


**Figure 27.** Calculated planar pentacoordinate carbon configurations in CSi<sub>5</sub><sup>2-</sup> (a and b), CSi<sub>4</sub>P<sup>-</sup> (c), and CSi<sub>3</sub>P<sub>2</sub> (d and e). The bond lengths are given in Å.

the  $D_{5h}$ -symmetric CSi<sub>5</sub><sup>2-</sup> dianion (**27a**), and its isoelectronic analogues  $C_{2v}$ -CSi<sub>4</sub>P<sup>-</sup> (**27c**) and  $C_{2v}$ -CSi<sub>3</sub>P<sub>2</sub> (**27d**, **27e**) are minima with ppCs at the B3LYP/6-311+G\* level of theory. However, they may not be global minima, because a detailed isomer search revealed that **27b** is 8.9 kcal mol<sup>-1</sup> lower in energy than **27a**. Note that the p–π occupation in these clusters is also a little larger than 1.0 e.

Building blocks similar to those in Figure 25 but based on ptC are also possible, and several examples are given in Figure 28. Integrating the ptC building blocks such as **28a** and **28b** into compounds can generate a large family of ptC compounds, such as **28c** and **28d**.

Inspired by the discovery of the aromatic M<sub>5</sub>(μ-H)<sub>5</sub> (M = Cu, Ag, Cu) hydrometal rings,<sup>[57,67]</sup> Li and co-workers extended their study on the planar tetracoordinate non-metal complexes<sup>[58]</sup> to pentacoordinate analogues.<sup>[68]</sup> A systematic theoretical investigation revealed that **29a–l** with

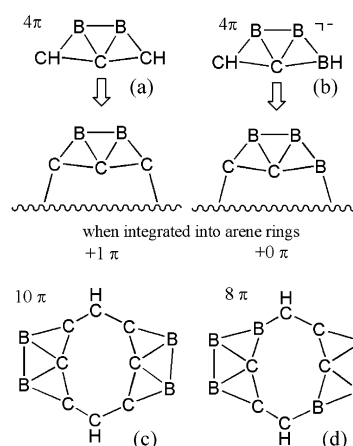


**Figure 28.** Design principles for ptC compounds.

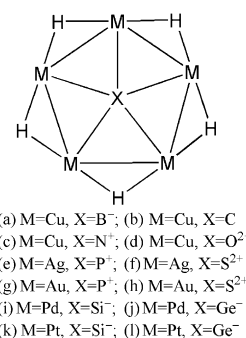


**Figure 29.** Planar pentacoordinate motifs centered in hydrometal M<sub>5</sub>H<sub>5</sub> rings.

planar pentacoordinate non-metal centers are local minima on the potential-energy surface (Figure 29). However, it remains unclear if these structures are the global minima or not. These species are aromatic in nature, as indicated by the large negative NICS values above the rings.<sup>[68]</sup> A similar type of structure U@[c-U<sub>5</sub>(μ<sub>2</sub>-C)<sub>5</sub>] (**23f**) was also predicted by Tsiapis and co-workers.<sup>[60]</sup>

In 2008, Zeng and co-workers<sup>[69]</sup> computationally identified the first global minimum planar pentacoordinate carbon in CAI<sub>5</sub><sup>+</sup> and examined its aromaticity (Figure 30). In 2010, Wang and co-workers used isoelectronic substitution (Be replaces Al) to design CAI<sub>4</sub>Be and CAI<sub>3</sub>Be<sub>2</sub><sup>-</sup> (**31a**, **31b**; Figure 31).<sup>[70]</sup> In 2012, Wu and co-workers predicted that ppC molecules CAI<sub>2</sub>Be<sub>3</sub><sup>2-</sup> and LiCAI<sub>2</sub>Be<sub>3</sub><sup>-</sup> (**31c**, **31d**) obtained by further substitution are global minima.<sup>[71]</sup> Similarly, Castro et al. reported the completely Be-substituted ppC motifs in CBe<sub>5</sub>E<sup>-</sup> (E = Al, Ga, In, Tl),<sup>[72]</sup> but the ppC global minima are only found for E = Al and Ga in the CBe<sub>5</sub>E<sup>-</sup> series.

## 5. Planar Hexa- and Higher Coordinate Carbon

In the previous Section, we have seen that numerous ptC and ppC compounds are feasible. Is it possible to get planar carbon with higher coordination? For example, can a planar carbon adopt hexacoordination and reside in the center of



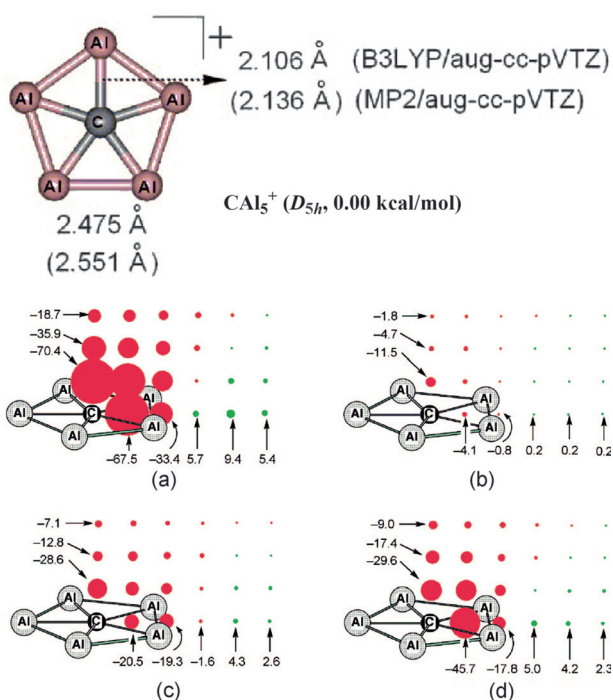


**Figure 30.** Predicted global minimum ppC  $\text{Al}_5^+$  and its aromaticity characterized by NICS (in ppm) plots (a–d).<sup>[69]</sup> (Reprinted with permission from Ref. [69], Copyright 2008 American Chemical Society.)

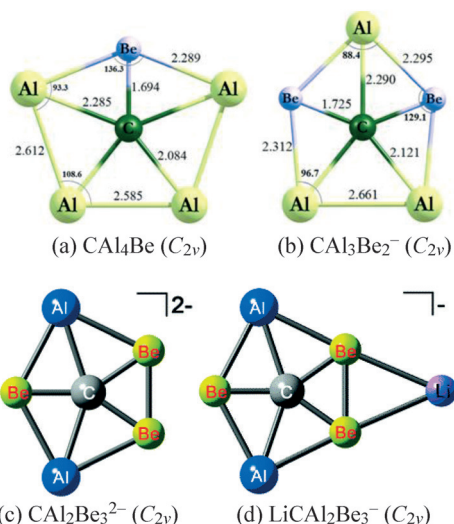


**Figure 31.** Predicted global ppC minima: a)  $\text{CA}_4\text{Be}$ , b)  $\text{CA}_3\text{Be}_2^-$ ,<sup>[70]</sup> c)  $\text{CA}_2\text{Be}_3^{2-}$ , d)  $\text{LiCA}_2\text{Be}_3^-$ .<sup>[71]</sup> The bond lengths are given in Å and angles in °. (Reprinted with permission from Ref. [70], Copyright 2010 The Royal Society of Chemistry; Ref. [71], Copyright 2012 American Chemical Society.)

a benzene ring? Many known compounds have hexacoordinate carbons, but they are involved in three-dimensional structures (see Figure 32).

As pointed out by Schleyer and Boldyrev in 1991,<sup>[20]</sup> the design of unusual molecular shapes requires the right fit of the constituent atoms, both geometrically and electronically. The interatomic distances must be in the normal ranges. The molecular orbitals patterns and degeneracies should be consistent with the molecular symmetry. Unusually high

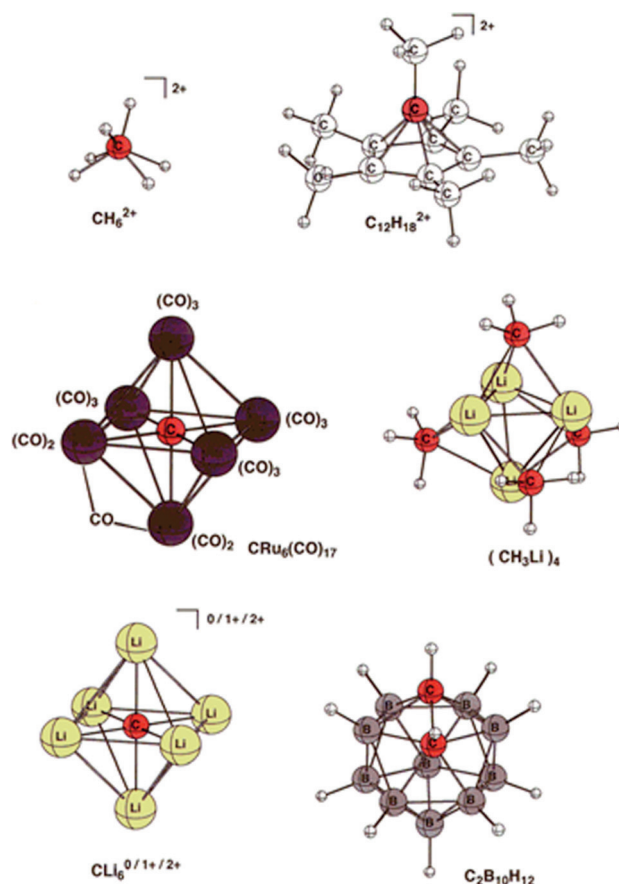


**Figure 32.** Some compounds with three-dimensional hexacoordinate carbons:  $\text{CH}_6^{2+}$ , Hogeveen's dication ( $\text{CCH}_3$ )<sub>6</sub>,  $[\text{CRu}_6(\text{CO})_{17}]$ , tetrameric  $\text{MeLi}$ ,  $\text{CLi}_6^{0/1+/2+}$ , and *ortho*- $\text{C}_2\text{B}_{10}\text{H}_{12}$ .<sup>[51a]</sup> (Reprinted with permission from Ref. [51a], Copyright 2000 AAAS.)

coordination of a central atom can best be achieved in cyclic systems or clusters in which all atom–atom contacts are bonding.

The first planar hexacoordinate carbon was achieved in 2000 by Exner and Schleyer in  $\text{CB}_6^{2-}$  (**33a**; Figure 33).<sup>[51a]</sup> In addition to the suitable size, there are no unfavorable orbitals populated in  $\text{CB}_6^{2-}$ . The HOMOs of **33g** are a degenerate  $\pi$  set ( $e_{1g}$ ), just like in benzene, and the third occupied  $\pi$  MO involving the p orbital at the central carbon ( $a_{2u}$ ) is low in energy.  $\text{CB}_6^{2-}$  is the first example of a six  $\pi$  aromatic molecule with a central hexacoordinate atom. Its aromaticity is confirmed by highly negative NICS values above the ring, and the diamagnetic  $\pi$ -ring current that circulates the molecule undisturbed by the central carbon atom.<sup>[73]</sup>

Neutral closed-shell carbon–boron systems with phC are also possible. All the heavy atoms in the doubly protonated  $\text{CB}_6\text{H}_2$  (**33b**) lie very nearly in a plane. Isoelectronic analogues of  $\text{CB}_6^{2-}$ , **33c–f**, all with phCs, are local minima. Compound **33f** has a hexacoordinate boron atom, is also a local minimum, and is 38.4 kcal mol<sup>−1</sup> lower in energy than the lowest energy phC isomer (**33e**) at B3LYP/6-311 + G\*. Although **33c–e** are not the lowest-energy isomers, and can rearrange to more stable isomers, the barriers should be sufficiently high to permit their experimental observation.

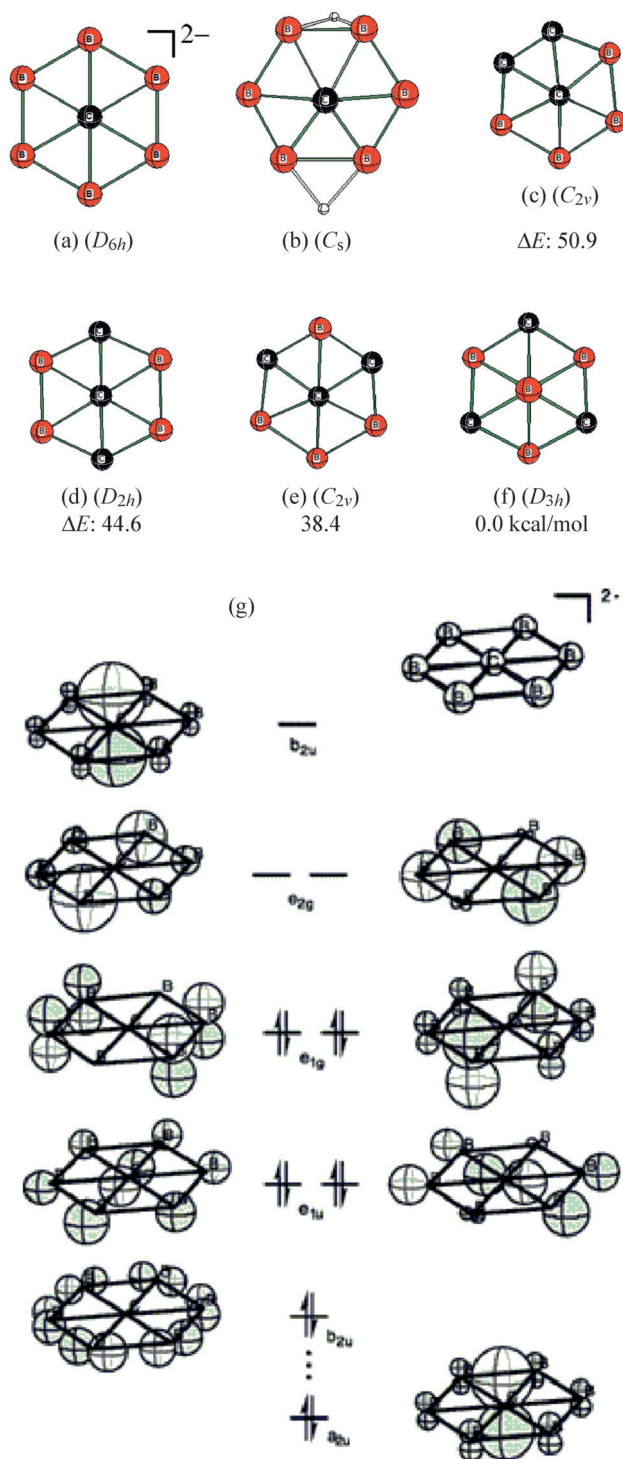


**Figure 33.** Predicted planar hexacoordinate carbon  $CB_6^{2-}$  (a), its protonated form (b), and isoelectronic species  $C_3B_4$  (c–f), orbital diagram (g). The MO Scheme for  $CB_6^{2-}$  with planar hexacoordinate carbon (at the B3LYP/6-311 +  $C^*$  level). The six  $\pi$  electrons are delocalized in the  $a_{2u}$  symmetric MO involving the p orbital on the central carbon and the two degenerate highest occupied MOs ( $e_{1u}$  symmetry).<sup>[51a]</sup> (Reprinted with permission from Ref. [51a], Copyright 2000 AAAS.)

A family of wheel-shaped molecules which contain quasi-planar penta- and hexacoordinate carbons (or isoelectronic

atoms, such as  $B^-$ ,  $Al^-$ , Si, or Ge) can also be formed by face-to-face conjugation of two units of two planar heptacoordinate (or hexacoordinate) carbon (or isoelectronic) atoms (**34a–l**).<sup>[74]</sup> The wheel isomers (W), but not the regular polyhedral (P) isomers follow Wade's rule *closo*.<sup>[75]</sup> Taking  $C_2B_{12}H_{12}$  (W) (**34a**) for example, its internal axial bond is characterized by a short C–C separation (1.597 Å), and a bonding HOMO (Figure 34m). However,  $C_2B_{12}H_{12}$  (**34b**) structures in the polyhedral singlet (PS) biradical or triplet states have long C–C separations, and have nonbonding HOMOs (Figure 34n), thus Wade's rule *closo* is not followed if the two unpaired electrons are added to the skeletal-electron-pair count.

Though the axial C–C bonding favors wheel-shapes, the concomitant cage increases the strain which destabilizes the wheel form. The competition between these two factors determine whether a W or a P isomer is favored. Except for **34c** and **34g**, W isomers are energetically favored over P isomers. To increase the relative stability of W over P isomers, the cage bonding, or the cage deformation strain of W isomers has to be reduced. This can be realized by electronegative substituents, such as fluorine atoms, as in **34e**, **34f**, **34k**, and **34l**.

As a follow-up study of the original work on  $CB_6^{2-}$ , Schleyer and co-workers<sup>[76]</sup> investigated the possibility of using  $CB_6^{2-}$  as a building block. They designed myriad planar hexacoordinate carbon molecules inviting synthesis (see Figure 35). Furthermore, the boron rings enclosing planar hypercoordinate Group 14 elements have been studied by Merino and co-workers.<sup>[51d]</sup> They found several planar hypercoordinate wheels as local minima.

Inspired by the breakthrough in phC, several groups focused on the prediction of compounds containing  $CB_6^{2-}$ . Li and co-workers<sup>[77]</sup> predicted the main-group metallocene-like complexes  $K[(\eta^6-B_6C)Ca]_n(\eta^6-B_6C)K$  ( $n=1-3$ ) and  $[(\eta^6-B_6C)Ca]_n(\eta^6-B_6C)^{2-}$  ( $n=1, 2$ ), as well as the related pyramidal  $[(\eta^6-B_6C)M]^{i-}$  ( $M=Na, K$ , and  $CaCl$ ,  $i=1$ ;  $M=Ca$ ,  $i=0$ ) and bipyramidal  $(\eta^6-B_6C)(CaCl)_2$  (see Figure 36), which involve phC-containing  $\eta^6-B_6C^{2-}$  ligands. Note that the pyramidal half-sandwich is unstable owing to the transformation into low-lying isomers from the viewpoint of thermodynamics. Furthermore, the metallocene-like complexes are quite unstable because of the strong tendency of  $CB_6^{2-}$  ligands to fuse (see details in Section 7). Shahbazian and co-workers<sup>[78]</sup> predicted the metal complexes of  $CB_6^{2-}$ , that is,  $[M(B_6C)]^-$  ( $M=Li, Na, K$ ) and ( $M=Be, Mg, Ca$ ) as viable targets for gas-phase synthesis. However, these materials may be difficult to prepare owing to their high instability and transformation into other low-lying isomers.

All the above mentioned phC species are only local minima. Recently, the first global minimum phC molecule,  $CO_3Li_3^+$  ( $D_{3h}$ ) (Figure 37), was found by Wu, Wang and co-workers after searching the viable candidates.<sup>[79]</sup> They also predicted another possible candidate  $CN_3Be_3^+$  ( $D_{3h}$ ), a deeply-lying kinetically viable local minimum.

Note that boron rings have been widely used to design planar hypercoordinate motifs by enclosing both main-group and transition-metal elements. The mixed carbon–boron clusters  $C_xB_y$  have been extensively studied to probe the



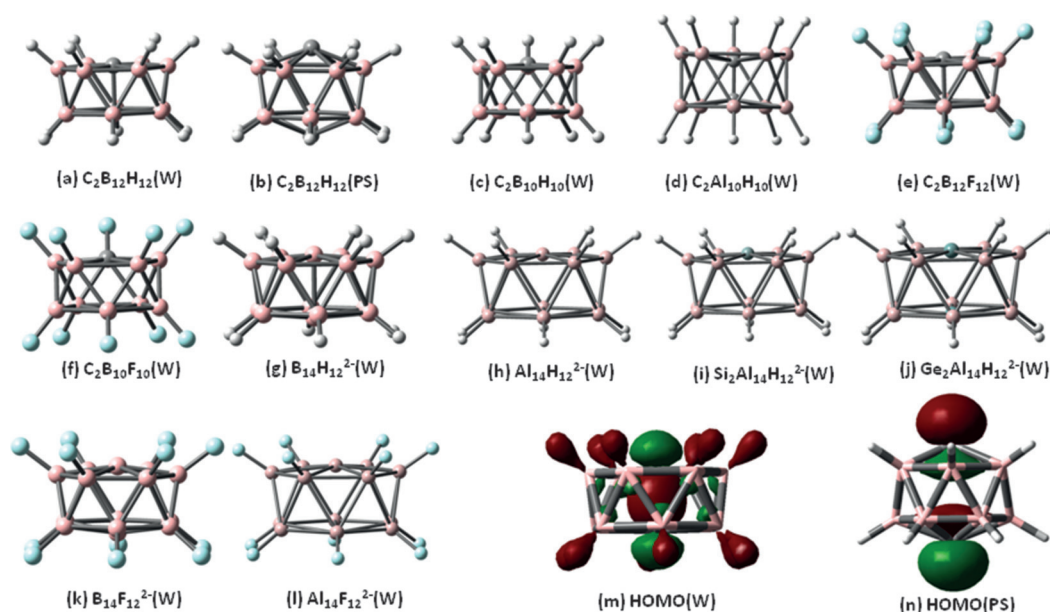


**Figure 34.** A family of wheel-shaped molecules containing nearly penta- and hexacoordinate carbons and isoelectronic species (a–l) have been predicted. Comparison of the HOMOs of (a) and (b) are also shown in (m) and (n). Structures replotted based on Ref. [74].

possible planar configurations. Both experimental and theoretical work demonstrate that the higher electronegativity of carbon compared to boron disfavors the hypercoordinate carbon forms.<sup>[51e–g,k]</sup> For example, for  $\text{CB}_6^-$ ,  $\text{CB}_6^{2-}$ ,  $\text{C}_2\text{B}_5^-$ ,<sup>[51f]</sup>  $\text{CB}_7^-$ ,<sup>[51e]</sup>  $\text{CB}_8^-$ ,<sup>[51g]</sup>  $\text{CB}_9^-$ , and  $\text{C}_2\text{B}_8^-$ ,<sup>[51k]</sup> the global minima prefer other locations for carbon atom(s) rather than central positions with the highest possible hypercoordination.

The size of the central atom in the

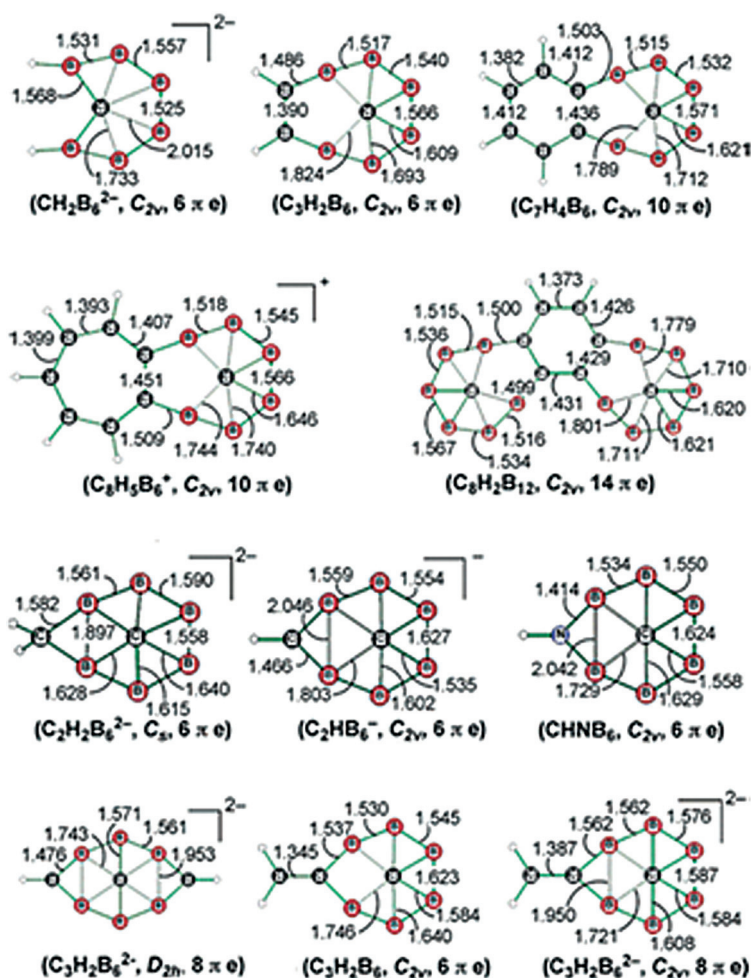


**Figure 35.** Examples of  $\text{CB}_6^{2-}$ -based phC molecules. Bond lengths are shown in Å. Structures replotted based on Ref. [76].

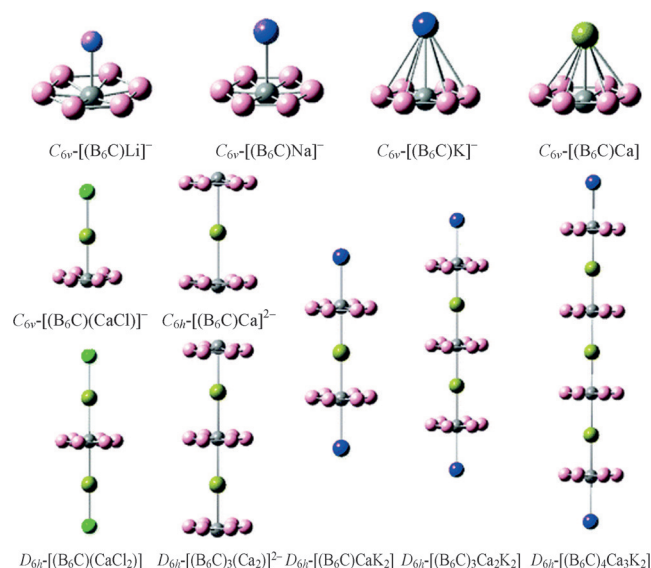


**Figure 36.** Optimized structures of  $C_{6v}[(\eta^6\text{-B}_6\text{C})\text{M}]^-$  ( $\text{M} = \text{Li}, \text{Na},$  and  $\text{K}$ ),  $C_{6v}[(\eta^6\text{-B}_6\text{C})\text{Ca}]$ ,  $C_{6v}[(\eta^6\text{-B}_6\text{C})\text{CaCl}]^-$ ,  $D_{6h}[(\eta^6\text{-B}_6\text{C})(\text{CaCl})_2]$ ,  $D_{6h}[(\eta^6\text{-B}_6\text{C})_{n+1}\text{Ca}_n]^{2-}$  ( $n = 1$  and  $2$ ), and  $D_{6h}[(\eta^6\text{-B}_6\text{C})_{n+1}\text{Ca}_n\text{K}_n]$  ( $n = 1, 2,$  and  $3$ ).<sup>[77]</sup> (Reprinted with permission from Ref. [77], Copyright 2007 American Chemical Society.)

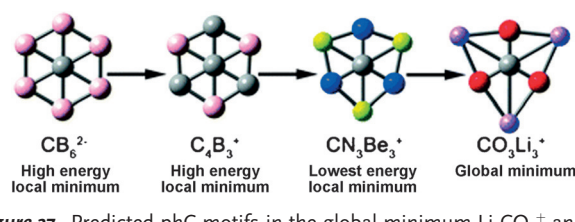


**Figure 37.** Predicted phC motifs in the global minimum  $\text{Li}_3\text{CO}_3^+$  and low-lying  $\text{CN}_3\text{Be}_3^+$ .<sup>[79]</sup> (Reprinted with permission from Ref. [79], Copyright 2012 The Royal Society of Chemistry.)

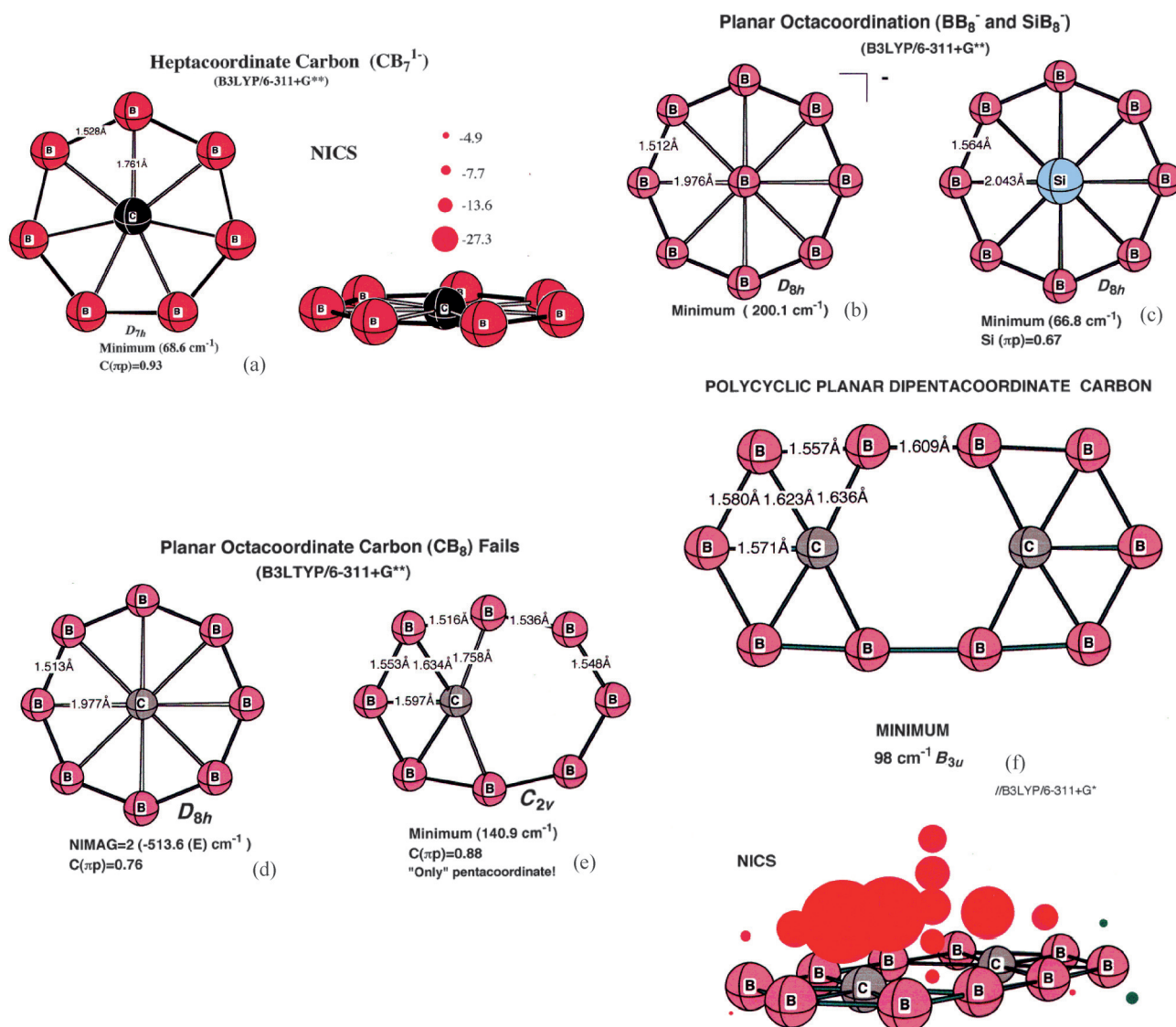


**Figure 38.** The optimized structures containing planar heptacoordinate carbon, planar octacoordinate carbon, boron, and silicon species, and the NICS (in ppm) plot of **38 f**.<sup>[51b]</sup> (Reprinted with permission from Ref. [51b], Copyright 2001 AAAS.)

boron ring is crucial to achieve planar hypercoordinate carbon or other planar hypercoordinate elements. For example, planar heptacoordinate carbon can be realized in  $D_{7h}$ - $B_7C^-$  (**38a**).  $D_{8h}$ - $B_9^-$  (**38b**) and  $D_{8h}$ - $B_8Si$  (**38c**) are local minima with planar octacoordinate boron and silicon (Figure 38). However, the  $B_6$  ring will not accommodate a central boron atom, and  $B_7^-$  adopts pyramidal structures.<sup>[80]</sup> Similarly, the carbon atom is too small to achieve good bonding to all eight boron atoms simultaneously, thus  $D_{8h}$ - $B_8C$  (**38d**) is a transition state, and distorts to a  $C_{2v}$  structure with a planar pentacoordinate carbon (**38e**). A polycyclic planar dipentacoordinate carbon compound (**38f**) is also predicted.

This concept can be extended to other elements as well. For example, planar boron-ring-based molecules,  $B_8^{2-}$  and  $B_9^-$  were detected in laser vaporization experiments.<sup>[81]</sup> This was the first experimental observation of hepta- and octacoordinate boron atoms. The chemical bonding analysis reveals that

the double ( $\sigma$  and  $\pi$ ) aromaticity is responsible for the wheel structures and the extreme coordination environments in  $B_8^{2-}$  and  $B_9^-$ . The molecular wheel  $B_8^{2-}$  was also experimentally detected as an inorganic ligand in  $LiB_8^-$  and its high stability suggests that it may be used as a new building block in chemistry.<sup>[82]</sup> Other planar hypercoordinate species await future experimental investigation. Recently, Chen and co-workers<sup>[83]</sup> predicted a series of  $M@B_n$  boron wheels to be local minima rather than global minima, except for triplet  $Be@B_8$  planar wheel which is a global minimum.

Using a similar procedure, Minyaev, Minkin, and co-workers<sup>[84]</sup> discovered planar hexacoordinate carbon and boron compounds **39a–f** (Figure 39), planar heptacoordinate carbon and nitrogen compounds  $B_7C^-$  (**38a**),  $B_7N$ , and their isoelectronic analogue  $B_6C_2$  (**39f**), and planar octacoordinate silicon and phosphorus compounds  $B_8Si$  (**38c**) and  $B_8P^+$ . Moreover, Park<sup>[85]</sup> computed various isomers of  $B_7C^-$  and its isoelectronic species  $B_6C_2$  and  $B_5C_3^+$ , and found their most



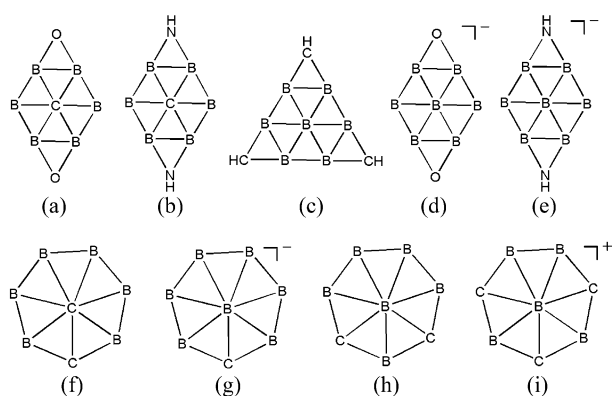


**Figure 39.** Predicted planar hexa- and heptacoordinate carbon and boron compounds.

stable isomers **39 g–i**. The energy differences are  $60.7 \text{ kcal mol}^{-1}$  between **39 g** and **38 a**, and  $60.2 \text{ kcal mol}^{-1}$  between **39 h** and **39 f**, respectively.

In 2009, the Wang and Boldyrev groups<sup>[51g]</sup> demonstrated the rational design of hypercoordinated planar chemical species using the adaptive natural density partitioning (AdNDP) method<sup>[86]</sup> which assesses delocalized bonding in chemical species. This method leads to partitioning of the charge density into elements with the highest possible degree of localization of electron pairs. If some part of the density cannot be localized in this manner, it is represented using completely delocalized objects, similar to canonical MOs, naturally incorporating the idea of delocalized bonding, such as  $n$ -center two-electron ( $nc$ - $2e$ ) bonds. Thus, AdNDP achieves a seamless description of different types of chemical bonds and has been applied recently to different chemical systems. The analysis explains why the  $B_9^-$  (**40 a**) cluster is a doubly aromatic high-symmetry wheel structure, while  $AlB_9$  (**40 c**) and  $FeB_9^-$  (**40 d**) species with octacoordinate Al and Fe are global minima or low-lying isomers. This analysis also explains why carbon atoms fit well into the central cavity of  $CaI_4^{2-}$  (**40 b**; Figure 40) and  $CaI_5^+$  (Figure 30). They suggested that to design a chemical species with a central hypercoordinate carbon atom, electropositive ligands, which would have lone pairs instead of  $2c$ - $2e$  peripheral bonds.

## 6. Other Planar Tetracoordinate (or Hypercoordinate) Elements

### 6.1. Boron

In addition to the planar hypercoordinate boron atoms, such as  $B_7^-$ ,  $B_8^{2-}$ , and  $B_9^-$  (see Section 5), many other planar hypercoordinated boron compounds have been theoretically and experimentally examined.<sup>[87]</sup> The groups of Boldyrev and Wang have published a series of theoretical/experimental papers on small boron clusters  $B_3^-$ – $B_{24}^-$  (see Figure 41).<sup>[87a]</sup> Starting with planar clusters,  $B_5^-$ ,<sup>[88]</sup>  $B_6^-$ ,<sup>[89]</sup>  $B_7^-$ ,<sup>[80]</sup>  $B_8^-$  and  $B_9^-$ ,<sup>[81]</sup> in 2003, Wang and co-workers prepared planar (or quasi-planar) clusters  $B_{10}^-$  to  $B_{15}^-$ .<sup>[90]</sup> All-boron aromatic clusters are potential new inorganic ligands and building blocks in chemistry.<sup>[87b]</sup> The work on all-boron bare clusters demonstrates that these anions have planar structures from  $B_3^-$  to  $B_{24}^-$ .<sup>[87a]</sup> Remarkably, even larger all-boron clusters, including quasiplanar structures, namely chiral  $B_{30}^-$ <sup>[91]</sup> and  $B_{35}^-$ <sup>[92]</sup> with a double-hexagonal vacancy (Figure 42) as well as a planar hexagonal  $B_{36}^-$ <sup>[93]</sup> (Figure 43), have been detected in the gas-phase and characterized by photoelectron spectroscopy and ab initio calculations.

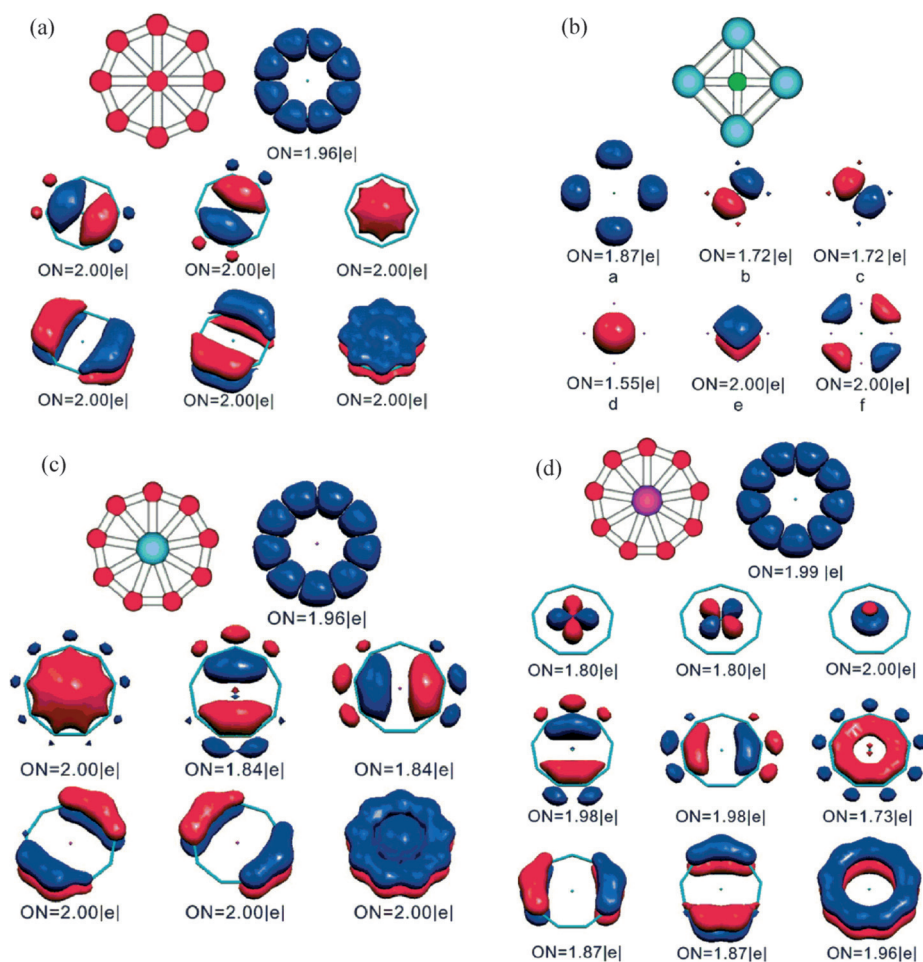


**Figure 40.** The chemical bonding analysis for  $B_9^-$  (a),  $CaI_4^{2-}$  (b),  $AlB_9$  (c), and  $FeB_9$  (d), all calculated by AdNDP analysis.<sup>[51g]</sup> (Reprinted with permission from Ref. [51g], Copyright 2009 The Royal Society of Chemistry.)

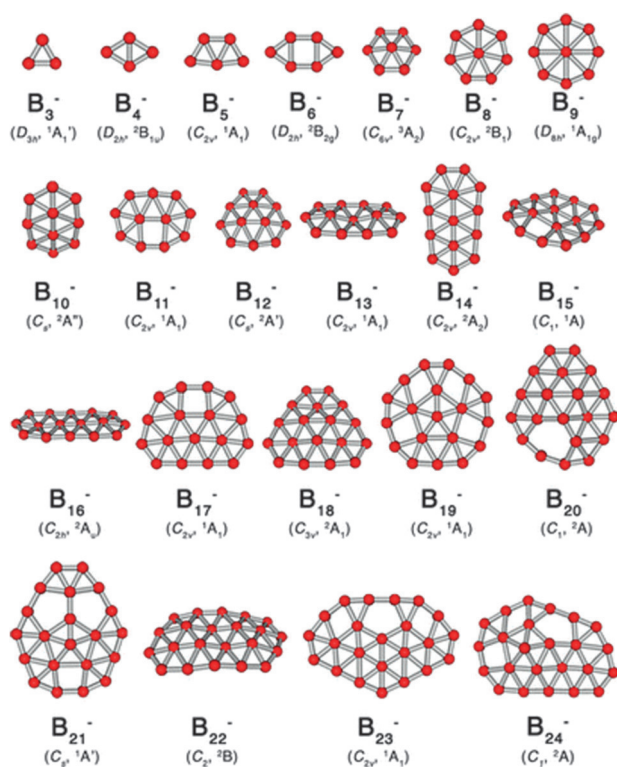


**Figure 41.** The lowest-energy structures calculated for  $B_3^-$  through  $B_{24}^-$ .<sup>[87a]</sup> The point group and electronic configuration of the ground-state structures are in parentheses. (Reprinted with permission from Ref. [87a], Copyright 2014 American Chemical Society.)

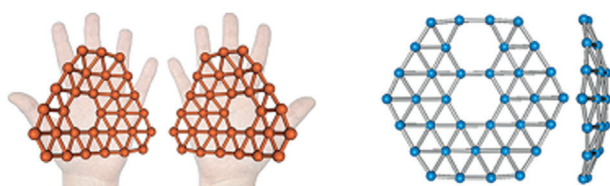


**Figure 42.** The observed quasiplanar boron clusters: chiral  $B_{30}^-$  (left)<sup>[91]</sup> and  $B_{35}^-$  (right) with a double-hexagonal vacancy.<sup>[92]</sup> (Reprinted with permission from Ref. [91], Copyright 2014 Wiley-VCH and Ref. [92], Copyright 2014 American Chemical Society.)

All-boron clusters have a rich chemistry. In particular,  $B_8^{-,2-}$ ,<sup>[81]</sup>  $B_9^{-}$ ,<sup>[81]</sup>  $B_{10}$ ,  $B_{11}^-$ , and  $B_{12}$ <sup>[90]</sup> can be viewed as analogues of benzene on the basis of their six  $\pi$  electrons, because they have  $\pi$ -molecular orbital patterns similar to those of benzene. A perfectly planar  $B_{16}^{2-}$  ( $D_{2h}$ )<sup>[94]</sup> with 10  $\pi$  electrons can be considered an all-boron naphthalene. Also, three neutral boron clusters  $B_{11}$ ,  $B_{16}$ , and  $B_{17}$  are shown to have planar or quasi-planar structures by vibrational spectroscopy and ab initio calculations.<sup>[95]</sup>  $B_{17}^-$  and  $B_{18}^-$ <sup>[96]</sup> have been predicted to be planar or quasi-planar.

Furthermore, a concentric planar doubly  $\pi$ -aromatic  $B_{19}^-$  cluster has been experimentally detected.<sup>[97]</sup> This ‘‘aromatic Wankel motor’’<sup>[98]</sup> contains two concentric  $\pi$  systems, with two  $\pi$  electrons delocalized over the central pentagonal  $B_5$  unit, and another ten  $\pi$  electrons responsible for the bonding between the central pentagonal unit and the outer ring. Such

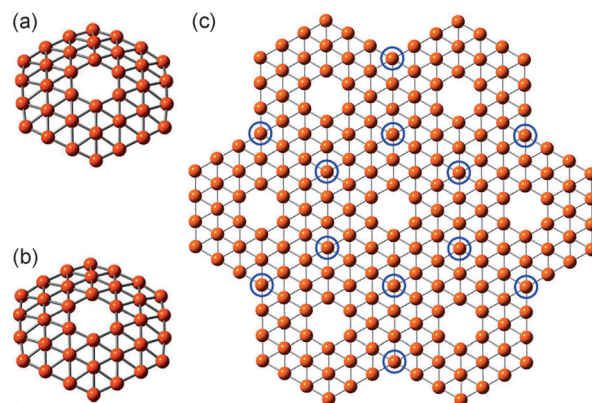


**Figure 43.** Calculated structure of a)  $B_{36}^-$  and b)  $B_{36}$ , and c) proposed extended boron sheets based on  $B_{36}$  units.<sup>[93]</sup> (Reprinted with permission from Ref. [93], Copyright 2014 Macmillan Publishers Ltd: Nature Communications.)

peculiar chemical bonding does not exist in organic compounds, it is only found in clusters.

With increasing numbers of atoms, the geometric structure will evolve from planar or quasi-planar (2D) to three dimensional (3D). Interestingly,  $B_{20}^-$ <sup>[99]</sup> and  $B_{21}^-$ <sup>[100]</sup> are still planar.  $B_{22}^{2-}$  and  $B_{23}^-$  can be considered to be boron analogues of anthracene and phenanthrene.<sup>[101]</sup> Note that the energies of quasi-planar and 3D tubular structures are quite close for  $B_{20}^-$ <sup>[99]</sup> and  $B_{22}^-$ ,<sup>[101]</sup> and it was suggested that the 2D–3D structural transition would occur at  $B_{20}$ .<sup>[99]</sup> However,  $B_{24}^-$ <sup>[102]</sup> (Figure 41),  $B_{30}^-$ ,<sup>[91]</sup> and  $B_{35}^-$ <sup>[92]</sup> (Figure 42) were characterized to be quasi-planar, whereas  $B_{36}^-$ <sup>[93]</sup> (Figure 43) was confirmed to be planar hexagonal and proposed as a basis for extended single layer boron sheets. Interestingly, the very recent joint experimental and theoretical investigations by Wang and co-workers led to the discovery of borospherenes  $B_{39}^-$ <sup>[103]</sup> and  $B_{40}^-$ ,<sup>[104]</sup> which provide evidence for the structure transition from 2D to 3D. However, the exact number of boron atoms for the transition from 2D to 3D is a tricky question since the motifs of boron clusters are very sensitive to the charge states, spin multiplicity, and number of atoms. The structure of large boron clusters becomes very complicated because several motifs (e.g., quasi-planar, bowl, tube, fullerene, etc.) can crossover, be mixed together, and coexist as lowest-lying isomers.

From the perspective of structural motifs, these all-boron bare clusters resemble large rafts, with two to four boron atoms in the center surrounded by a peripheral ring of boron atoms. They exhibit size-dependent aromatic and antiaromatic behavior following the Hückel rules, akin to planar hydrocarbons. Aromatic boron clusters are more stable and have more-circular shapes, whereas antiaromatic boron clusters are less stable and elongated. For example, the  $B_{10}$ ,  $B_{11}^-$ , and  $B_{12}$  clusters have six delocalized  $\pi$  electrons, and  $B_{15}^-$  has 10 delocalized  $\pi$  electrons, thus these clusters have circular planar structures and are highly stable. In contrast, the  $B_{13}^-$  and  $B_{14}$  clusters have eight delocalized  $\pi$  electrons and are antiaromatic, with elongated oval shapes analogous to the square-to-rectangular distortion in the antiaromatic cyclobutadiene.<sup>[105]</sup>

Based on topological resonance energy (TRE) computations, Aihara and co-workers<sup>[106]</sup> argued that all these planar boron clusters are highly aromatic with large positive TREs even if they have  $4n$   $\pi$  electrons. This notion was later refuted by Boldyrev and Wang.<sup>[87b]</sup> As an extension of their work, Boldyrev and Wang proposed all-boron aromatic clusters as potential new inorganic ligands and building blocks in chemistry,<sup>[87b]</sup> exemplified by half sandwich-like compounds  $\text{LiB}_8^-$ ,<sup>[82]</sup>  $\text{LiB}_6^-$ ,<sup>[107]</sup>  $\text{Ta}_2\text{B}_6^-$ ,<sup>[108]</sup>  $\text{CoB}_{12}^-$ ,<sup>[109]</sup> and  $\text{RhB}_{12}^-$ <sup>[109]</sup> in the gas phase, and bulk phase  $\text{Ti}_7\text{Rh}_4\text{Ir}_2\text{B}_8$  in solid state,<sup>[110]</sup> and also many other predicted sandwich-like compounds.

In addition to the all-boron bare cluster anions ( $\text{B}_n^-$ ) detected by photoelectron spectroscopy and the corresponding neutral species studied with ab initio calculations, there are also reports on small cationic clusters. Oger and co-workers presented a detailed study on the evolution of structures of boron cluster cations (from  $\text{B}_{12}^+$  to  $\text{B}_{25}^+$ ; Figure 44) ranging from planar to cylindrical motifs.<sup>[111]</sup> A

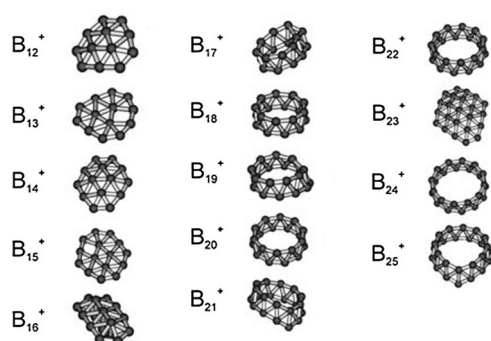


**Figure 44.** The lowest energy global minima structures of  $\text{B}_{12}^+$  to  $\text{B}_{25}^+$ .<sup>[111]</sup> (Reprinted with permission from Ref. [111], Copyright 2007 Wiley-VCH.)

typical case is  $\text{B}_{13}^+$ ,<sup>[112]</sup> which has anomalously high stability and low reactivity in comparison with other cationic boron clusters, consistent with its aromatic nature. Recently, Alexandrova and co-workers predicted  $\text{B}_{13}^+$  to be a photodriven molecular Wankel engine, which can be driven by circularly polarized infrared electromagnetic radiation.<sup>[113]</sup> Additionally, Wang and co-workers prepared and characterized several boron–gold alloy clusters (Figure 45), such as  $\text{B}_6\text{Au}_n^-$  ( $n = 1-3$ )<sup>[114]</sup> and  $\text{B}_7\text{Au}_2^-$ ,<sup>[115]</sup> which contain planar tetracoordinate boron motifs.

Carboranes with planar tetracoordinate boron atoms, **46a** and **46b**, have been detected experimentally.<sup>[116]</sup> Boranes with planar tetracoordinate boron atoms have also been pursued both theoretically<sup>[117]</sup> and experimentally (Figure 46).<sup>[118]</sup> Theoretically, the prototype anion **46c** is doubly aromatic, with a planar tetracoordinate boron atom forming a three-center, two-electron (3c-2e)  $\sigma$  bond as well as a 3c-2e  $\pi$  bond with the two other boron atoms.<sup>[119]</sup> Upon protonation, the classical B–B bond in **46c** is transformed into a 3c-2e B–H–B bond in **46d**, which is also doubly aromatic. In tetraborane **46e**, the hydrogen bridge in **46d** is replaced by a planar  $\text{BH}_2$  bridge, but it is less stable than its distorted tetrahedral isomer. The diamond-shaped tetraborane ( $\text{R} = \text{SiMe}_3$ ) **46f**

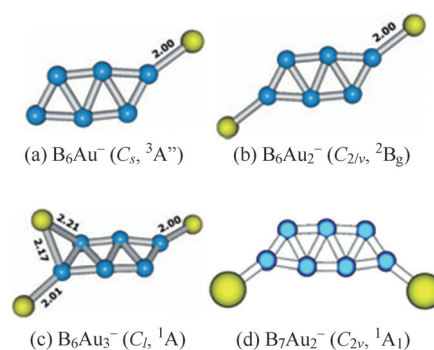


**Figure 45.** Experimental and theoretical global-minimum structures of  $\text{B}_6\text{Au}_n^-$  ( $n = 1-3$ ),<sup>[114]</sup> and  $\text{B}_7\text{Au}_2^-$ .<sup>[115]</sup> The bond lengths are given in Å. (Reprinted with permission from Ref. [114], Copyright 2013 American Institute of Physics and Ref. [115], Copyright 2006 American Chemical Society.)

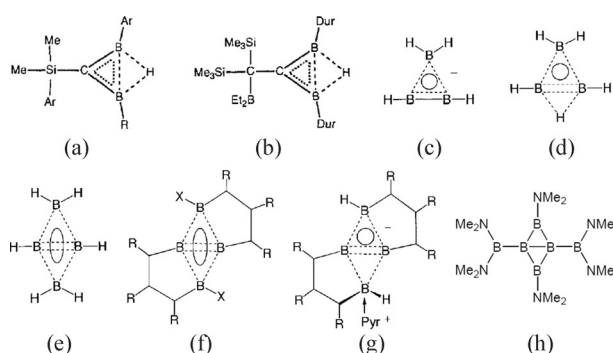


**Figure 46.** Experimentally and/or theoretically known planar tetracoordinate boron and its chemical bonding. a), b) from Ref. [116], c)–g) from Ref. [118a], h) from Ref. [118b]. (Reprinted with permission from Ref. [116], Copyright 1995 Wiley-VCH, Ref. [118a], Copyright 2002 Wiley-VCH, and Ref. [118b], Copyright 2002 Wiley-VCH.)

and its pyridine adduct **46g** are the first aromatic compounds in which two  $\pi$  electrons display cyclic delocalization over four and three boron centers, respectively. **46h** displays a planar, diamond-shaped  $\text{B}_4$  ring containing a central B–B bond (1.633 Å).

## 6.2. Nitrogen

Compounds with a planar tetracoordinate nitrogen (ptN) arrangement,  $\text{NAl}_4^-$  (**4b**) and  $\text{NSiAl}_3$  (**4c**), were predicted by Schleyer and Boldyrev in 1991.<sup>[20]</sup>  $\text{NAl}_4^-$  was later experimentally observed by Rao and co-workers in 1999,<sup>[120]</sup> as we discussed in Figure 4 in Section 2 on pentaatomic ptC species. Furthermore,  $\text{NAl}_5^-$  (**4s**) with a ptN motif was also observed and characterized together with  $\text{NAl}_4^-$  (**4b**) by Wang and Boldyrev in 2006.<sup>[28]</sup> Encouraged by the fact that the planar boron rings can serve as convenient frameworks for the stabilization of planar tetra- and hypercoordinate main-group elements, Minyaev and co-workers<sup>[121]</sup> predicted the species **47a–e**, with planar tetracoordinate nitrogen atoms (Figure 47).



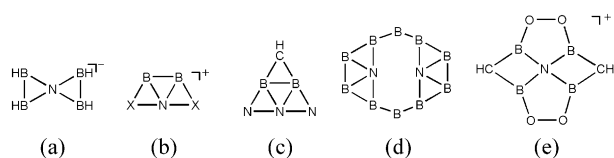


Figure 47. Predicted planar tetracoordinate nitrogen species.

### 6.3. Oxygen and Sulfur

$\text{Al}_4\text{O}$  ( $D_{4h}$ , **4a**) with planar tetracoordinate oxygen was found by Schleyer and Boldyrev in 1991.<sup>[20]</sup> In 2004, Li and co-workers discussed hydrometal complexes  $D_{4h}$ - $\text{Cu}_4\text{H}_4\text{O}^{2+}$  (**21d**) and  $\text{Ni}_4\text{H}_4\text{O}^{2+}$  (**21h**),<sup>[58]</sup> as well as  $D_{5h}$ - $\text{Cu}_5\text{H}_5\text{O}^{2+}$  (**29d**).<sup>[68]</sup> In 2011, Zhang and co-workers<sup>[122]</sup> experimentally detected a perfectly square-planar tetracoordinated oxygen atom (**48**) in a tetracopper cluster-based coordination polymer (Figure 48).

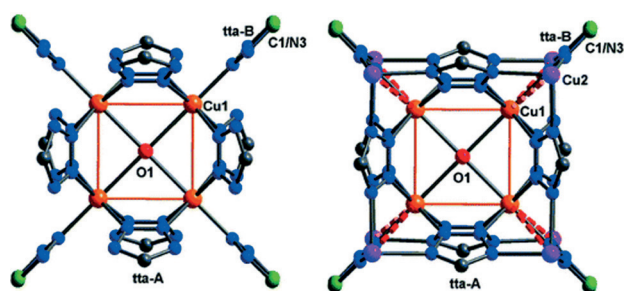


Figure 48. Planar tetracoordinate oxygen in a tetracopper cluster coordination polymer. (Reprinted with permission from Ref. [122], Copyright 2011 American Chemical Society.)

In 1996, Müller and Henkel<sup>[123]</sup> successfully synthesized  $[\text{Ni}_5\text{S}(\text{StBu})_5]^-$  (**49**), which features a planar pentacoordinate sulfur atom (Figure 49). This unprecedented pentanuclear sulfide thiolate cluster anion has a fivefold symmetry and contains a pentagonal nickel frame capped by a  $\mu_5$  sulfide ion. In 2005, species with planar hypercoordinate sulfur were found in hydrometal complexes  $\text{Ag}_5\text{H}_5\text{S}^{2+}$  (**29f**) and  $\text{Au}_5\text{H}_5\text{S}^{2+}$  (**29h**; Figure 29).<sup>[68b]</sup>

### 6.4. Silicon and Germanium

In 1970, when ptC was proposed by HAW, planar tetracoordinate silicon was also considered. In 1979, Würthwein and Schleyer<sup>[124]</sup> proposed that planar tetracoordinate silicon should be favored by electronegative,  $\pi$ -donor substituents. For example, the energy of planar (**50a**; Figure 50) was found to be only  $32.9 \text{ kcal mol}^{-1}$  less stable than the tetrahedral form (using MNDO and B3LYP/6-311 + G\* with ZPE correction), whereas this difference was  $116.3 \text{ kcal mol}^{-1}$  for its carbon analogue. In 1992, Boldyrev, Schleyer, and Keese reported computational results that polynitrogen[5,5,5]-sila-fenestrene (**50b**) has a minimum at the HF/3-21G level.<sup>[125]</sup> Keese and co-workers synthesized **50c**, but only pyramidal coordinated silicon was found.<sup>[126]</sup>

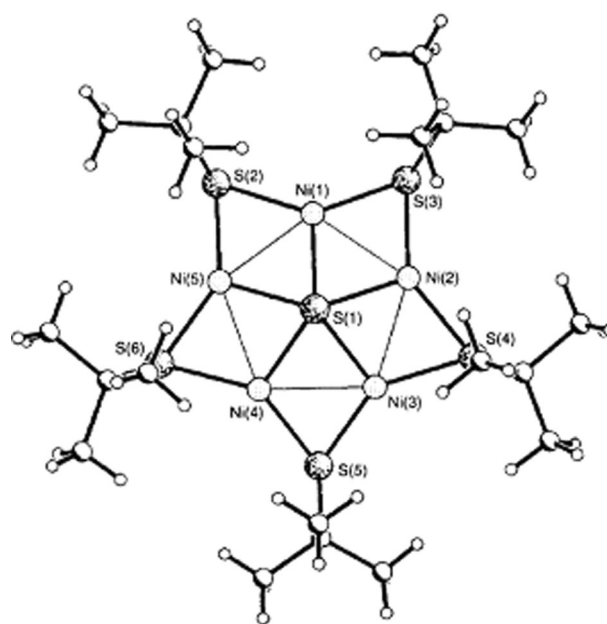


Figure 49. Molecular structure of  $[\text{Ni}_5\text{S}(\text{StBu})_5]^-$  featuring a planar pentacoordinate sulfur with fivefold symmetry.<sup>[123]</sup> (Reprinted with permission from Ref. [123], Copyright 1996 The Royal Society of Chemistry.)

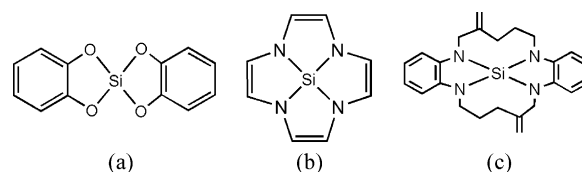
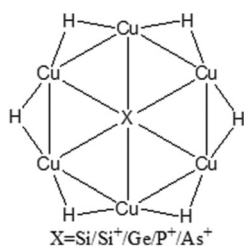


Figure 50. Computationally predicted compounds containing planar tetracoordinate silicon (a and b), and experimentally synthesized molecule with pyramidal silicon (c).

Smaller rings in the central  $\text{SiN}_4$  core are required to realize the planarization of **50b**.

Boron and hydrometal rings have been used to stabilize planar hypercoordinate silicon, as in  $\text{B}_8\text{Si}$  (**38c**),<sup>[51b]</sup>  $\text{Pd}_5\text{H}_5\text{Si}^-$  (**29i**),  $\text{Pt}_5\text{H}_5\text{Si}^-$  (**29k**),<sup>[68b]</sup> and  $\text{Cu}_6\text{H}_6\text{Si}^{0,+}$  (**51**).<sup>[127]</sup> The  $\text{Cu}_6\text{H}_6$  ring can also stabilize larger elements, such as Ge, P, and As (**51**; Figure 51).<sup>[127]</sup> However, it's not clear whether these  $\text{Cu}_6\text{H}_6\text{X}$  molecules are global minima or not. In 2004, Li and co-workers<sup>[128]</sup> reported a scheme to incorporate planar hypercoordinate silicon in the  $\text{C}_{2v}\text{-B}_n\text{E}_2\text{Si}$  series ( $\text{E} = \text{CH}$ ,  $\text{BH}$ , or  $\text{Si}$ ;  $n = 2-5$ ) as in **52a-d** (Figure 52) and  $D_{8h}\text{-B}_8\text{Si}$ . These  $\text{C}_{2v}\text{-B}_n\text{E}_2\text{Si}$  clusters feature fan-shaped structures (partial molecular wheels) which “grow” gradually along the fan peripheries as the number of the boron atoms increases. These finally achieve a perfect closed octagon at  $\text{B}_8\text{Si}$ . These planar clusters are the valence electron analogues of the experimentally known planar boron clusters,<sup>[80-81, 88-89]</sup> and are aromatic in nature. This structural pattern is formally robust, but may be difficult to synthesize experimentally. In total, 61 molecules containing planar hypercoordinate Si and other elements (B, C, Ge, P, As, Al, and Ga) were reported.<sup>[128]</sup> Molecules with double planar tetra-, penta-, and hexacoordi-



**Figure 51.** Planar motifs of Si, Ge, P, As enclosed by a  $\text{Cu}_6\text{H}_6$  ring.

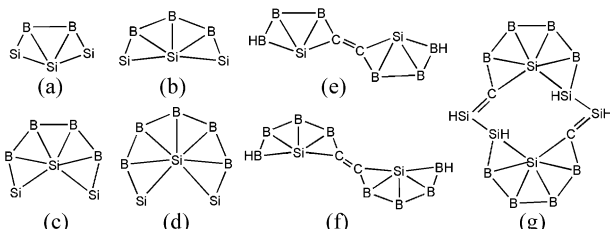


**Figure 52.** a–d) Planar tetra-, penta-, hexa-, and heptacoordinate silicon. e–g) Molecules with double planar tetra-, penta-, and hexacoordinate silicon.

nate silicon (ptSi, ppSi, phSi; see **52e–g**) were also obtained by Li and co-workers.<sup>[129]</sup> However, these beautiful planar motifs (ptSi, ppSi, phSi) are only local minima with low thermodynamic stability, and their experimental observation is expected to be difficult.

Compared with silicon, planar hypercoordinate germanium has rarely been investigated. Early semi-empirical (CNDO/2, ETH) calculations on  $T_d$  and  $D_{4h}$  symmetry  $\text{EH}_4$  and  $\text{EF}_4$  ( $E = \text{C}, \text{Si}, \text{Ge}$ ) showed that it is easier to form planar structures as one increases the atomic number of the central atom and with increasing electronegativity of the substituents.<sup>[130]</sup> Recent examples include hydrometal complexes  $\text{Pd}_5\text{H}_5\text{Ge}^-$  (**29j**),  $\text{Pt}_5\text{H}_5\text{Ge}^-$  (**29l**),<sup>[68b]</sup>  $\text{Cu}_6\text{H}_6\text{Ge}$  (**51**)<sup>[127]</sup>, and the boron wheel  $\text{B}_9\text{Ge}^+$ .<sup>[83]</sup>

Pentatomic planar tetracoordinate silicon- and germanium-containing molecules  $\text{SiAl}_4^-$  (**4k**) and  $\text{GeAl}_4^-$  (**4l**; Figure 4) were experimentally detected in 2000.<sup>[24c]</sup> Calculations showed that the anions with  $C_{2v}$  planar structures are of lowest energy, and the neutral molecules  $\text{SiAl}_4$  and  $\text{GeAl}_4$  clusters also remain planar. This is different from the case of their  $\text{CAI}_4^{n-}$  ( $n = 0, 1$ ) analogues, whose anion is planar while the neutral species is tetrahedral.<sup>[21]</sup>

### 6.5. Phosphorus and Arsenic

In 1992, polynitrogen-[5,5,5,5]-phosphofenestrene (**53a**) containing a planar tetracoordinate phosphorus (ptP) was computed as a local minimum (Figure 53).<sup>[125]</sup> However, the first compound with a planar tetracoordinate phosphorus was not realized until Driess and co-workers synthesized (**53b**,  $E = \text{P}$ ) in 1999,<sup>[131]</sup> and its heavier arsenic analogue (**53b**,  $E = \text{As}$ ) was prepared in 2002 by the same group.<sup>[132]</sup> Furthermore, ab initio calculations on a series of isoelectronic model  $\text{ER}_4$  compounds ( $E = \text{B}^-, \text{C}, \text{N}^+, \text{Al}^-, \text{Si}, \text{P}^+, \text{As}^+, \text{Sb}^+$ ;  $R =$

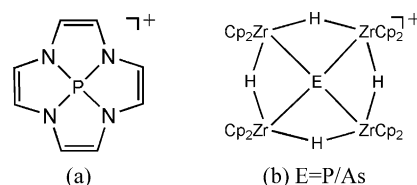


**Figure 53.** Predicted planar tetracoordinate phosphorus and arsenic species.

$\text{ZrHCp}_2$ ) showed that the organometallic substituent  $R$  represents a facile and universal ligand for the stabilization of elusive anti-van't Hoff/Le Bel configurations of various main-group elements including  $\text{Al}^-$ ,  $\text{Si}$  and  $\text{P}^+$ ,  $\text{As}^+$  and  $\text{Sb}^+$ .<sup>[131,132]</sup> The main factor responsible for the planar structure has been attributed to the  $\text{Zr}-E$   $\pi$  bonding and the ensuing delocalization of the  $E$  lone pair. Planar hypercoordinate arsenic was also found in the hydrometal complex  $\text{Cu}_6\text{H}_6\text{As}^+$  (**51**) predicted by Li and co-workers.<sup>[127]</sup>

### 6.6. Transition Metals

Such unusual planar hypercoordinate configurations are not only limited to main-group elements. In the following Section, we discuss planar transition-metal motifs with coordination numbers from four to ten.

In 2003, Lievens and co-workers<sup>[133]</sup> prepared  $\text{Au}_5\text{Zn}^+$  clusters (Figure 54) by cationic photo-fragmentation mass spectrometry. They detected planar tetracoordinate Au, and planar tetra/pentacoordinate Zn motifs stabilized by  $\sigma$  aromaticity.

Planar tetracoordinate and pentacoordinate motifs in  $\text{Ag}_5\text{X}^{0,+}$  ( $X = \text{Sc}, \text{Ti}, \text{V}, \text{Cr}, \text{Mn}, \text{Fe}, \text{Co},$  and  $\text{Ni}$ )<sup>[134]</sup> and  $\text{Au}_5\text{X}^+$  ( $X = \text{Au}, \text{Sc}, \text{Ti}, \text{Cr}, \text{Fe}$ )<sup>[135]</sup> clusters were investigated by Lievens, Nguyen and co-workers. Frenking and co-workers<sup>[136]</sup> found that because of the strong electron delocalization, iron can adopt planar pentacoordination in  $\text{FeSb}_5^+$  and  $\text{FeBi}_5^+$  in  $D_{5h}$  symmetry as local minima but not global minima on the potential-energy surface. Furthermore, planar pentacoordinate uranium in neutral  $\text{U}@[c\text{-U}_5(\mu_2\text{-C})_5]$  molecule (**23f**) was predicted by Tsipis and co-workers,<sup>[60]</sup> which extends the planar motifs from transition metals into actinoids. But, it is not clear if this structure is a global minimum or not.

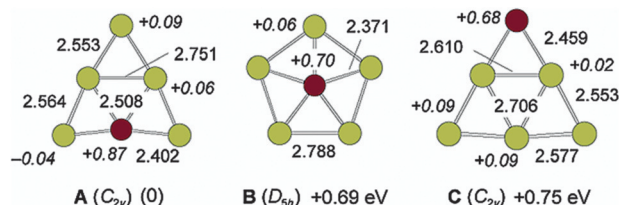


**Figure 54.** Optimized structures, charge populations, and relative stability of  $\text{Au}_5\text{Zn}^+$  calculated at the MP2 level of theory. Bond lengths are in Å. Charge populations are given in italics.<sup>[133]</sup> (Reprinted with permission from Ref. [133], Copyright 2003 American Chemical Society.)

Planar hexacoordinate species were observed in  $M@Au_6^-$  ( $M = Ti, V, Cr$ ) (**55**) by Wang and co-workers in 2005 (Figure 55).<sup>[137]</sup> Similar configurations have been predicted in  $M@Au_6$  ( $M = Sc, Ti, V, Cr, Mn, Fe, Co, Ni$ ) clusters by Luo and co-workers in 2009.<sup>[138]</sup> Furthermore, planar hepta-coordinated copper was computationally predicted in the  $Cu_7Sc$  ( $D_{7h}$ ) cluster (**56**) by Nguyen and co-workers<sup>[139]</sup> in 2008 (Figure 56).

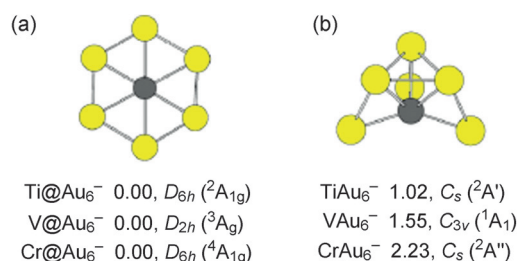


**Figure 55.** Molecular structures of  $M@Au_6^-$  ( $M = Ti, V, Cr$ ) feature planar hexacoordinate motifs.<sup>[137]</sup> Relative energies are given in eV. a) The most stable isomer; b) the next most-stable isomer. (Reprinted with permission from Ref. [137], Copyright 2005 The American Physical Society.)

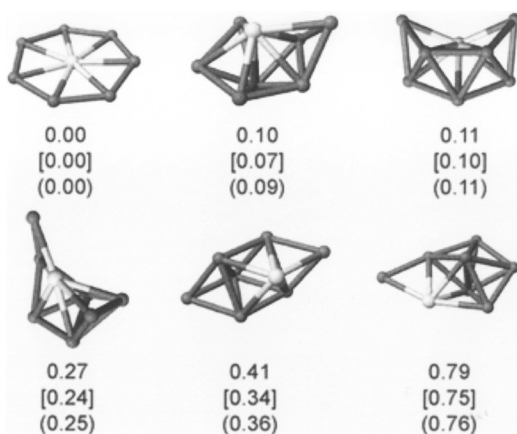


**Figure 56.** Ground-state structure of heptacoordinated  $Cu_7Sc$  cluster.<sup>[139]</sup> The two lowest lying isomers and their relative energies in eV are also shown. The Sc atom is light gray. (Reprinted with permission from Ref. [139], Copyright 2008 Wiley-VCH.)

In 2008, Li and co-workers<sup>[140]</sup> comprehensively explored the planar hypercoordinate (hepta-, octa-, nona-, and deca-coordinate) top-row d-block metals enclosed by boron rings. They predicted many neutral and charged molecules  $M@B_n$  ( $n = 7-10$ ), including several global minima with planar hypercoordinate motifs. Examples include  $Fe@B_8^{2-}$  ( $D_{8h}$ ),  $Co@B_8^-$  ( $D_{8h}$ ), and  $Fe@B_9^-$  ( $D_{9h}$ ) (Figure 57). Two of them,  $Co@B_8^-$  ( $D_{8h}$ ) and  $Fe@B_9^-$  ( $D_{9h}$ ), were later experimentally verified by Wang and Boldyrev.<sup>[141]</sup>

A groups of Wang and Boldyrev performed a series of experimental observations and theoretical characterizations of planar hypercoordinate species (see Figure 57). These include  $Ru@B_9^-$  ( $D_{9h}$ ),<sup>[141a]</sup>  $M@B_9^-$  ( $M = Rh, Ir$ ) ( $D_{9h}$ ),<sup>[142]</sup> slightly distorted  $Fe@B_8^-$  ( $C_{8v}$ ),<sup>[141b]</sup>  $M@B_{10}^-$  ( $M = Ta, Nb$ )

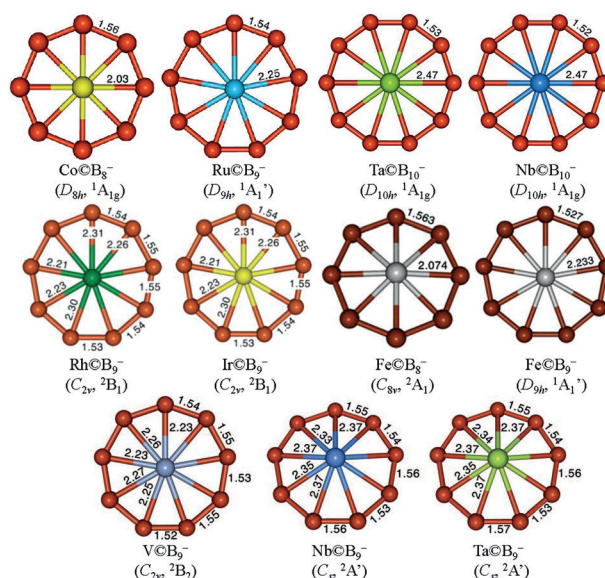


**Figure 57.** Experimentally observed transition-metal-centered boron molecular wheels,  $Co@B_8^-$  ( $D_{8h}$ ) and  $Ru@B_9^-$  ( $D_{9h}$ ),<sup>[141a]</sup>  $M@B_9^-$  ( $M = Rh, Ir$ ) ( $D_{9h}$ ),<sup>[142]</sup>  $Fe@B_8^-$  ( $C_{8v}$ ) and  $Fe@B_9^-$  ( $D_{9h}$ ),<sup>[141b]</sup>  $M@B_{10}^-$  ( $M = Ta, Nb$ ) ( $D_{10h}$ ),<sup>[143]</sup>  $M@B_9^-$  ( $M = V$ ) ( $C_{2v}$ ),  $Nb$  ( $C_s$ ),  $Ta$  ( $C_s$ )).<sup>[144]</sup> The bond lengths are given in Å. (Reprinted with permission from Ref. [141a], Copyright 2011 Wiley-VCH; Ref. [142], Copyright 2012 American Chemical Society; Ref. [141b], Copyright 2012 Elsevier; Ref. [143], Copyright 2012 Wiley-VCH; Ref. [144], Copyright 2013 American Institute of Physics.)

( $D_{10h}$ ),<sup>[143]</sup> planar  $V@B_9^-$  ( $C_{2v}$ ),<sup>[144]</sup> and slightly distorted  $M@B_9^-$  ( $M = Nb, Ta$ ) ( $C_s$ ).<sup>[144]</sup> Considering geometric and electronic factors, Wang, Boldyrev, and co-workers derived an electron-counting rule  $n + q + x = 12$  for the rational design of transition-metal-centered boron molecular wheels  $M^{(x)}@B_n^{k-}$ , where  $x$  is the formal valence of the transition metal,  $q$  is the charge, and  $n$  is the size of the boron ring.<sup>[144,145]</sup>

## 7. Sandwich-Type Complexes and Extended Systems

The ultimate goal of ptC chemistry is to design novel one-dimensional (1D), two-dimensional (2D), and three-dimensional (3D) cluster-assembled materials based on the “ptC” concept.<sup>[146]</sup> As Radom commented, “...the design of such new types of solids will be a further, very exciting development...”<sup>[147]</sup> Incorporating ptC units into assembled molecular materials could bridge the gap from isolated clusters in molecular beams to potential macroscopic solid materials.<sup>[146]</sup> These unusual materials might exhibit unique electronic, magnetic, optical, mechanical, or catalytic properties.

Individual planar hypercoordinate molecules can also serve as building blocks for larger structures or even potentially bulk solids. In 2002, Boldyrev and co-workers<sup>[24f]</sup> reported the  $(Na_2[CaI_4])_2$  dimer. The most stable structure reported by Boldyrev’s group is consistent with Yang and Ding’s “homo-decked sandwich” compound  $[(CaI_4^{2-})(Na^+)_4(CaI_4^{2-})]$ .<sup>[146]</sup> This concept can be extended to  $[(CaI_4^{2-})(K^+)_4(CaI_4^{2-})]$ . These two “homo-decked sandwich” com-



pounds can be viewed as two  $(\text{CAL}_4^{2-})$  decks sandwiching a  $(\text{Na}^+)_4$  or  $(\text{K}^+)_4$  cluster.<sup>[146,148]</sup>

In 2004, linking the central ptC of the  $\text{C}_5^{2-}$  units with two three-membered rings led to extensions of ptC into one, two, and three dimensions. Derived from the monomer and dimer models, and using a simple model of the bonding capabilities of the  $\text{C}_5^{2-}$  units, Hoffmann and co-workers proposed a variety of extended networks, including  $\text{C}_5\text{M}_x$  ( $x = 1$ ,  $\text{M} = \text{Pt}$ ,  $\text{Zn}$ ,  $\text{Be}$  and  $x = 2$ ,  $\text{M} = \text{Li}$ ) (Figure 58).<sup>[149]</sup> In general, these novel solids have relatively large band gaps, suggesting insulating behavior.

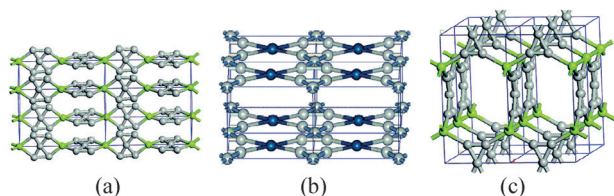


**Figure 58.** Optimized structures of a)  $\text{C}_5\text{Zn}$  1D network, b)  $\text{C}_5\text{Pt}$  2D network, and c)  $\text{C}_5\text{M}$  ( $\text{M} = \text{Zn}$ ,  $\text{Be}$ ) 3D network.<sup>[149]</sup> (Reprinted with permission from Ref. [149], Copyright 2004 American Chemical Society.)

Another example is the transition-metal ( $\text{Fe}$ ,  $\text{Co}$ ,  $\text{Ni}$ ) sandwich-type complexes containing hypercoordinate carbon, nitrogen, or boron (such as **59a–c**, Figure 59) modelled by Li and co-workers.<sup>[150]</sup> Conceptually, extended systems and more heterocyclic analogues could be designed using the same procedure. As pointed out by Li and co-workers, “the sandwich structural pattern developed may be extended along the six-fold molecular axis to form  $[(\text{B}_6\text{C})\text{M}]_n$  chains ( $n \geq 3$ ) linked with alkali-metal cations and the hexagonal  $\text{B}_6$  centered with  $\text{C}$  or  $\text{N}$  may be modified to form various heterocyclic ligands.”<sup>[150]</sup> Similar sandwich-type motifs of main-group metals,  $\text{K}[(\eta^6\text{-B}_6\text{C})\text{Ca}]_n(\eta^6\text{-B}_6\text{C})\text{K}$  ( $n = 1\text{--}3$ ) and  $[(\eta^6\text{-B}_6\text{C})\text{Ca}]_n(\eta^6\text{-B}_6\text{C})^{2-}$  ( $n = 1, 2$ ), were predicted in 2007 by Li and co-workers.<sup>[77]</sup>

However, Li and co-workers’ transition-metal ( $\text{Fe}$ ,  $\text{Co}$ ,  $\text{Ni}$ ) sandwich-type complexes may be difficult to prepare, since the configuration with two fused  $\text{B}_6\text{X}$  ( $\text{X} = \text{C}$ ,  $\text{B}$ ,  $\text{N}$ ) units is energetically much lower than that of sandwich-type complexes. For example, the energy of the fusion isomer of  $(\text{B}_6\text{N})_2\text{Fe}$  is much lower than that of the sandwich-like form by  $183.9 \text{ kcal mol}^{-1}$  at the B3LYP/6-311 + G(d) + ZPVE level.<sup>[151]</sup> Thus the “homo-decked sandwich” compounds

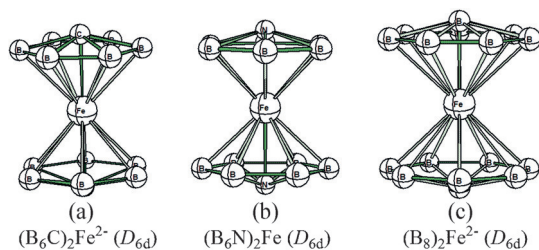
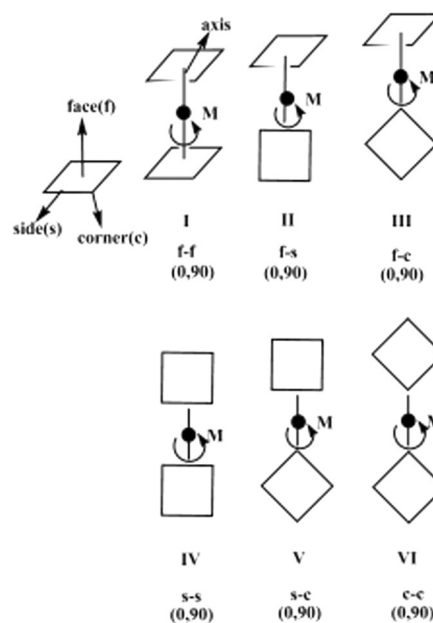


**Figure 59.** Sandwich-like structures based on planar hypercoordinate units a)  $\text{CB}_6^{2-}$ , b)  $\text{NB}_6^-$ , and c)  $\text{B}_8^{2-}$ .

$[(\text{B}_6\text{X})_2\text{M}]^{q-}$  ( $\text{X} = \text{C}$ ,  $\text{B}$ ,  $\text{N}$ ) are thermodynamically quite unstable and therefore may be difficult to synthesize.

Yang and Ding<sup>[146,148]</sup> redefined the concept of sandwich-type complexes and explored sandwich-like compounds in various interaction forms (such as, face–face (f–f), face–side (f–s), face–corner (f–c), side–side (s–s), side–corner (s–c), and corner–corner (c–c); see Scheme 9). The decks can be organic, inorganic, all-metal, homocyclic, or heterocyclic ligands. The cores can be transition-metal, main-group-metal, nonmetal atoms, or clusters. The coordination number of the ligand in the sandwich compounds could be one to eight, or even bigger. The new definition could cover various types of sandwich-like compounds with diverse decks, cores, and coordination numbers.



**Scheme 9.** Six types of deck-metal-deck  $[\text{DMD}]^{q-}$  sandwiches. Lowest energy states are found for rotations of  $0^\circ$  and  $90^\circ$ .<sup>[148d]</sup> (Reprinted with permission from Ref. [148d], Copyright 2007 Wiley-VCH.)

Using the newly proposed “hetero-decked sandwich” scheme, Yang and Ding successfully assembled and stabilized computationally a series of planar motif bricks ( $\text{CAL}_4^{2-}$ ,<sup>[146]</sup>  $\text{CAL}_4^-$ ,<sup>[148f]</sup>  $\text{CAL}_3\text{Si}$ ,<sup>[148b]</sup>  $\text{CAL}_3\text{Si}^-$ ,<sup>[148e]</sup>  $\text{CB}_6^{2-}$ ,<sup>[148g]</sup>  $\text{CSi}_2\text{Ga}_2$ ,<sup>[148i]</sup>  $\text{CAL}_2\text{Si}_2$ ,<sup>[152]</sup>  $\text{Al}_4\text{N}^-$ ,<sup>[148c]</sup>  $\text{B}_6^{2-}$ ,<sup>[148h]</sup>  $\text{B}_3^-$ ,<sup>[148m]</sup>  $\text{Al}_4^{2-}$ ,<sup>[148d]</sup>  $\text{SiAl}_3^-$ ,<sup>[148k]</sup>  $\text{Al}_3^-$ ,<sup>[148a]</sup>  $\text{Ga}_3^-$ ,<sup>[148h]</sup> into “hetero-decked sandwich” compounds (see Figure 60). We consider the “hetero-decked sandwich” scheme to be a promising direction for the assembly and stabilization of planar units in the future. Interestingly, we found that the side (s) interaction of ptC units in both “homo-decked sandwich” and “hetero-decked sandwich” complexes is more stable than that of face (f) interaction. This is in sharp contrast to the traditional “homo-decked sandwich” compounds, such as  $[\text{Fe}(\text{C}_5\text{H}_5)_2]$  and  $[\text{Cr}(\text{C}_6\text{H}_6)_2]$  (Figure 60), where the face (f) interaction is dominant and more important than side (s) or corner (c) interactions.

Recently, there has been growing interest in nanoscale materials and 2D sheets containing planar tetracoordinate

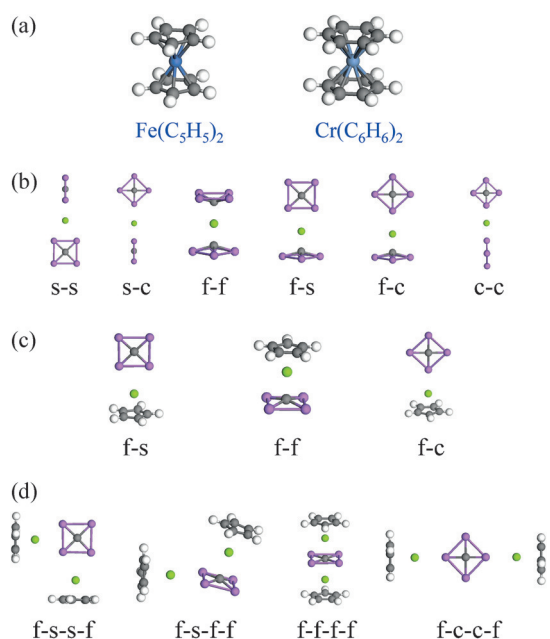


**Figure 60.** Traditional “homo-decked sandwich” compounds (a), calculated “homo-decked sandwich” complexes  $\text{M}(\text{CAl}_4)_2^{q-}$  (b), “hetero-decked sandwich” complexes  $[\text{CpM}(\text{CAl}_4)]^{q-}$  (c), and extended “hetero-decked sandwich” complexes  $\text{CpM}(\text{CAl}_4)\text{MCp}$  (d).<sup>[146]</sup>

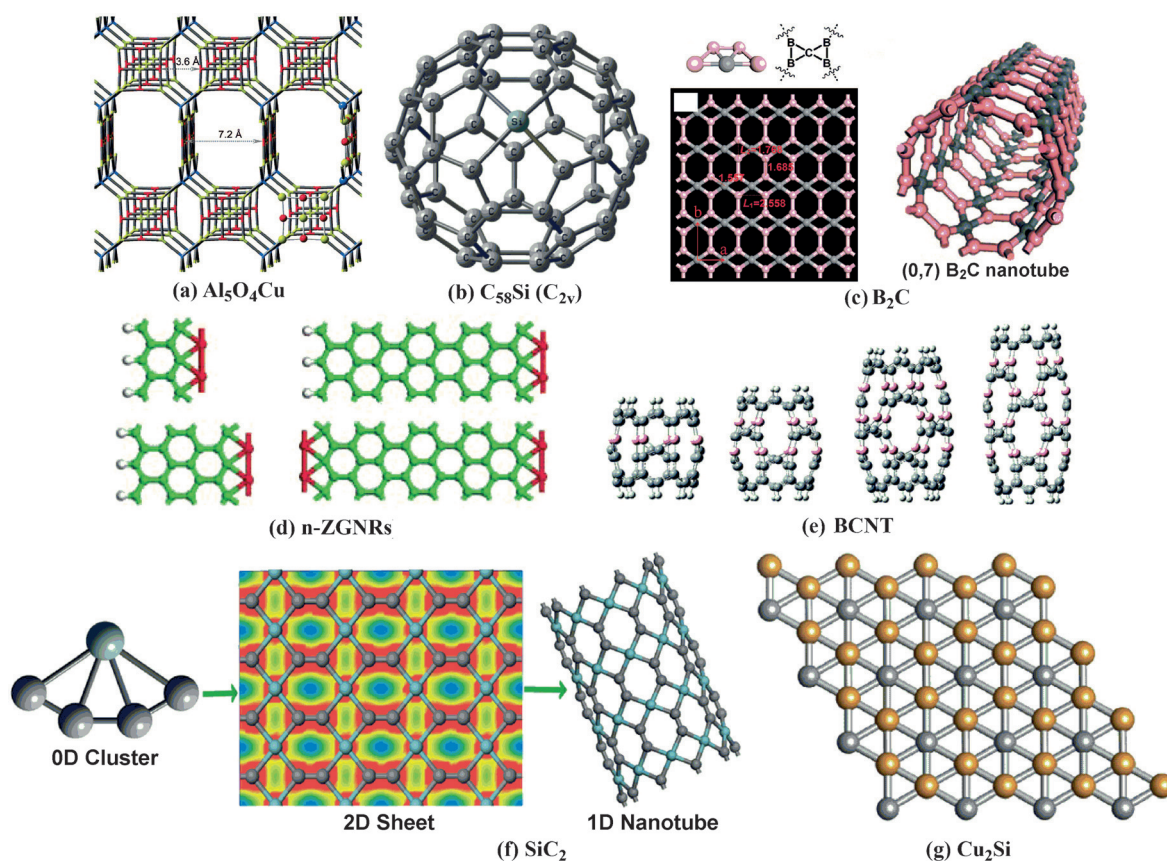


**Figure 61.** Calculated planar tetragonal motifs in nanostructures and nanosheets: a)  $\text{Al}_5\text{O}_4\text{Cu}$ ,<sup>[153]</sup> b)  $\text{C}_{58}\text{Si}$ ,<sup>[154]</sup> c)  $\text{B}_2\text{C}$  graphene, nanotubes, and nanoribbons,<sup>[155]</sup> d) zigzag graphene nanoribbon (n-ZGNRs),<sup>[156]</sup> e) zigzag boron–carbon nanotubes (BCNT),<sup>[160]</sup> f)  $\text{SiC}_2$  silagraphene and its one-dimensional derivatives,<sup>[161]</sup> g)  $\text{Cu}_2\text{Si}$  monolayer featuring phSi and phCu.<sup>[167]</sup> (Reprinted with permission from Ref. [153], Copyright 2008 American Chemical Society; Ref. [154], Copyright 2008 Elsevier; Ref. [155], Copyright 2009 American Chemical Society; Ref. [156], Copyright 2010 American Chemical Society; Ref. [160], Copyright 2008 American Chemical Society; Ref. [161], Copyright 2011 American Chemical Society; Ref. [167], Copyright 2015 American Chemical Society).

motifs (Figure 61). In 2008,  $\text{Al}_5\text{O}_4^-$  with a highly symmetric ( $D_{4h}$ ) planar ring structure was proposed to be a superatom, using  $\text{Al}_5\text{O}_4\text{M}$  ( $\text{M} = \text{Li}, \text{Na}, \text{K}, \text{etc.}$ ) as building blocks, new 1D, 2D, and 3D extended networks featuring both planar tetracoordinate aluminum (ptAl) and planar tetracoordinated oxygen (ptO) (**61a**) were designed.<sup>[153]</sup> Liu and Jalbout predicted that ptSi can reside in  $\text{C}_{58}\text{Si}$  (**61b**).<sup>[154]</sup>

Theoretical calculations showed that ptC elements can be found in  $\text{B}_2\text{C}$  graphene, nanotubes, and nanoribbons (**61c**).<sup>[155]</sup> They can also be observed in edge-decorated zigzag graphene nanoribbons (**61d**),<sup>[156]</sup> and at graphene nanoribbon edges. ptC strips can also be formed by beryllium and boron decoration.<sup>[157]</sup> Multi-ptC motifs can be formed in tri-wing graphene nano-paddle-wheels.<sup>[158]</sup> Remarkably, ptC and ptSi coexist in edge-decorated SiC nanoribbons.<sup>[159]</sup> Zigzag boron–carbon nanotubes featuring quasi-ptC (**61e**)<sup>[160]</sup> and  $\text{SiC}_2$  silagraphene featuring ptSi (**61f**) were also predicted.<sup>[161]</sup> In 2011, Luo, Xiang, and co-workers<sup>[162]</sup> predicted B-rich 2D boron–carbon compounds featuring ptC motifs. More recently, Chen, and co-workers<sup>[163]</sup> predicted  $\text{C}_{12}\text{B}_{68}$  fullerenes with quasi-ptC configurations.

Li, Chen and co-workers<sup>[164]</sup> predicted a  $\text{Be}_2\text{C}$  monolayer featuring quasi-planar hexacoordinate carbon, a concept originally proposed by Exner and Schleyer.<sup>[51a]</sup> This is the

first report involving extended structures containing quasi-phC motifs. Zeng and co-workers<sup>[165]</sup> have reported other inorganic materials, namely AlC, Al<sub>2</sub>C, and Al<sub>3</sub>C monolayers featuring planar tetracoordinate carbon. Independently, the Al<sub>2</sub>C monolayer and nanoribbons were also predicted by Li, Chen, and co-workers.<sup>[166]</sup> Quite recently, Yang and co-workers<sup>[167]</sup> reported the first global minimum Cu<sub>2</sub>Si monolayer featuring planar hexacoordinate silicon (phSi) and planar hexacoordinate copper (phCu). Notably, the monolayer structures are global minima on the 2D potential surface, which make these novel structures promising for experimental realization.

## 8. Experimental Realization of Planar Motifs

It is a great challenge to synthesize compounds containing planar tetracoordinate carbon that are stable enough to be isolated, investigated, and handled under ambient conditions. There have therefore been many attempts to construct hydrocarbon frameworks that can incorporate and stabilize tetravalent carbon in this unstable planar coordination geometry. Many experimental chemists have explored possible planar motif compounds since Hoffmann and co-workers<sup>[7a]</sup> proposed the ptC concept in 1970. A number of compounds stable at room temperature have been isolated and characterized. These compounds feature electronically stabilized planar tetracoordinate atoms within an organometallic framework.<sup>[12b]</sup>

The divanadium complex **1b**, the first compound featuring a ptC motif, was prepared experimentally by Cotton and Millar<sup>[11]</sup> in 1977. In the divanadium complex, the planar configuration exists because of a multicenter bond formed by the carbon sp<sup>2</sup> orbital of the phenyl anion, similar to the binding in the C<sub>2v</sub> form of methane. The structurally related

dizirconocene complex **62** reported by Buchwald and co-workers<sup>[168]</sup> in 1989 has the same stabilization scheme for the ptC (Figure 62).

In 1989, Cayton and co-workers<sup>[169]</sup> reported the ditungsten allene complex **63** in which the central carbon atom of the allene has the coordination characteristics of a ptC (Figure 63). The bonding of the allene to the W<sub>2</sub> unit is unique. In the angled C<sub>3</sub> ligand, three 2p orbitals form bonding, nonbonding, and antibonding combinations, and the central carbon atom has an empty p orbital orthogonal to the three 2p combinations.

The allene functions as a 4e donor, and one of the W<sub>2</sub> p bonds interacts with the empty 2p orbital of the ptC.

Many ptC-containing organometallic compounds were reported in the 1990s. Herein, we pay special attention to Erker's group, which was the major contributor to the ptC-organometallic chemistry in this period. During the 1990s, remarkably, Erker and co-workers<sup>[12b]</sup> synthesized more than 50 organometallic compounds featuring ptC elements. Some

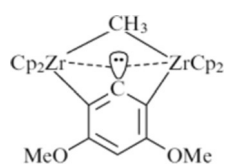


**Figure 62.** Dizirconocene complex featuring planar tetracoordinate carbon.<sup>[168]</sup> (Reprinted with permission from Ref. [168], Copyright 1989 American Chemical Society.)

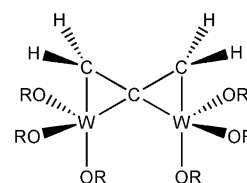


**Figure 63.** Ditungsten allene complex with planar tetracoordinate carbon.<sup>[169]</sup>

of these materials were also studied by X-ray diffraction. These experimental results confirmed the theoretical predictions for ptCs and greatly expanded the number of ptC materials that had been prepared.

The prototypical ptC containing dicobalt complex **64** belongs to an extensive set of dinuclear complexes in which ptC atoms are linked to transition (or non-transition) metal atoms Figure 64.<sup>[170]</sup> Many examples of these complexes exist with structures similar to compounds **62–64**. Details of the synthesis methods can be found in the literature.<sup>[12b,e]</sup>

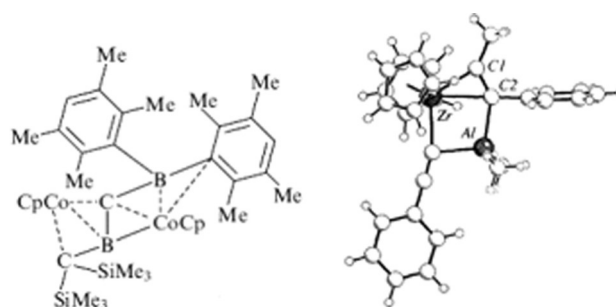


**Figure 64.** Left: A typical example of a dimetallic ptC containing organometallic complex;<sup>[170]</sup> Right: 3D representation of another ptC molecule from Erker's group.<sup>[12b]</sup> (Reprinted with permission from Ref. [170], Copyright 1997 Wiley-VCH.)

Gas-phase experimental observations were already covered in earlier Sections of this Review. Thus we will only mention that many small gas-phase clusters with planar motifs were observed by the Wang and Boldyrev groups between 2001 and 2014.<sup>[24g,87a,b,145]</sup>

In 2003, Messerle and co-workers<sup>[171]</sup> synthesized a dinuclear propynylidene complex **65a** arising from double C–H activation of an allene ligand. This complex featured a ptC motif and unusual bonding (Figure 65b).

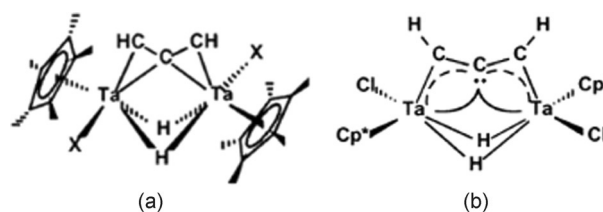


**Figure 65.** Organometallic propynylidene complex containing the ptC configuration.<sup>[171]</sup> (Reprinted with permission from Ref. [171], Copyright 2003 American Chemical Society.)



Some planar motifs with metal centers have been synthesized. A typical example is planar tetracoordinate nickel (ptNi; **66**, Figure 66).<sup>[172]</sup> In 2008, Li et al.<sup>[172]</sup> reported the synthesis and characterization of a slightly distorted square-planar nickel compound  $[2\text{-C(H)NDippC}_6\text{H}_4\text{NH}]_2\text{Ni}$  (Dipp = 2,6-*i*Pr<sub>2</sub>C<sub>6</sub>H<sub>3</sub>) containing a ptNi (**66**). Note that Ni<sup>II</sup> has mostly planar tetracoordinate structure, which also holds true for Pd<sup>II</sup> and Pt<sup>II</sup>.

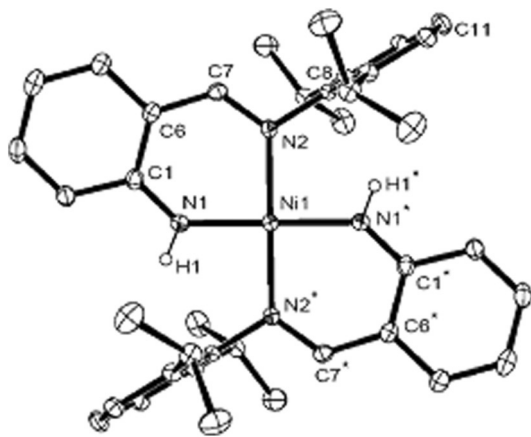


**Figure 66.** Experimentally synthesized planar tetracoordinate nickel complex.<sup>[172]</sup> (Reprinted with permission from Ref. [172], Copyright 2008 American Chemical Society.)

In 2010, Cooper and co-workers<sup>[173]</sup> synthesized a monomeric dilithio methandiide (**67**) with a distorted *trans*-planar four-coordinate carbon (Figure 67). The properties of this material were studied using X-ray diffraction as well as quantum chemistry calculations.

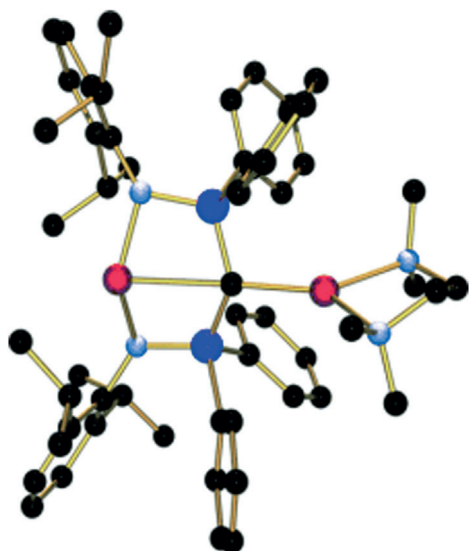
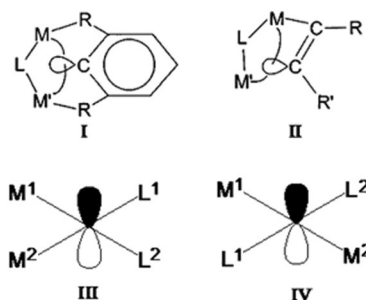


**Figure 67.** A distorted *trans*-planar four-coordinate carbon found in a monomeric dilithio methandiide.<sup>[173]</sup> C black, P blue, N light blue, Li red, (Reprinted with permission from Ref. [173], Copyright 2010 Wiley-VCH.)

Many of the reported ptC-based organometallic compounds can be abstracted into small models, as Siebert and Gunale summarized in 1999 (see Scheme 10).<sup>[12e]</sup> These



**Scheme 10.** Organometallic compounds featuring ptC motifs with metal atoms M<sup>1</sup> and M<sup>2</sup> and ligands L<sup>1</sup> and L<sup>2</sup>.<sup>[12e]</sup> (Reprinted with permission from Ref. [12e], Copyright 1999 The Royal Society of Chemistry.)

models are reminiscent of Hoffmann's planar methane model. In these cases, metals (including transition metals) as ligands provide  $\sigma$ -donating bonds and  $\pi$ -accepting properties for back-bonding from the filled 2p lone pair at the central carbon atom. The ligands are preferentially bonded to each other, forming a perimeter.

Up till now, our discussion of the experimental synthesis of planar motifs has mainly focused on dinuclear complexes in organometallic chemistry because transition metals are favored ligands to stabilize planar configurations. Moreover, the synergistic combination of the properties of both metal atoms is very useful in the synthesis of ptC species.

Now we will discuss the experimental progress on non-carbon planar motifs. For example, the pentaatomic planar motifs of heavier Group IV elements, silicon and germanium,  $\text{XAl}_4^{0-}$ , X = Si/Ge (**4q,r**) were detected and characterized by a joint photoelectron spectroscopy and high-level ab initio study in 2000.<sup>[24c]</sup> Considering second-row elements, planar boron motifs have been detected in a series of small pure boron clusters (at least up to 24 atoms) by a joint photoelectron spectroscopy and high-level ab initio study.<sup>[87a]</sup> The planar configuration of planar tetracoordinate aluminum was also detected in  $\text{Al}_5^-$  (**4p**) in 2000.<sup>[24b]</sup> The origin of the planar nature of  $\text{Al}_5^-$  was ascribed to a four-center peripheral bond. In the same year, Köhnlein et al.<sup>[174]</sup> synthesized a metalloid  $\text{Al}_{14}$  cluster with coupled  $\text{AlAl}_6$  nanowheels featuring quasi-planar hexacoordinate aluminum (phAl) (**68**; Figure 68).

In 1992, Schollenberger et al.<sup>[175]</sup> reported the preparation of pentagonal planar coordinate indium in  $[(\mu_5\text{-In})[\text{Mn}(\text{CO})_4]_5]^{2-}$  (see Figure 69). Planar tetracoordinate nitrogen (ptN) has been detected in  $\text{NAl}_4^-$  in 1999,<sup>[176]</sup> and  $\text{NAl}_5^-$  in 2006.<sup>[28]</sup> The planar configurations of P and As, ptP and ptAs in  $\text{X}[\text{Zr}(\text{H})\text{Cp}_2]_4^+(\text{BPh}_4)^-$ , (X = P and As)<sup>[132,177]</sup> have also been synthesized (Figure 53b).

In 2011, Zhang and co-workers<sup>[178]</sup> synthesized a tetracoper cluster-based coordination polymer and confirmed its crystal structure featuring a perfectly square-planar tetra-coordinated oxygen atom (Figure 48). Earlier observations of

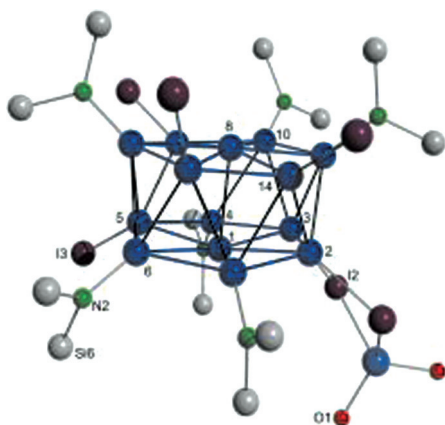


**Figure 68.** Planar hexacoordinate aluminum in a metalloid  $\text{Al}_{14}$  cluster with coupled  $\text{AlAl}_6$  nanowheels.<sup>[174]</sup>  $\text{AlAl}_6$  is in blue (Reprinted with permission from Ref. [174], Copyright 2000 Wiley-VCH.)

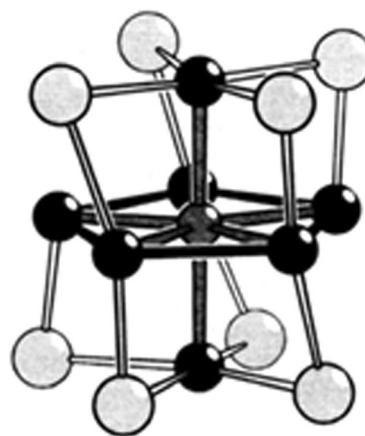


**Figure 70.** Molecular structure of  $\text{Bi}_7\text{Rh}_8\text{Br}_8$  features planar pentacoordinate rhodium motif.<sup>[181]</sup> Bi black, Rh gray, Br light gray (Reprinted with permission from Ref. [181], Copyright 1997 Wiley-VCH.)

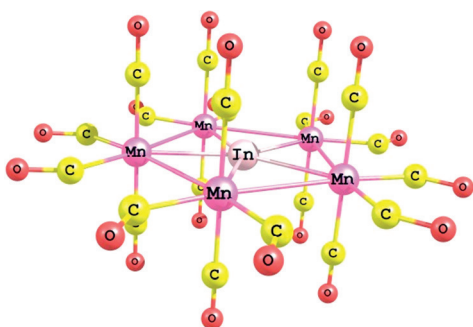


**Figure 69.** Molecular structure of  $[(\mu_5\text{-In})[\text{Mn}(\text{CO})_4]_s]^{2-}$  featuring planar pentacoordinate indium motif.<sup>[175]</sup>

ptO include  $[\text{Cu}_4\text{H}_4\text{O}]^{2+}$  in 2004,<sup>[179]</sup> and  $\text{Al}_4\text{O}$  in 1991.<sup>[180]</sup> ptO in a bulk solid structure was predicted in 2008.<sup>[153]</sup>

The planar configuration of sulfur was synthesized earlier than that of ptO. In 1996, Müller and Henkel<sup>[123]</sup> reported the synthesis of  $[\text{Ni}_5\text{S}(\text{tBu})_5]^-$ , featuring a planar pentacoordinate sulfur motif (see Figure 49). This unprecedented pentanuclear sulfide thiolate cluster anion has a five-fold symmetry and contains a regularly shaped pentagonal nickel frame capped by a  $\mu_5$ -sulfide ion.

Several planar tetracoordinate structures have been observed in transition metals. In 1997, Ruck<sup>[181]</sup> prepared the planar pentacoordinate rhodium in  $\text{Bi}_7\text{Rh}_8\text{Br}_8$  (**70**; Figure 70). In 2003, Tanaka, Lievens, and co-workers<sup>[133]</sup> probed the planar motifs in the binary alloy  $\text{ZnAu}_5^+$  (**54**) using mass spectroscopy. In 2005, Wang, and co-workers<sup>[137]</sup> detected planar hexacoordinate transition metal (Ti, V, Cr) centers in  $\text{M@Au}_6^-$  ( $\text{M} = \text{Ti, V, Cr}$ ) (**55**) using photoelectron spectroscopy. Additionally, Köhler<sup>[182]</sup> reported a new material,  $\text{SrFeO}_2$ , in which a high-spin  $\text{Fe}^{2+}$  exhibits a square-planar coordination.

In summary, the organometallic compounds (especially, complexed arenes, allenes, and olefins) and related species are the major categories for experimental synthesis in the field of planar hypercoordinate chemistry. These achievements form a solid basis for the future development of planar hypercoordinate chemistry.

What are the potential applications of planar hypercoordinate molecules? To date, little is known about this possibility. We hope that further research will explore whether these unusual materials can have unique catalytic functionality or exotic chemical reactivity, or can be used in photoelectronics. Accordingly, recent theoretical studies have identified several promising applications. For example, a 2D  $\text{B}_2\text{C}$  monolayer including ptC elements is a promising superconductor with an estimated transition temperature of 19.2 K.<sup>[183]</sup> a  $\text{Be}_2\text{C}$  monolayer<sup>[164]</sup> featuring quasi-planar hexacoordinate carbon, and a  $\text{Al}_2\text{C}$  monolayer<sup>[165–166]</sup> containing ptCs are both semiconducting with a moderate band gap, and thus are promising for potential applications in electronics, optoelectronics and photovoltaics. Furthermore, the recently predicted highly stable metallic  $\text{Cu}_2\text{Si}$  monolayer,<sup>[167]</sup> with exact planar hexacoordinate silicon and planar hexacoordinate copper, might be used as a superthin electrode in future nanoelectronics.

## 9. Conclusion

After 200 years of organic chemistry, more than 14 000 000 carbon compounds with traditional  $\text{sp}$ ,  $\text{sp}^2$ , and  $\text{sp}^3$  hybridization have been synthesized. Even the fundamental and most widely held structural rules of chemistry are violated by the planar hypercoordinate species described in this Review. Van't Hoff and Le Bel's tetrahedral carbon model went unchallenged for a century until the first planar arrangements of four (or more) substituents were predicted computationally and realized experimentally. Strain (e.g., small rings) and electronic (e.g., multicenter bonding) strategies, especially in combination, can overcome the much higher energies normally associated with these increasingly recognized planar arrangements. Such structures may have various main-group element and transition-metal centers in up to ten-membered ring perimeters. The seemingly unlikely planar hypercoordinate carbon compounds are now well established. As clusters, nano sheets, and bulk solids are also included, these unusual materials offer novel properties and have opened new research fields.

We thank all the scientists involved in the advancement of these topics, and especially the former Schleyer group members Prof. Alexander I. Boldyrev and Dr. Kai Exner. L.-M.Y. acknowledges the support from the Fellowship of Hanse-Wissenschafts-Kolleg (HWK) (Institute for Advanced Study) and Research Scholarship of University of Bremen. This work was financially supported by National Science Foundation Grant CHE-0209857. Support to Z.C. by Department of Defense (Grant W911NF-12-1-0083) and NSF (Grant EPS-1010094) is gratefully acknowledged. We thank Ariel Ganz for her contribution to the frontispiece, and Matthew Dornfeld for his assistance with the manuscript. Finally, we thank Prof. Thomas Heine for translating the manuscript into German, and also for his comments and suggestions to improve the manuscript.

**How to cite:** *Angew. Chem. Int. Ed.* **2015**, *54*, 9468–9501  
*Angew. Chem.* **2015**, *127*, 9602–9637

- [1] V. I. Minkin, R. M. Minjaev, J. A. Ždanov, *Nonclassical Structures of Organic Compounds*, Mir, Moscow, **1987**.
- [2] [http://upload.wikimedia.org/wikipedia/commons/b/b3/Molecular\\_Model\\_of\\_Methane\\_Hofmann.jpg](http://upload.wikimedia.org/wikipedia/commons/b/b3/Molecular_Model_of_Methane_Hofmann.jpg).
- [3] J. H. van't Hoff, *Arch. Neerl. Sci. Exactes Nat.* **1874**, *9*, 44.
- [4] J. A. Le Bel, *Bull. Soc. Chim. Fr.* **1874**, *22*, 337.
- [5] H. Wynberg, G. L. Hekkert, J. P. M. Houbiers, H. W. Bosch, *J. Am. Chem. Soc.* **1965**, *87*, 2635–2639.
- [6] H. J. Monkhorst, *Chem. Commun.* **1968**, 1111.
- [7] a) R. Hoffmann, R. W. Alder, C. F. Wilcox, *J. Am. Chem. Soc.* **1970**, *92*, 4992; b) R. Hoffmann, *Pure Appl. Chem.* **1971**, *28*, 181–194.
- [8] J. B. Collins, J. D. Dill, E. D. Jemmis, Y. Apeloig, P. von R. Schleyer, R. Seeger, J. A. Pople, *J. Am. Chem. Soc.* **1976**, *98*, 5419–5427.
- [9] M. J. M. Pepper, I. Shavitt, P. von R. Schleyer, M. N. Glukhovtsev, R. Janoschek, M. Quack, *J. Comput. Chem.* **1995**, *16*, 207–225.
- [10] Z. X. Wang, P. von R. Schleyer, *J. Am. Chem. Soc.* **2001**, *123*, 994–995.
- [11] F. A. Cotton, M. Millar, *J. Am. Chem. Soc.* **1977**, *99*, 7886–7891.
- [12] a) K. Sorger, P. von R. Schleyer, *J. Mol. Struct. THEOCHEM* **1995**, *338*, 317–346; b) D. Röttger, G. Erker, *Angew. Chem. Int. Ed. Engl.* **1997**, *36*, 812–827; *Angew. Chem.* **1997**, *109*, 840–856; c) L. Radom, D. R. Rasmussen, *Pure Appl. Chem.* **1998**, *70*, 1977–1984; d) G. Erker, *Chem. Soc. Rev.* **1999**, *28*, 307–314; e) W. Siebert, A. Gunale, *Chem. Soc. Rev.* **1999**, *28*, 367–371; f) V. I. Minkin, R. M. Minyaev, R. Hoffmann, *Russ. Chem. Rev.* **2002**, *71*, 869–892; g) R. Keese, *Chem. Rev.* **2006**, *106*, 4787–4808; h) G. Merino, M. A. Mendez-Rojas, A. Vela, T. Heine, *J. Comput. Chem.* **2007**, *28*, 362–372.
- [13] U. Salzner, P. von R. Schleyer, *Chem. Phys. Lett.* **1992**, *199*, 267–274.
- [14] D. M. Golden, R. Walsh, S. W. Benson, *J. Am. Chem. Soc.* **1965**, *87*, 4053–4057.
- [15] a) B. Bredenkötter, U. Flörke, D. Kuck, *Chem. Eur. J.* **2001**, *7*, 3387–3400; b) H. Hopf in *Classics in Hydrocarbon Chemistry*, Wiley-VCH, Weinheim, **2000**, pp. 81–102; c) M. Thommen, R. Keese, *Synlett* **1997**, 231; d) W. Luef, R. Keese in *Advances in Strain in Organic Chemistry, Vol. 3* (Ed.: B. Halton), JAI, Greenwich, **1993**, S. 229–267; e) W. C. Agosta in *The Chemistry of Alkanes and Cycloalkanes* (Eds.: S. Patai, Z. Rappoport), Wiley, New York, **1992**, pp. 927–962; f) A. K. Gupta, X. Y. Fu, J. P. Snyder, J. M. Cook, *Tetrahedron* **1991**, *47*, 3665–3710; g) K. Krohn in *Organic Synthesis Highlights* (Eds.: J. Mulzer, H.-J. Altenbach, M. Braun, K. Krohn, H.-U. Reissig), Wiley-VCH, Weinheim, **1991**, pp. 121–125; h) B. R. Venepalli, W. C. Agosta, *Chem. Rev.* **1987**, *87*, 399–410; i) R. Keese in *Organic Synthesis: Modern Trends* (Ed.: O. Chizhov), Blackwell, Oxford, **1987**, pp. 43–52; j) R. Keese, *Nachr. Chem. Tech. Lab.* **1982**, *30*, 844–849.
- [16] a) M. P. McGrath, L. Radom, *J. Am. Chem. Soc.* **1993**, *115*, 3320–3321; b) J. E. Lyons, D. R. Rasmussen, M. P. McGrath, R. H. Nobes, L. Radom, *Angew. Chem. Int. Ed. Engl.* **1994**, *33*, 1667–1668; *Angew. Chem.* **1994**, *106*, 1722–1724.
- [17] D. R. Rasmussen, L. Radom, *Angew. Chem. Int. Ed.* **1999**, *38*, 2875–2878; *Angew. Chem.* **1999**, *111*, 3051–3054.
- [18] a) P. Babinec, J. Leszczynski, *Int. J. Quantum Chem.* **1999**, *72*, 319–324; b) M. W. Wong, L. Radom, *J. Am. Chem. Soc.* **1989**, *111*, 1155–1156; c) B. M. Gimarc, *Tetrahedron Lett.* **1977**, *18*, 1859–1862; d) A. W. Hanner, T. F. Moran, *Org. Mass Spectrom* **1981**, *16*, 512–513; e) J. A. Pople, B. Tidor, P. von R. Schleyer, *Chem. Phys. Lett.* **1982**, *88*, 533–537; f) P. E. M. Siegbahn, *Chem. Phys.* **1982**, *66*, 443–452.
- [19] M. B. Krogh-Jespersen, J. Chandrasekhar, E. U. Würthwein, J. R. Collins, P. von R. Schleyer, *J. Am. Chem. Soc.* **1980**, *102*, 2263–2268.
- [20] P. von R. Schleyer, A. I. Boldyrev, *J. Chem. Soc. Chem. Commun.* **1991**, 1536–1538.
- [21] X. Li, L. S. Wang, A. I. Boldyrev, J. Simons, *J. Am. Chem. Soc.* **1999**, *121*, 6033–6038.
- [22] X. Li, H. F. Zhang, L. S. Wang, G. D. Geske, A. I. Boldyrev, *Angew. Chem. Int. Ed.* **2000**, *39*, 3630–3632; *Angew. Chem.* **2000**, *112*, 3776–3778.
- [23] L. S. Wang, A. I. Boldyrev, X. Li, J. Simons, *J. Am. Chem. Soc.* **2000**, *122*, 7681–7687.
- [24] a) A. I. Boldyrev, J. Simons, *J. Am. Chem. Soc.* **1998**, *120*, 7967–7972; b) G. D. Geske, A. I. Boldyrev, X. Li, L. S. Wang, *J. Chem. Phys.* **2000**, *113*, 5130–5133; c) A. I. Boldyrev, X. Li, L. S. Wang, *Angew. Chem. Int. Ed.* **2000**, *39*, 3307–3310; *Angew. Chem.* **2000**, *112*, 3445–3448; d) X. Li, L. S. Wang, N. A. Cannon, A. I. Boldyrev, *J. Chem. Phys.* **2002**, *116*, 1330–1338; e) X. Li, H. J. Zhai, L. S. Wang, *Chem. Phys. Lett.* **2002**, *357*, 415–419; f) G. D. Geske, A. I. Boldyrev, *Inorg. Chem.* **2002**, *41*, 2795–2798; g) A. I. Boldyrev, L. S. Wang, *J. Phys. Chem. A* **2001**, *105*, 10759–10775.
- [25] a) A. N. Alexandrova, M. J. Nayhouse, M. T. Huynh, J. L. Kuo, A. V. Melkonian, G. Chavez, N. M. Hernando, M. D. Kowal, C. P. Liu, *Phys. Chem. Chem. Phys.* **2012**, *14*, 14815–14821; b) A. C. Castro, M. Audiffred, J. M. Mercero, J. M. Ugalde, M. A. Mendez-Rojas, G. Merino, *Chem. Phys. Lett.* **2012**, *519*–20, 29–33.
- [26] a) S. M. Gao, H. P. He, Y. H. Ding, *Chem. J. Chin. Univ.* **2013**, *34*, 185–191; b) K. Zhou, *Comput. Theor. Chem.* **2013**, *1009*, 30–34; c) H. P. He, Y. H. Ding, *Acta Chim. Sin.* **2010**, *68*, 13–18; d) Z. H. Cui, C. B. Shao, S. M. Gao, Y. H. Ding, *Phys. Chem. Chem. Phys.* **2010**, *12*, 13637–13645; e) Z. H. Cui, Y. H. Ding, *Phys. Chem. Chem. Phys.* **2011**, *13*, 5960–5966; f) D. Roy, C. Corminboeuf, C. S. Wannere, R. B. King, P. von R. Schleyer, *Inorg. Chem.* **2006**, *45*, 8902–8906.
- [27] A. I. Boldyrev, J. Simons, X. Li, L. S. Wang, *J. Chem. Phys.* **1999**, *111*, 4993–4998.
- [28] B. B. Averkiev, A. I. Boldyrev, X. Li, L.-S. Wang, *J. Chem. Phys.* **2006**, *125*, 124305.
- [29] G. A. Olah, G. Klopman, *Chem. Phys. Lett.* **1971**, *11*, 604–608.
- [30] Z. X. Wang, P. von R. Schleyer, *J. Am. Chem. Soc.* **2002**, *124*, 11979–11982.
- [31] A. Streitwieser, S. M. Bachrach, A. Dorigo, P. von R. Schleyer in *Lithium Chemistry, A Theoretical and Experimental Overview* (Hrsg.: A. M. Sapse, P. von R. Schleyer), Wiley, New York, **1994**, S. 1.
- [32] Y. Xie, H. F. Schaefer, *Chem. Phys. Lett.* **1991**, *179*, 563–567.
- [33] B. J. Smith, *Chem. Phys. Lett.* **1993**, *207*, 403–406.



- [34] a) S. Harder, J. Boersma, L. Brandsma, A. Van Heteren, J. A. Kanters, W. Bauer, P. von R. Schleyer, *J. Am. Chem. Soc.* **1988**, *110*, 7802–7806; b) H. Dietrich, W. Mahdi, W. Storch, *J. Organomet. Chem.* **1988**, *349*, 1–10.
- [35] Z.-X. Wang, T. K. Manojkumar, C. Wannere, P. von R. Schleyer, *Org. Lett.* **2001**, *3*, 1249–1252.
- [36] Z.-X. Wang, C.-G. Zhang, Z. Chen, P. von R. Schleyer, *Inorg. Chem.* **2008**, *47*, 1332–1336.
- [37] Y. Wang, *J. Comput. Chem.* **2009**, *30*, 2122–2126.
- [38] D. R. Rasmussen, L. Radom, *Chem. Eur. J.* **2000**, *6*, 2470–2483.
- [39] a) K. Lammertsma, P. von R. Schleyer, *J. Phys. Chem.* **1988**, *92*, 881–886; b) Z. X. Wang, P. von R. Schleyer, unpublished results.
- [40] “Zwitterionic ‘Neutral’ and ‘Anionic’ Carbocation Analogs”: C. S. Wannere, Z. Chen, P. von R. Schleyer in *Carbocation Chemistry* (Eds.: G. A. Olah, G. K. S. Prakash), Wiley, Hoboken, **2004**, pp. 43–71.
- [41] P. M. Esteves, N. B. P. Ferreira, R. J. Corrêa, *J. Am. Chem. Soc.* **2005**, *127*, 8680–8685.
- [42] a) G. Merino, M. A. Mendez-Rojas, A. Vela, *J. Am. Chem. Soc.* **2003**, *125*, 6026–6027; b) G. Merino, M. A. Mendez-Rojas, H. I. Beltraan, C. Corminboeuf, T. Heine, A. Vela, *J. Am. Chem. Soc.* **2004**, *126*, 16160–16169.
- [43] T. N. Gribanova, R. M. Minyaev, V. I. Minkin, *Collect. Czech. Chem. Commun.* **1999**, *64*, 1780–1789.
- [44] N. Perez, T. Heine, R. Barthel, G. Seifert, A. Vela, M. A. Mendez-Rojas, G. Merino, *Org. Lett.* **2005**, *7*, 1509–1512.
- [45] a) U. D. Priyakumar, A. S. Reddy, G. N. Sastry, *Tetrahedron Lett.* **2004**, *45*, 2495–2498; b) U. D. Priyakumar, G. N. Sastry, *Indian J. Chem. Sect. A* **2004**, *43*, 455–457.
- [46] N. Perez-Peralta, M. Sanchez, J. Martin-Polo, R. Islas, A. Vela, G. Merino, *J. Org. Chem.* **2008**, *73*, 7037–7044.
- [47] C. L. Firme, N. B. P. Barreiro, P. M. Esteves, R. J. Correa, *J. Phys. Chem. A* **2008**, *112*, 686–692.
- [48] R. M. Minyaev, V. E. Avakyan, A. G. Starikov, T. N. Gribanova, V. I. Minkin, *Dokl. Chem.* **2008**, *419*, 101–107.
- [49] a) W. Sun, C. Zhang, Z. Cao, *J. Phys. Chem. C* **2008**, *112*, 351–357; b) C. Zhang, P. Wang, J. Liang, W. Jia, Z. Cao, *J. Mol. Struct. THEOCHEM* **2010**, *941*, 41–46.
- [50] V. I. Minkin, V. E. Avakyan, R. M. Minyaev, *Russ. Chem. Bull.* **2011**, *60*, 2188–2195.
- [51] a) K. Exner, P. von R. Schleyer, *Science* **2000**, *290*, 1937–1940; b) Z. X. Wang, P. von R. Schleyer, *Science* **2001**, *292*, 2465–2469; c) S. Erhardt, G. Frenking, Z. Chen, P. von R. Schleyer, *Angew. Chem. Int. Ed.* **2005**, *44*, 1078–1082; *Angew. Chem.* **2005**, *117*, 1102–1106; d) R. Islas, T. Heine, K. Ito, P. von R. Schleyer, G. Merino, *J. Am. Chem. Soc.* **2007**, *129*, 14767–14774; e) L.-M. Wang, W. Huang, B. B. Averkiev, A. I. Boldyrev, L.-S. Wang, *Angew. Chem. Int. Ed.* **2007**, *46*, 4550–4553; *Angew. Chem.* **2007**, *119*, 4634–4637; f) B. B. Averkiev, D. Y. Zubarev, L.-M. Wang, W. Huang, L.-S. Wang, A. I. Boldyrev, *J. Am. Chem. Soc.* **2008**, *130*, 9248; g) B. B. Averkiev, L.-M. Wang, W. Huang, L.-S. Wang, A. I. Boldyrev, *Phys. Chem. Chem. Phys.* **2009**, *11*, 9840–9849; h) L.-M. Wang, B. B. Averkiev, J. A. Ramiłowski, W. Huang, L.-S. Wang, A. I. Boldyrev, *J. Am. Chem. Soc.* **2010**, *132*, 14104–14112; i) Z. H. Cui, M. Contreras, Y. H. Ding, G. Merino, *J. Am. Chem. Soc.* **2011**, *133*, 13228–13231; j) T. R. Galeev, A. S. Ivanov, C. Romanescu, W.-L. Li, K. V. Bozhenko, L.-S. Wang, A. I. Boldyrev, *Phys. Chem. Chem. Phys.* **2011**, *13*, 8805–8810; k) T. R. Galeev, W.-L. Li, C. Romanescu, I. Černušák, L.-S. Wang, A. I. Boldyrev, *J. Chem. Phys.* **2012**, *137*, 234306; l) I. A. Popov, V. F. Popov, K. V. Bozhenko, I. Černušák, A. I. Boldyrev, *J. Chem. Phys.* **2013**, *139*, 114307; m) J. Shao, C. He, R. Shi, C. Wang, X. Zhu, X. Lu, *J. Mol. Struct. THEOCHEM* **2010**, *961*, 17–28; n) C. He, J. Shao, R. Shi, X. Zhu, *Comput. Theor. Chem.* **2011**, *967*, 59–66.
- [52] a) Y.-B. Wu, J.-L. Jiang, R.-W. Zhang, Z.-X. Wang, *Chem. Eur. J.* **2010**, *16*, 1271–1280; b) Y.-B. Wu, J.-L. Jiang, H.-G. Lu, Z.-X. Wang, N. Perez-Peralta, R. Islas, M. Contreras, G. Merino, J. I. C. Wu, P. von R. Schleyer, *Chem. Eur. J.* **2011**, *17*, 714–719.
- [53] Y.-B. Wu, J.-L. Jiang, R.-W. Zhang, Z.-X. Wang, *Chem. Eur. J.* **2010**, *16*, 1271.
- [54] J. Chandrasekhar, E. D. Jemmis, P. von R. Schleyer, *Tetrahedron Lett.* **1979**, *20*, 3707–3710.
- [55] U. D. Priyakumar, G. N. Sastry, *Tetrahedron Lett.* **2004**, *45*, 1515–1517.
- [56] R. M. Minyaev, T. N. Gribanova, V. I. Minkin, A. G. Starikov, R. Hoffmann, *J. Org. Chem.* **2005**, *70*, 6693–6704.
- [57] A. C. Tsipis, C. A. Tsipis, *J. Am. Chem. Soc.* **2003**, *125*, 1136–1137.
- [58] S. D. Li, G. M. Ren, C. Q. Miao, Z. H. Jin, *Angew. Chem. Int. Ed.* **2004**, *43*, 1371–1373; *Angew. Chem.* **2004**, *116*, 1395–1397.
- [59] S. D. Li, G. M. Ren, C. Q. Miao, *J. Phys. Chem. A* **2005**, *109*, 259–261.
- [60] A. C. Tsipis, C. E. Kefalidis, C. A. Tsipis, *J. Am. Chem. Soc.* **2008**, *130*, 9144–9155.
- [61] M.-D. Su, *Inorg. Chem.* **2005**, *44*, 4829–4833.
- [62] C. Crigger, B. K. Wittmaack, M. Tawfik, G. Merino, K. J. Donald, *Phys. Chem. Chem. Phys.* **2012**, *14*, 14775–14783.
- [63] F. Y. Naumkin, *J. Phys. Chem. A* **2008**, *112*, 4660–4668.
- [64] Y.-B. Wu, H.-G. Lu, S.-D. Li, Z.-X. Wang, *J. Phys. Chem. A* **2009**, *113*, 3395–3402.
- [65] Y.-B. Wu, J.-L. Jiang, H. Li, Z. Chen, Z.-X. Wang, *Phys. Chem. Chem. Phys.* **2010**, *12*, 58–61.
- [66] a) P. von R. Schleyer, C. Maerker, A. Dransfeld, H. Jiao, N. J. R. van Eikema Hommes *J. Am. Chem. Soc.* **1996**, *118*, 6317–6318; b) P. von R. Schleyer, H. Jiao, N. J. R. van Eikema Hommes, V. G. Malkin, O. L. Malkina, *J. Am. Chem. Soc.* **1997**, *119*, 12669–12670; c) P. von R. Schleyer, M. Manoharan, Z. X. Wang, B. Kiran, H. Jiao, R. Puchta, N. J. R. van Eikema Hommes, *Org. Lett.* **2001**, *3*, 2465–2468; d) T. Heine, C. Corminboeuf, P. von R. Schleyer, G. Seifert, R. Reviakine, J. Weber, *J. Phys. Chem. A* **2003**, *107*, 6470–6475; e) “Aromaticity indices from magnetic shieldings”: Z. Chen, T. Heine, P. von R. Schleyer, D. Sundholm in *Calculation of NMR and EPR Parameters, Theory and Applications* (Eds.: M. Kaupp, M. Bühl, V. G. Malkin), Wiley-VCH, Weinheim, **2004**; f) Z. Chen, C. S. Wannere, C. Corminboeuf, R. Puchta, P. von R. Schleyer, *Chem. Rev.* **2005**, *105*, 3842–3888.
- [67] C. A. Tsipis, E. E. Karagiannis, P. F. Kladou, A. C. Tsipis, *J. Am. Chem. Soc.* **2004**, *126*, 12916–12929.
- [68] a) S. D. Li, C. Q. Miao, G. M. Ren, *Eur. J. Inorg. Chem.* **2004**, 2232–2234; b) S. D. Li, C. Q. Miao, *J. Phys. Chem. A* **2005**, *109*, 7594–7597.
- [69] Y. Pei, W. An, K. Ito, P. von R. Schleyer, X. C. Zeng, *J. Am. Chem. Soc.* **2008**, *130*, 10394–10400.
- [70] J. O. C. Jimenez-Halla, Y.-B. Wu, Z.-X. Wang, R. Islas, T. Heine, G. Merino, *Chem. Commun.* **2010**, *46*, 8776–8778.
- [71] Y.-B. Wu, Y. Duan, H.-G. Lu, S.-D. Li, *J. Phys. Chem. A* **2012**, *116*, 3290–3294.
- [72] A. C. Castro, G. Martinez-Guajardo, T. Johnson, J. M. Ugalde, Y.-b. Wu, J. M. Mercero, T. Heine, K. J. Donald, G. Merino, *Phys. Chem. Chem. Phys.* **2012**, *14*, 14764–14768.
- [73] R. W. A. Havenith, P. W. Fowler, E. Steiner, *Chem. Eur. J.* **2002**, *8*, 1068–1073.
- [74] Z.-X. Wang, P. von R. Schleyer, *Angew. Chem. Int. Ed.* **2002**, *41*, 4082–4085; *Angew. Chem.* **2002**, *114*, 4256–4259.
- [75] K. Wade, *J. Chem. Soc. D* **1971**, 792–793.
- [76] K. Ito, Z. Chen, C. Corminboeuf, C. S. Wannere, X. H. Zhang, Q. S. Li, P. von R. Schleyer, *J. Am. Chem. Soc.* **2007**, *129*, 1510.
- [77] Q. Luo, X. H. Zhang, K. L. Huang, S. Q. Liu, Z. H. Yu, Q. S. Li, *J. Phys. Chem. A* **2007**, *111*, 2930–2934.

- [78] S. Shahbazian, S. Alizadeh, *J. Phys. Chem. A* **2008**, *112*, 10365–10377.
- [79] Y. B. Wu, Y. Duan, G. Lu, H. G. Lu, P. Yang, P. von R. Schleyer, G. Merino, R. Islas, Z. X. Wang, *Phys. Chem. Chem. Phys.* **2012**, *14*, 14760–14763.
- [80] A. N. Alexandrova, A. I. Boldyrev, H. J. Zhai, L. S. Wang, *J. Phys. Chem. A* **2004**, *108*, 3509–3517.
- [81] H. J. Zhai, A. N. Alexandrova, K. A. Birch, A. I. Boldyrev, L. S. Wang, *Angew. Chem. Int. Ed.* **2003**, *42*, 6004–6008; *Angew. Chem.* **2003**, *115*, 6186–6190.
- [82] A. N. Alexandrova, H. J. Zhai, L. S. Wang, A. I. Boldyrev, *Inorg. Chem.* **2004**, *43*, 3552–3554.
- [83] Y. Liao, C. L. Cruz, P. von R. Schleyer, Z. Chen, *Phys. Chem. Chem. Phys.* **2012**, *14*, 14898–14904.
- [84] a) T. N. Gribanova, R. M. Minyaev, V. I. Minkin, *Mendeleev Commun.* **2001**, *11*, 169–170; b) R. M. Minyaev, T. N. Gribanova, *Russ. Chem. Bull.* **2000**, *49*, 783–796; c) R. M. Minyaev, T. N. Gribanova, A. G. Starikov, V. I. Minkin, *Mendeleev Commun.* **2001**, *11*, 213–214; d) R. M. Minyaev, T. N. Gribanova, A. G. Starikov, V. I. Minkin, *Dokl. Chem.* **2002**, *382*, 41–45; e) V. I. Minkin, R. M. Minyaev, *Mendeleev Commun.* **2004**, *14*, 43–46; f) See Ref. [12f].
- [85] S. S. Park, *Bull. Korean Chem. Soc.* **2005**, *26*, 63–71.
- [86] a) D. Y. Zubarev, A. I. Boldyrev, *Phys. Chem. Chem. Phys.* **2008**, *10*, 5207–5217; b) T. R. Galeev, B. D. Dunnington, J. R. Schmidt, A. I. Boldyrev, *Phys. Chem. Chem. Phys.* **2013**, *15*, 5022–5029.
- [87] a) A. P. Sergeeva, I. A. Popov, Z. A. Piazza, W.-L. Li, C. Romanescu, L.-S. Wang, A. I. Boldyrev, *Acc. Chem. Res.* **2014**, *47*, 1349–1358; b) A. N. Alexandrova, A. I. Boldyrev, H.-J. Zhai, L.-S. Wang, *Coord. Chem. Rev.* **2006**, *250*, 2811–2866; c) D. Y. Zubarev, A. I. Boldyrev, *J. Comput. Chem.* **2007**, *28*, 251–268.
- [88] H. J. Zhai, L. S. Wang, A. N. Alexandrova, A. I. Boldyrev, *J. Chem. Phys.* **2002**, *117*, 7917–7924.
- [89] A. N. Alexandrova, A. I. Boldyrev, H. J. Zhai, L. S. Wang, E. Steiner, P. W. Fowler, *J. Phys. Chem. A* **2003**, *107*, 1359–1369.
- [90] H. J. Zhai, B. Kiran, J. Li, L. S. Wang, *Nat. Mater.* **2003**, *2*, 827–833.
- [91] W.-L. Li, Y.-F. Zhao, H.-S. Hu, J. Li, L.-S. Wang, *Angew. Chem. Int. Ed.* **2014**, *53*, 5540–5545; *Angew. Chem.* **2014**, *126*, 5646–5651.
- [92] W.-L. Li, Q. Chen, W.-J. Tian, H. Bai, Y.-F. Zhao, H.-S. Hu, J. Li, H.-J. Zhai, S.-D. Li, L.-S. Wang, *J. Am. Chem. Soc.* **2014**, *136*, 12257–12260.
- [93] Z. A. Piazza, H.-S. Hu, W.-L. Li, Y.-F. Zhao, J. Li, L.-S. Wang, *Nat. Commun.* **2014**, *5*, 3113.
- [94] A. P. Sergeeva, D. Y. Zubarev, H.-J. Zhai, A. I. Boldyrev, L.-S. Wang, *J. Am. Chem. Soc.* **2008**, *130*, 7244.
- [95] C. Romanescu, D. J. Harding, A. Fielicke, L.-S. Wang, *J. Chem. Phys.* **2012**, *137*, 014317.
- [96] A. P. Sergeeva, B. B. Averkiev, H.-J. Zhai, A. I. Boldyrev, L.-S. Wang, *J. Chem. Phys.* **2011**, *134*, 224304.
- [97] a) W. Huang, A. P. Sergeeva, H.-J. Zhai, B. B. Averkiev, L.-S. Wang, A. I. Boldyrev, *Nat. Chem.* **2010**, *2*, 202–206; b) J. O. C. Jiménez-Halla, R. Islas, T. Heine, G. Merino, *Angew. Chem. Int. Ed.* **2010**, *49*, 5668–5671; *Angew. Chem.* **2010**, *122*, 5803–5806.
- [98] See Ref. [97b].
- [99] B. Kiran, S. Bulusu, H. J. Zhai, S. Yoo, X. C. Zeng, L. S. Wang, *Proc. Natl. Acad. Sci. USA* **2005**, *102*, 961–964.
- [100] Z. A. Piazza, W.-L. Li, C. Romanescu, A. P. Sergeeva, L.-S. Wang, A. I. Boldyrev, *J. Chem. Phys.* **2012**, *136*, 104310.
- [101] A. P. Sergeeva, Z. A. Piazza, C. Romanescu, W. L. Li, A. I. Boldyrev, L. S. Wang, *J. Am. Chem. Soc.* **2012**, *134*, 18065–18073.
- [102] I. A. Popov, Z. A. Piazza, W.-L. Li, L.-S. Wang, A. I. Boldyrev, *J. Chem. Phys.* **2013**, *139*, 144307.
- [103] Q. Chen, W.-L. Li, Y.-F. Zhao, S.-Y. Zhang, H.-S. Hu, H. Bai, H.-R. Li, W.-J. Tian, H.-G. Lu, H.-J. Zhai, S.-D. Li, J. Li, L.-S. Wang, *ACS Nano* **2015**, *9*, 754–760.
- [104] H.-J. Zhai, Y.-F. Zhao, W.-L. Li, Q. Chen, H. Bai, H.-S. Hu, Z. A. Piazza, W.-J. Tian, H.-G. Lu, Y.-B. Wu, Y.-W. Mu, G.-F. Wei, Z.-P. Liu, J. Li, S.-D. Li, L.-S. Wang, *Nat. Chem.* **2014**, *6*, 727–731.
- [105] R. Breslow, *Acc. Chem. Res.* **1973**, *6*, 393–398.
- [106] J. Aihara, H. Kanno, T. Ishida, *J. Am. Chem. Soc.* **2005**, *127*, 13324–13330.
- [107] A. N. Alexandrova, A. I. Boldyrev, H.-J. Zhai, L.-S. Wang, *J. Chem. Phys.* **2005**, *122*, 054313.
- [108] W.-L. Li, L. Xie, T. Jian, C. Romanescu, X. Huang, L.-S. Wang, *Angew. Chem. Int. Ed.* **2014**, *53*, 1288–1292; *Angew. Chem.* **2014**, *126*, 1312–1316.
- [109] I. A. Popov, W.-L. Li, Z. A. Piazza, A. I. Boldyrev, L.-S. Wang, *J. Phys. Chem. A* **2014**, *118*, 8098–8105.
- [110] B. P. T. Fokwa, M. Hermus, *Angew. Chem. Int. Ed.* **2012**, *51*, 1702–1705; *Angew. Chem.* **2012**, *124*, 1734–1737.
- [111] E. Oger, N. R. M. Crawford, R. Kelting, P. Weis, M. M. Kappes, R. Ahlrichs, *Angew. Chem. Int. Ed.* **2007**, *46*, 8503–8506; *Angew. Chem.* **2007**, *119*, 8656–8659.
- [112] a) J. E. Fowler, J. M. Ugalde, *J. Phys. Chem. A* **2000**, *104*, 397–403; b) J. Aihara, *J. Phys. Chem. A* **2001**, *105*, 5486–5489.
- [113] J. Zhang, A. P. Sergeeva, M. Sparta, A. N. Alexandrova, *Angew. Chem. Int. Ed.* **2012**, *51*, 8512–8515; *Angew. Chem.* **2012**, *124*, 8640–8643.
- [114] Q. Chen, H.-J. Zhai, S.-D. Li, L.-S. Wang, *J. Chem. Phys.* **2013**, *138*, 084306.
- [115] H. J. Zhai, L. S. Wang, D. Y. Zubarev, A. I. Boldyrev, *J. Phys. Chem. A* **2006**, *110*, 1689–1693.
- [116] M. Menzel, D. Steiner, H. J. Winkler, D. Schweikart, S. Mehle, S. Fau, G. Frenking, W. Massa, A. Berndt, *Angew. Chem. Int. Ed. Engl.* **1995**, *34*, 327–329; *Angew. Chem.* **1995**, *107*, 368–370.
- [117] a) M. Krempp, R. Damrauer, C. H. DePuy, Y. Keheyuan, *J. Am. Chem. Soc.* **1994**, *116*, 3629; b) A. A. Korkin, P. von R. Schleyer, M. L. McKee, *Inorg. Chem.* **1995**, *34*, 961; c) M. L. McKee, *Inorg. Chem.* **1999**, *38*, 321; d) A. Neu, T. Mennekes, U. Englert, P. Paetzold, M. Hofmann, P. von R. Schleyer, *Angew. Chem. Int. Ed. Engl.* **1997**, *36*, 2117–2119; *Angew. Chem.* **1997**, *109*, 2211–2213.
- [118] a) C. Präsang, M. Hofmann, G. Geiseler, W. Massa, A. Berndt, *Angew. Chem. Int. Ed.* **2002**, *41*, 1526–1529; *Angew. Chem.* **2002**, *114*, 1597–1599; b) A. Maier, M. Hofmann, H. Pritzkow, W. Siebert, *Angew. Chem. Int. Ed.* **2002**, *41*, 1529–1532; *Angew. Chem.* **2002**, *114*, 1600–1602.
- [119] M. Unverzagt, G. Subramanian, M. Hofmann, P. v. R. Schleyer, S. Berger, K. Harms, W. Massa, A. Berndt, *Angew. Chem. Int. Ed. Engl.* **1997**, *36*, 1469–1472; *Angew. Chem.* **1997**, *109*, 1567–1569.
- [120] S. K. Nayak, B. K. Rao, P. Jena, X. Li, L. S. Wang, *Chem. Phys. Lett.* **1999**, *301*, 379–384.
- [121] T. N. Gribanova, R. M. Minyaev, V. I. Minkin, *Mendeleev Commun.* **2002**, *12*, 170–172.
- [122] X.-M. Zhang, J. Lv, F. Ji, H.-S. Wu, H. Jiao, P. von R. Schleyer, *J. Am. Chem. Soc.* **2011**, *133*, 4788–4790.
- [123] A. Müller, G. Henkel, *Chem. Commun.* **1996**, 1005–1006.
- [124] E. U. Würthwein, P. von R. Schleyer, *Angew. Chem. Int. Ed. Engl.* **1979**, *18*, 553–554; *Angew. Chem.* **1979**, *91*, 588–589.
- [125] A. I. Boldyrev, P. von R. Schleyer, R. Keese, *Mendeleev Commun.* **1992**, *2*, 93–95.
- [126] B. Ding, R. Keese, H. Stoeckli-Evans, *Angew. Chem. Int. Ed.* **1999**, *38*, 375–376; *Angew. Chem.* **1999**, *111*, 387–388.
- [127] S. D. Li, G. M. Ren, C. Q. Miao, *Inorg. Chem.* **2004**, *43*, 6331–6333.



- [128] S. D. Li, C. Q. Miao, J. C. Guo, G. M. Ren, *J. Am. Chem. Soc.* **2004**, *126*, 16227–16231.
- [129] S. D. Li, J. C. Guo, C. Q. Miao, G. M. Ren, *J. Phys. Chem. A* **2005**, *109*, 4133–4136.
- [130] G. Scholz, R. Lück, L. Kolditz, *Z. Anorg. Allg. Chem.* **1986**, *532*, 57–64.
- [131] M. Driess, J. Aust, K. Merz, C. van Wüllen, *Angew. Chem. Int. Ed.* **1999**, *38*, 3677–3680; *Angew. Chem.* **1999**, *111*, 3967–3970.
- [132] M. Driess, H. Ackermann, J. Aust, K. Merz, C. van Wüllen, *Angew. Chem. Int. Ed.* **2002**, *41*, 450–453; *Angew. Chem.* **2002**, *114*, 467–470.
- [133] H. Tanaka, S. Neukermans, E. Janssens, R. E. Silverans, P. Lievens, *J. Am. Chem. Soc.* **2003**, *125*, 2862–2863.
- [134] a) E. Janssens, X.-J. Hou, M. T. Nguyen, P. Lievens, *J. Chem. Phys.* **2006**, *124*, 1843191–1843198; b) X.-J. Hou, E. Janssens, P. Lievens, M. T. Nguyen, *Chem. Phys.* **2006**, *330*, 365–379.
- [135] E. Janssens, H. Tanaka, S. Neukermans, R. E. Silverans, P. Lievens, *Phys. Rev. B* **2004**, *69*, 085402.
- [136] M. Lein, J. Frunzke, G. Frenking, *Angew. Chem. Int. Ed.* **2003**, *42*, 1303–1306; *Angew. Chem.* **2003**, *115*, 1341–1345.
- [137] X. Li, B. Kiran, L. F. Cui, L. S. Wang, *Phys. Rev. Lett.* **2005**, *95*, 253401.
- [138] M. Zhang, L.-M. He, L.-X. Zhao, X.-J. Feng, Y.-H. Luo, *J. Phys. Chem. C* **2009**, *113*, 6491–6496.
- [139] T. Hóltzl, E. Janssens, N. Veldeman, T. Veszprémi, P. Lievens, M. T. Nguyen, *ChemPhysChem* **2008**, *9*, 833–838.
- [140] a) K. Lto, Z. Pu, Q.-S. Li, P. von R. Schleyer, *Inorg. Chem.* **2008**, *47*, 10906–10910; b) Z. Pu, K. Ito, P. von R. Schleyer, Q.-S. Li, *Inorg. Chem.* **2009**, *48*, 10679–10686.
- [141] a) C. Romanescu, T. R. Galeev, W.-L. Li, A. I. Boldyrev, L.-S. Wang, *Angew. Chem. Int. Ed.* **2011**, *50*, 9334–9337; *Angew. Chem.* **2011**, *123*, 9506–9509; b) C. Romanescu, T. R. Galeev, A. P. Sergeeva, W.-L. Li, L.-S. Wang, A. I. Boldyrev, *J. Organomet. Chem.* **2012**, *721–722*, 148–154.
- [142] W.-L. Li, C. Romanescu, T. R. Galeev, Z. A. Piazza, A. I. Boldyrev, L.-S. Wang, *J. Am. Chem. Soc.* **2012**, *134*, 165–168.
- [143] T. R. Galeev, C. Romanescu, W.-L. Li, L.-S. Wang, A. I. Boldyrev, *Angew. Chem. Int. Ed.* **2012**, *51*, 2101–2105; *Angew. Chem.* **2012**, *124*, 2143–2147.
- [144] C. Romanescu, T. R. Galeev, W.-L. Li, A. I. Boldyrev, L.-S. Wang, *J. Chem. Phys.* **2013**, *138*, 134315.
- [145] C. Romanescu, T. R. Galeev, W.-L. Li, A. I. Boldyrev, L.-S. Wang, *Acc. Chem. Res.* **2013**, *46*, 350–358.
- [146] L.-m. Yang, Y.-h. Ding, C.-c. Sun, *J. Am. Chem. Soc.* **2007**, *129*, 658–665.
- [147] E. Wilson, *Chem. Eng. News* **2000**, *78*, 8.
- [148] a) L.-m. Yang, Y.-h. Ding, C.-c. Sun, *ChemPhysChem* **2006**, *7*, 2478–2482; b) L.-m. Yang, Y.-h. Ding, C.-c. Sun, *J. Am. Chem. Soc.* **2007**, *129*, 1900; c) L.-m. Yang, Y.-h. Ding, C.-c. Sun, *J. Phys. Chem. A* **2007**, *111*, 10675–10681; d) L.-M. Yang, Y.-H. Ding, C.-C. Sun, *Chem. Eur. J.* **2007**, *13*, 2546–2555; e) L.-M. Yang, Y.-H. Ding, C.-C. Sun, *Theor. Chem. Acc.* **2008**, *119*, 335–342; f) L.-m. Yang, Y.-h. Ding, W. Q. Tian, C.-c. Sun, *Phys. Chem. Chem. Phys.* **2007**, *9*, 5304–5314; g) L.-M. Yang, H.-P. He, Y.-H. Ding, C.-C. Sun, *Organometallics* **2008**, *27*, 1727–1735; h) L.-m. Yang, X.-p. Li, Y.-h. Ding, C.-c. Sun, *Eur. J. Inorg. Chem.* **2008**, 2099–2106; i) L.-m. Yang, X.-p. Li, Y.-h. Ding, C.-c. Sun, *J. Mol. Model.* **2009**, *15*, 97–104; j) L.-m. Yang, C.-b. Shao, Y.-h. Ding, C.-c. Sun, *Phys. Chem. Chem. Phys.* **2008**, *10*, 2020–2025; k) L.-M. Yang, J. Wang, Y.-H. Ding, C.-C. Sun, *Organometallics* **2007**, *26*, 4449–4455; l) L.-m. Yang, J. Wang, Y.-h. Ding, C.-c. Sun, *Phys. Chem. Chem. Phys.* **2008**, *10*, 2316–2320; m) L.-m. Yang, N. Wang, Y.-h. Ding, C.-c. Sun, *J. Phys. Chem. A* **2007**, *111*, 9122–9129; n) H.-P. He, L.-M. Yang, Y.-H. Ding, *Chem. J. Chin. Univ. Chin.* **2009**, *30*, 2464–2468.
- [149] P. D. Pancharatna, M. A. Mendez-Rojas, G. Merino, A. Vela, R. Hoffmann, *J. Am. Chem. Soc.* **2004**, *126*, 15309–15315.
- [150] S. D. Li, J. C. Guo, C. Q. Miao, G. M. Ren, *Angew. Chem. Int. Ed.* **2005**, *44*, 2158–2161; *Angew. Chem.* **2005**, *117*, 2196–2199.
- [151] C.-b. Shao, Y.-h. Ding, *Phys. Chem. Chem. Phys.* **2010**, *12*, 13153–13157.
- [152] H.-P. He, L.-M. Yang, Y.-H. Ding, *Chem. J. Chin. Univ.* **2009**, *30*, 2464–2468.
- [153] U. Das, K. Raghavachari, *J. Chem. Theory Comput.* **2008**, *4*, 2011–2019.
- [154] F.-L. Liu, A. F. Jalbout, *J. Mol. Graphics Modell.* **2008**, *26*, 1327–1332.
- [155] X. Wu, Y. Pei, X. C. Zeng, *Nano Lett.* **2009**, *9*, 1577–1582.
- [156] M. Wu, Y. Pei, X. C. Zeng, *J. Am. Chem. Soc.* **2010**, *132*, 5554.
- [157] B. Xiao, Y.-h. Ding, C.-c. Sun, *Phys. Chem. Chem. Phys.* **2011**, *13*, 2732–2737.
- [158] M. Wu, Y. Pei, J. Dai, H. Li, X. C. Zeng, *J. Phys. Chem. C* **2012**, *116*, 11378–11385.
- [159] M. Wu, Y. Pei, X. C. Zeng, *Chem. Phys. Lett.* **2013**, *580*, 78–81.
- [160] C. Zhang, W. Sun, Z. Cao, *J. Am. Chem. Soc.* **2008**, *130*, 5638.
- [161] Y. Li, F. Li, Z. Zhou, Z. Chen, *J. Am. Chem. Soc.* **2011**, *133*, 900–908.
- [162] X. Luo, J. Yang, H. Liu, X. Wu, Y. Wang, Y. Ma, S.-H. Wei, X. Gong, H. Xiang, *J. Am. Chem. Soc.* **2011**, *133*, 16285–16290.
- [163] F. Li, D.-e. Jiang, Z. Chen, *J. Mol. Model.* **2014**, *20*, 2085.
- [164] Y. Li, Y. Liao, Z. Chen, *Angew. Chem. Int. Ed.* **2014**, *53*, 7248–7252; *Angew. Chem.* **2014**, *126*, 7376–7380.
- [165] J. Dai, X. Wu, J. Yang, X. C. Zeng, *J. Phys. Chem. Lett.* **2014**, *5*, 2058–2065.
- [166] Y. Li, Y. Liao, P. von R. Schleyer, Z. Chen, *Nanoscale* **2014**, *6*, 10784–10791.
- [167] L.-M. Yang, V. Bačić, I. A. Popov, A. I. Boldyrev, T. Heine, T. Frauenheim, E. Ganz, *J. Am. Chem. Soc.* **2015**, *137*, 2757–2762.
- [168] S. L. Buchwald, E. A. Lucas, W. M. Davis, *J. Am. Chem. Soc.* **1989**, *111*, 397.
- [169] R. H. Cayton, S. T. Chacon, M. H. Chisholm, M. J. Hampden-Smith, J. C. Huffman, K. Folting, P. D. Ellis, B. A. Huggins, *Angew. Chem. Int. Ed. Engl.* **1989**, *28*, 1523–1525; *Angew. Chem.* **1989**, *101*, 1547–1548.
- [170] I. Hyla-Kryspin, R. Gleiter, M.-M. Rohmer, J. Devemy, A. Gunale, H. Pritzkow, W. Siebert, *Chem. Eur. J.* **1997**, *3*, 294–299.
- [171] J.-H. Huang, J. J. Luci, T.-Y. Lee, D. C. Swenson, J. H. Jensen, L. Messerle, *J. Am. Chem. Soc.* **2003**, *125*, 1688–1689.
- [172] J.-F. Li, H.-B. Song, C.-M. Cui, J.-P. Cheng, *Inorg. Chem.* **2008**, *47*, 3468–3470.
- [173] O. J. Cooper, A. J. Wooles, J. McMaster, W. Lewis, A. J. Blake, S. T. Liddle, *Angew. Chem. Int. Ed.* **2010**, *49*, 5570–5573; *Angew. Chem.* **2010**, *122*, 5702–5705.
- [174] H. Köhnlein, G. Stösser, E. Baum, E. Möllhausen, U. Huniar, H. Schnöckel, *Angew. Chem. Int. Ed.* **2000**, *39*, 799–801; *Angew. Chem.* **2000**, *112*, 828–830.
- [175] M. Schollenberger, B. Nuber, M. L. Ziegler, *Angew. Chem. Int. Ed. Engl.* **1992**, *31*, 350–351; *Angew. Chem.* **1992**, *104*, 329–331.
- [176] See Ref. [120].
- [177] See Ref. [131].
- [178] See Ref. [122].
- [179] See Ref. [58].
- [180] A. I. Boldyrev, P. von R. Schleyer, *J. Am. Chem. Soc.* **1991**, *113*, 9045–9054.
- [181] M. Ruck, *Angew. Chem. Int. Ed. Engl.* **1997**, *36*, 1971–1973; *Angew. Chem.* **1997**, *109*, 2059–2062.
- [182] J. Köhler, *Angew. Chem. Int. Ed.* **2008**, *47*, 4470–4472; *Angew. Chem.* **2008**, *120*, 4544–4546.
- [183] J. Dai, Z. Li, J. Yang, J. Hou, *Nanoscale* **2012**, *4*, 3032.

Received: October 23, 2014

Published online: June 26, 2015